INTERPRETATION OF INFRARED INTENSITIES

By

JAMES HENRY NEWTON

A DISSERTATION PRESENTED TO THE GRADUATE
COUNCIL OF THE UNIVERSITY OF FLORIDA IN PARTIAL
FULFILLMENT OF THE REQUIREMENTS FOR THE DEGREE OF
DOCTOR OF PHILOSOPHY

UNIVERSITY OF FLORIDA
1974

This thesis is gratefully dedicated to my wife, Tina, whose patience, good nature, encouragement, and sacrifice have made this work possible; and to my daughter, Pauline, whose unknowing sacrifice and ever-present high spirits have been a continual source of inspiration.

ACKNOWLEDGEMENTS

I would like to express my personal thanks and gratitude to Dr. W.B. Person, whose guidance, encouragement, friendship, and willingness to help have played a major role in my graduate education. The hours of discussion on the topics in this thesis (and many other related and unrelated topics) are gratefully acknowledged.

I would also like to express my thanks to past and present members of Dr. Person's research group for their friendship over the past few years, in particular Dr. G. Jiang, Dr. T. C. Jao, Dr. S. Kondo, Miss B. Zilles, Mr. R. Levine, and Dr. Ken Brown. Their friendship has been, and will continue to be, invaluable.

The partial support of NSF Grant GP-17818 is gratefully acknowledged, as well as a grant from the Division of Sponsored Research at the University of Florida.

We are grateful to the NERDC for partial support for computer time.

I am grateful to my wife for her patience and diligence in typing the rough drafts and final copy of this thesis, and to my sister-in-law, Mrs. Stan Sheldon, for her valuable assistance in putting this thesis together. Her sense of humor and willingness to help are gratefully acknowledged.

TABLE OF CONTENTS

LIST OF TABLES

LIST OF FIGURES

Abstract of Dissertation Presented to the Graduate Council of the University of Florida in Partial Fulfillment of the Requirements for the Degree of Doctor of Philosophy

INTERPRETATION OF INFRARED INTENSITIES

By

James Henry Newton

December, 1974

Chairman: Willis B. Person
Major Department: Chemistry

The infrared intensity data for the methyl halides have been interpreted in terms of the atomic polar tensors first introduced by Biarge, Herranz, and Morcillo (1961). By using the principal of isotopic invariance and the approximate quantum mechanical CNDO/2 technique, a unique sign choice for the $\partial\vec{p}/\partial Q$'s for CH_3F and CH_3Cl was determined. By analogy the signs for the $\partial\vec{p}/\partial Q$'s for CH_3Br and CH_3I were inferred. The errors in the polar tensor elements were estimated by comparing the CH_3X and CD_3X tensors. In addition, a normal coordinate analysis of the CH_3X and CD_3X molecules was carried out to insure consistency in coordinate definitions using the most recent GF force fields of Duncan et al. (1972).

The magnitudes of the dipole moment change vectors, $(\Delta P)_\tau^\alpha$, associated with the atomic polar tensors were shown

to have smooth trends through the CH_3X series, suggesting that these vectors may be predictable and transferable intensity parameters. Similar trends were observed for the angle between the $(\Delta P)^H_\tau$ vectors and the C-H bond.

The effective charges, ξ_α , first defined by King, Mast and Blanchette (1972) for the αth atom in the CH_3X series were computed. From the effective charges of CH_3F, the effective charges for CF_4, CF_3H, CF_2H_2, and CH_4 were predicted and compared to the experimentally observed intensity sums for these molecules.

The CNDO/2 results for CH_3F and CH_3Cl were critically analyzed and the absolute intensities, A_i , predicted by CNDO, are compared to the experimental data. In general, the results for CH_3F are much better than for CH_3Cl. For example, we found that the CNDO/2 calculated bond moment for C-Cl is positive, which seems contrary to chemical intuition.

CHAPTER 1

INTRODUCTION

Infrared spectroscopy has long been recognized as an aid in the elucidation of the structures of complex molecular systems (1). The facts that different spatial arrangements of the atoms give rise to different spectral features and that in many cases the spectral features are sensitive to the intramolecular (as well as intermolecular) environments, together with the relative ease with which the spectra are obtained, have made the infrared spectrometer a common tool in most chemical laboratories. In the past, the emphasis has been on the interpretation of the spectra in terms of frequencies of functional groups or of chemical bonds, and extensive correlation charts have been derived that are quite useful for qualitative analysis. Moreover, the theoretical basis for such correlations is firmly established (see Reference 1, for example). Much less attention has been given to the infrared band intensities to obtain the additional useful information about the molecular environment which they may contain (2). The infrared band intensity is a function of the change in the dipole moment when the molecule is distorted from equilibrium; it is a direct reflection of the changes in the electron distribu-

tion in the molecule as a whole. As a consequence, the band intensity is expected to reflect any distortion of the electron cloud produced by substituents and/or by the immediate environment of the molecule. Wexler (2) has developed an empirical correlation chart for band intensities, similar to the frequency correlation charts, that demonstrates quite well the potential usefulness of the band intensities as an additional probe for the study of molecular structure and environments.

In general, the use of infrared band intensities has been limited to a semi-quantitative tool with such ambiguous terms as "strong (s)," "medium (m)," or "weak (w)" used to describe the band intensities. There are understandable reasons for the lack of quantitative infrared band intensity data for all but the simplest molecules. Reliable measurements of the absolute (or even of relative) band intensities is not a routine procedure, although the technique has been fairly well standardized (3). This problem may well be eliminated with the advent of the computerized spectrometer, and reliable band intensity measurements may soon become as routinely available as the spectrum itself. There is, however, a more fundamental problem associated with the routine use of infrared intensity data; that is, the lack of a uniform, coherent theoretical basis for interpreting them (4).

Hence, while it seems that the measurement of accurate band intensities may be fast approaching the "routine," it now seems appropriate that the theoretical tools should be

developed in order to offer a platform for interpretation.

The Morcillo Theory

One of the primary purposes of this thesis is to illustrate a procedure for the reduction of the experimental intensity data to a form which we believe is susceptible to theoretical scrutiny and interpretation. The procedure was first introduced by Biarge, Herranz, and Morcillo (5) and independently rediscovered by Person, Peyton, and Jiang (6), but has attracted little attention since its conception in 1961. With the exception of two revealing papers by Morcillo and his co-workers on the application of the technique (7 and 8), little work has been done employing the procedure. As a consequence, the usefulness of the procedure as a theoretical basis and an interpretative tool has been relatively unexplored.

The technique is discussed in Chapter 2, where we refer to it as the "polar tensor" or "Morcillo technique." It involves the reduction of the experimentally determined complete infrared band intensity data to a set of "atomic polar tensors"; one for each atom in the molecule, defined in a space-fixed Cartesian coordinate system for the molecule. The polar tensor for the αth atom in the molecule is defined as (5):

$$\underline{P}_X^{\alpha} = \begin{pmatrix} \partial p_x/\partial x_\alpha & \partial p_x/\partial y_\alpha & \partial p_x/\partial z_\alpha \\ \partial p_y/\partial x_\alpha & \partial p_y/\partial y_\alpha & \partial p_y/\partial z_\alpha \\ \partial p_z/\partial x_\alpha & \partial p_z/\partial y_\alpha & \partial p_z/\partial z_\alpha \end{pmatrix} . \quad (1\text{-}1)$$

Here α stands for the αth atom in the molecule and the αth tensor is composed of elements measuring the change in the dipole moment components with respect to an infinitesimal change along the Cartesian axes (x, y, or z) on the αth atom.

The atomic polar tensors quantitatively reflect the contributions of each atom to the total intensity of the infrared bands in the molecule. In the past, the band intensities have been interpreted in terms of bond dipole moments and/or of dipole moment changes with respect to a set of defined internal coordinates (3). The procedures, though useful in their own way, have not proved to be generally satisfactory. The bond moment hypothesis, for example, which assumes that the dipole moment change occurs parallel to the bond for a bond-stretching motion and perpendicular to the bonds for an angle-bending motion, and which might result in an attractively simple theory, has never been accepted (9).

Since the polar tensor technique resolves the band intensities into atomic contributions, we are able to examine atom by atom the contributions to the intensities. In essence the polar tensors offer a more detailed breakdown of the infrared band intensities that we believe is one of its major advantages.

One of the more significant advances in terms of the theoretical interpretations of band intensities in the last decade has been the application of ab initio and approximate quantum mechanical techniques to the calculation of band in-

tensities (4). As we shall show, the polar tensor technique presents the experimental data in a simple, straightforward form that can readily be compared with quantum mechanical calculations of theoretical polar tensors.

The most significant and potentially useful feature of the polar tensor technique is that the associated vectors and individual elements of the tensors in a series of structurally similar molecules exhibit simple and useful trends. The fact that certain polar tensor elements are quite insensitive to changes in substituents and others vary in a predictable manner suggests that it may be possible to predict quantitatively the infrared spectra of more complex systems from a knowledge of the polar tensors of simpler systems.

King, Mast, and Blanchette (KMB) have defined a quantity which they called the effective charge, ξ_α, for the αth atom in a molecule (10), and which bears a simple relationship to the intensity sum rule (11). They found that the effective charge of the hydrogen atoms in a series of hydrocarbons was constant. It has been shown that the squared effective charge derived by KMB is equal to the trace of the product of the αth atomic polar tensor with its transpose (12). This tensor invarient, ξ_α, appears to be another transferable or predictable intensity parameter, as we shall show later in Chapter 4.

Infrared Gas Phase Band Intensities

As discussed by Overend (3), the experimentally determined intensity (Γ_i) of the ith fundamental absorption band is related to the transition moment $< \Psi^*_{v''} \; |\hat{p}| \; \Psi_{v'} >$ by:

$$\Gamma_i = (1/n\ell)\int_{band} \{\ln(I_0/I)\}\, d(\ln\nu)$$

$$= 8\pi^2 N/3hc \; < \Psi^*_{v''} \; |\hat{p}| \; \Psi_{v'} >^2 \quad . \qquad (1\text{-}2)$$

Here n is the concentration, ℓ is the pathlength, I_0 is the intensity of the incident radiation of wavenumber, ν, and I is the intensity of the radiation after passage through the sample; $\Psi^*_{v''}$ and $\Psi_{v'}$ are the wave functions for the ground and excited vibrational states respectively (and are usually taken to be harmonic oscillator functions), and $\hat{p}$ is the dipole moment operator. The concentration term N and h, and c have their usual meanings. Assuming both mechanical and electric harmonicity, Equation 1-2 reduces to the simple form for the gas phase infrared band intensities:

$$\Gamma_i = (N\pi/3c^2\nu_i)\; (\partial\vec{p}/\partial Q_i)^2 \quad , \qquad (1\text{-}3)$$

where ν_i is the harmonic wavenumber (in cm^{-1}) of the ith fundamental band. The quantity $\partial\vec{p}/\partial Q_i$ is the dipole moment derivative relative to the ith normal coordinate, Q_i. As Overend has pointed out, even though Equation 1-3 is approximate, the errors involved in the approximations are generally regarded as negligible relative to the error involved in the actual integration of the spectrum (3), and Equation 1-3 is quite sufficient for the interpretation of molecular systems

of general interest.

The dimensions of Γ are (concentration x length)$^{-1}$. Another vibrational intensity measure, A, is often used, and it is related to Γ by:

$$A_i \simeq \Gamma_i \nu_i = (N\pi/3c^2)(\partial p/\partial Q_i)^2 \quad , \qquad (1\text{-}4)$$

and has dimensions of (wavenumber/concentration x length). The units of Γ are generally cm^2/mol, or in SI units (4) where the concentration is in mol m^{-3}, the pathlength in m, and the wavenumber in m^{-1}; Γ has the units m^2/mol. The SI units of A are m mol^{-1} where the pathlength is in m and the concentration in mol m^{-3} (Equation 1-2). In this work we shall use the intensity measurement Γ in units of cm^2/mol. The dipole moment derivatives have dimensions of charge x length/ length, and we shall use the units of $D\mathring{A}^{-1}$, or electrons ($\underline{e}$) (1.0 D $\mathring{A}^{-1}$=0.208 $\underline{e}$). In terms of SI units the dipole moment is expressed in Coulombs meters (Cm), with 1 esu · cm = 1 D = 3.335 x 10^{-20} Cm. Thus $D\mathring{A}^{-1}$ expressed in SI units becomes 1 $D\mathring{A}^{-1}$ = 3.335 x 10^{-20}C = 3.335 x 10^{-2} aC, and 1 $\underline{e}$ = 4.8 x 10^{-10} $D\mathring{A}^{-1}$ = 16.02 x 10^{-2} aC.

In Equation 1-4 we see that either measure of the experimental intensity is directly proportional to the square of the dipole moment derivative. Hence Equation 1-4 gives the relationship between these experimentally observed quantities and a set of molecular parameters subject to theoretical interpretation and computation. Only the magnitude of $\partial\vec{p}/\partial Q_i$ can be determined from such experimental in-

tensity measurements; if the band intensity is to be interpreted in terms of changes in the electron density (or dipole moment derivatives with respect to internal coordinates), the sign of $\partial\vec{p}/\partial Q_i$ must be determined as well. As we have pointed out, the data are usually reduced to a set of dipole moment derivatives with respect to a set of defined internal displacement coordinates (3) or, as in the case of the polar tensors, to the set of Cartesian displacement coordinates. We shall not pursue this subject further since the procedures are described in detail in Chapter 2. It will suffice here to point out that even when the data are reduced in polar tensor form, the sign ambiguity is still present and a complete description of the normal coordinates is still required. For the reduction of the data, or for a description of Q_i if $\partial\vec{p}/\partial Q_i$ is to form the basis of interpretation, the normal coordinate transformation matrix, $\underline{L}$, is required. The point to be made here is that for a meaningful interpretation of infrared band intensities, we must not only have accurate intensity measurements, but also some rules to determine the signs of the $\partial\vec{p}/\partial Q_i$'s and a rather complete knowledge of the force field with a normal coordinate analysis of the molecular system to give $\underline{L}$ (13).

Sign of Dipole Moment Derivatives

In recent years the application of ab initio and approximate quantum mechanical techniques has proven quite helpful in determining the signs of the dipole moment derivatives. The CNDO/2 approximate quantum technique (14) has been

highly successful, and a fairly high degree of confidence has been expressed in its ability to predict signs for molecules containing first row elements. This subject was recently reviewed in some detail (4).

There are also two experimental procedures which aid in the determination of the relative signs of the dipole derivatives. The first involves a detailed analysis of the Coriolis perturbation between two fundamental vibrational modes of appropriate symmetry; from these studies the relative signs of the two $\partial\vec{p}/\partial Q_i$'s for the coupled modes can be determined (15). The second method involves the comparison of the integrated band intensities of a molecule with its isotopically substituted species and has been referred to as the "isotopic invariance principle" (11). (We shall discuss these two techniques in more detail in Chapter 3.) Thus, if the pertinent Coriolis data and if the intensities of isotopically substituted molecules are both available, one may eliminate a large number of possible sign combinations of the $\partial\vec{p}/\partial Q_i$'s. These two procedures, coupled with the quantum mechanical calculations, make the choice of the signs of the $\partial\vec{p}/\partial Q_i$'s more objective, as we shall demonstrate in Chapter 3, and requires less reliance on chemical intuition, but usually they are insufficient to determine only one set of signs.

The Methyl Halides

The methyl halides (CH_3F, CH_3Cl, CH_3Br, and CH_3I) are perhaps the best series of structurally similar molecules for use as a model system to demonstrate the polar tensor

technique and its potential usefulness.

During the last decade, the methyl halides have been the subject of several extensive studies, especially calculations to establish their force fields. Notable among these are the classic papers by Aldous and Mills that appeared in 1962 (16) and 1963 (17), where an attempt was made to determine the general harmonic force fields for the molecules in the series. In their force constant refinement calculations, they utilized frequency data for the CH_3X and CD_3X molecules, as well as Coriolis constants and centrifugal distortion constants for both CH_3X and CD_3X. In all, twenty-one pieces of independent experimental data were used to calculate twelve harmonic force constants for each CH_3X molecule. In spite of the large number of experimental data used, they were not completely successful in fixing the force fields. {The general problem involved here is discussed thoroughly by Aldous and Mills (16), by Mills (13), and also briefly again in Chapter 2.} For CH_3F they found that two off-diagonal force constants in the A_1 class were essentially undetermined and that the E class force constants converged to two alternative sets. For CH_3Cl the force field did not converge, but wandered slowly through a family of solutions, each of which gave a good fit to the experimental data. For CH_3Br and for CH_3I one set of force constants was reported for each molecule, but these sets were not significant since they were just one arbitrary choice from a family of possible solutions.

In 1966, Russell, Needham, and Overend (RNO) (18) carried

out a force constant refinement calculation on the methyl halides, using, in addition to the data used by Aldous and Mills, the frequencies of the CHD_2X and CH_2DX molecules. Although these data are not independent (19), the calculations converged to a unique set of force constants for each molecule. However, several of the off-diagonal force constants had such large dispersions that they were essentially undetermined.

Duncan, Allen, and McKean in 1970 (20) and Duncan, McKean and Speirs in 1972 (21) used isotope frequencies from ^{13}C substituted molecules, together with all the data previously used by Overend, finally to fix the general harmonic force constants within a fairly narrow uncertainty range for all four methyl halides. The force constants found by Duncan, et al. (21) (hereafter cited as Duncan) were quite similar to those of Overend, but with significantly smaller dispersions for many of the force constants. In general, the dispersions in the off-diagonal force constants in Duncan's force field were an order of magnitude smaller than those for the force field of RNO. In particular the off-diagonal force constants (f_{12}, f_{13}) that were undetermined in Overend's work have been determined fairly well by Duncan's work. (In RNO's work, the dispersions for these force constants ranged from 100 to 200% of their values, whereas in Duncan's work the uncertainty is reduced to less than 20 to 50% of the force constant for the series.)

The infrared band intensities of the fundamentals of

CH_3X and CD_3X (where X is Cl, Br, or I), have been measured fairly accurately by Dickson, Mills, and Crawford (22). The band intensities of CH_3F and CD_3F have been measured by Barnett and Eggers (as reported by RNO). With the exception of CD_3I, the intensity measurements were complicated by overlapping bands, the most serious of which occurred in CH_3F and CD_3F. With the exception of the fluoride, however, the errors in the band intensities, including the estimated errors involved in band separation, ranged from about 5 to 20% for the series. For CH_3F and CD_3F each fundamental band is overlapped with one other fundamental, and the intensities of two bands, ν_2 of CH_3F and ν_5 of CD_3F, have estimated errors of about 100% and 200% respectively. The other bands in the fluoride molecules have estimated errors of about 10 to 20% (18). Although the errors for the methyl halide intensities may appear excessive, they are of the magnitude one must expect for intensity measurements of this kind. The problem of overlapping band separation has been very aptly described: "...separation is a major source of error, demanding, as it usually does, a keen eye, a sharp pencil, a certain artistic talent, and simple faith in the symmetry of vibrational-rotational bands and the cooperation of nature" (18).

Russell, Needham, and Overend's work (18) on the methyl halide series gives the best previous estimate of the $\partial\vec{p}/\partial Q_i$'s for CH_3X and CD_3X molecules. Although many sign combinations of the $\partial\vec{p}/\partial Q_i$'s were eliminated, they were not able to select a unique set of $\partial\vec{p}/\partial Q_i$'s for any molecule in

the series. The primary purpose of their work was to illustrate the procedure for calculating the errors in dipole moment derivatives and normal coordinates, and this provides another reason for our choice of this series as a model system: we can use the errors reported by them as a starting point, and propagate them through to the polar tensors to give a measure of their reliability.

In the remaining chapters of this thesis, we shall attempt to show the potential of the polar tensor technique using the methyl halide series as a model system. Our primary purpose will be to illustrate the technique and show how it can be used for interpretive purposes. In addition, we shall point out trends in the tensors that we believe are indicative of the predictive nature of the polar tensors.

We shall use the approximate quantum mechanical technique, CNDO/2, to aid in our choice of signs for the $\partial\vec{p}/\partial Q_i$'s and critically analyze the results of the calculations for CH_3F and CH_3Cl. In doing this we also hope to illustrate the potential of the polar tensor technique for quantum mechanical calculations and theoretical interpretations.

CHAPTER 2

POLAR TENSORS

As we pointed out in the last chapter, the polar tensor concept, though fairly old, is not well known among spectroscopists. In light of this fact we shall briefly develop in this chapter the concept of an atomic polar tensor as first introduced by Biarge, Herranz, and Morcillo (5), but using the revised notation of Person and Newton (12). In order to develop the mathematical expressions for the polar tensors and to familiarize the reader with the notation to be employed, we must digress momentarily and examine the mathematical transformations used in a normal coordinate analysis of molecular systems.

Normal Coordinate Transformations

The normal coordinate analysis procedures have been well documented (13, 23, 24) and we shall outline only the steps pertinent to the development of the polar tensors. For a molecular system containing N atoms there are 3N - 6 (or 3N - 5 if the molecule is linear) normal modes of vibration. In order to determine the nature of these normal modes, one generally begins with a space-fixed Cartesian coordinate system on which the instantaneous location of individual atoms are given by the Cartesian displacement coordinates.

These 3N Cartesian displacement coordinates can be represented by a column vector $\underline{X}$ of dimensions 3N x 1 as shown below:

$$\underline{X} = \begin{pmatrix} x_1 \\ y_1 \\ z_1 \\ x_2 \\ y_2 \\ z_2 \\ \cdot \\ \cdot \\ \cdot \\ z_N \end{pmatrix}$$

Here x_i, y_i, and z_i refer to the Cartesian displacement coordinates of atom i and the i subscript runs from 1 to N. The normal coordinates can be expressed in terms of this coordinate system, but it has been found more convenient to give the normal coordinates in terms of molecule-fixed internal coordinates or symmetry coordinates.

The transformation from Cartesian displacement coordinates to internal displacement coordinates (r_j, where j identifies the jth internal coordinate) is achieved by the transformation matrix $\underline{B}$.

$$\underline{R} = \underline{B}\ \underline{X}. \qquad (2\text{-}1)$$

Here $\underline{R}$ is a (3N - 6) x 1 column vector of the independent internal displacement coordinates (bond stretches or bends),

expressed as linear combinations of the Cartesian displacement coordinates. $\underline{B}$ is a (3N - 6) x 3N transformation matrix with elements of the form $b_{ij} = \partial r_i / \partial x_j$ so that an r_i element of $\underline{R}$ has the form

$$r_i = \sum_{j=1}^{3N} (\partial r_i / \partial x_j)\, x_j = \sum_{j=1}^{3N} b_{ij} x_j \,. \qquad (2\text{-}2)$$

The transformation matrix $\underline{B}$ (or its element, b_{ij}) is obtained by inspection of the geometry of the molecule and a convenient prescription for the evaluation of the elements has been given by Wilson, Decius, and Cross (23). It should be pointed out that the transformation just described transforms a set of 3N space-fixed Cartesian displacement coordinates into a set of 3N - 6 molecule-fixed internal displacement coordinates. The space-fixed coordinate system includes, in addition to the coordinatesof the vibrational degrees of freedom, coordinates for the three rotational and three translational degrees of freedom, for in the space-fixed axis system, the displacements cause the molecules to translate and rotate relative to a fixed axis system. In the molecule-fixed axis system, the coordinate axis rotates and translates with the molecule as the atoms are displaced, and only the 3N - 6 vibrational degrees of freedom are evident in this system. Although this may appear to be trivial now, it will be important in our development of the polar tensors and we shall return to this fact later in this chapter.

In order to take advantage of any symmetry of the molecule we can transform the internal coordinates to symmetry

coordinates by the following transformation:

$$\underline{S} = \underline{U}\,\underline{R} \ , \qquad (2\text{-}3)$$

where $\underline{S}$ is a (3N - 6) x 1 column vector of elements, S_i , composed of a linear combination of the internal displacement coordinates, r_j. $\underline{U}$ is a (3N - 6) x (3N - 6) orthogonal transformation matrix obtained by considering the symmetry point group to which the molecule belongs (25).

The normal coordinates (Q_i) are related to the symmetry displacement coordinates by :

$$\underline{S} = \underline{L}\,\underline{Q} \ , \text{ or } \underline{Q} = \underline{L}^{-1}\underline{S} \ . \qquad (2\text{-}4)$$

Here $\underline{Q}$ is a (3N - 6) x 1 column vector composed of elements, Q_i , which are linear combinations of the symmetry displacement coordinates. $\underline{L}$ is the (3N - 6) x (3N - 6) normal coordinate transformation matrix and $\underline{L}^{-1}$ is its inverse. The general form of an element of $\underline{L}$ is $L_{ij} = \partial S_i/\partial Q_j$ in terms of symmetry displacement coordinates or $l_{ij} = \partial r_i/\partial Q_j$ and $l_{ij} = \partial x_i/\partial Q_j$ in terms of internal displacement coordinates and Cartesian displacement coordinates, respectively. These three $\underline{L}$ matrices are not identical and the matrix is generally denoted (as here) by different symbols for each set of displacement coordinates. We shall not, however, make an explicit distinction in $\underline{L}$ for the different coordinates since we shall be speaking in general, or the particular set of coordinates will be obvious from the equations.

The evaluation of the $\underline{B}$ matrix and the $\underline{U}$ matrix is

straightforward, but the evaluation of $\underline{L}$ is not, in general, a trivial task, since it depends on the values of the force constants, as discussed by Mills (13). In general, these values are not known (see Reference 13). A great deal of effort has been expended in trying to evaluate good normal coordinates (that is, good $\underline{L}$ matrices) for polyatomic systems (see Reference 16 or 17 for examples). Although we are not explicitly interested in the details of the calculations, the results of such calculations, as we shall show, are of great importance in evaluating and interpreting the polar tensors. Once a set of internal displacement coordinates has been chosen, the $\underline{L}$ matrix can be evaluated from the solution of the eigenvalue equation

$$\underline{G}\,\underline{F}\,\underline{L} = \underline{L}\,\underline{\Lambda} \quad . \tag{2-5}$$

Here $\underline{G}$ is the symmetric inverse kinetic energy matrix and is related to the $\underline{B}$ matrix by

$$\underline{G} = \underline{B}'\,\underline{M}^{-1}\underline{B} \quad , \tag{2-6}$$

where $\underline{B}'$ is the transpose of $\underline{B}$ and $\underline{M}^{-1}$ is a 3N x 3N diagonal matrix whose elements are the reciprocal masses of the atoms of the molecule. $\underline{F}$ is the (3N - 6) x (3N - 6) symmetric force constant matrix comprised of elements, f_{ij}, which constitute the "force field" (2V = potential energy = the quadratic form, $\underline{R}'\underline{F}\,\underline{R}$) of the molecule. The $\underline{\Lambda}$ is the (3N - 6) x (3N - 6) diagonal eigenvalue matrix whose elements, λ_i, are the frequency parameters which are related to the (3N - 6)

frequencies of the normal modes of vibration. The matrix $\underline{L}$, the normal coordinate transformation matrix, is the eigenvector matrix of the $\underline{GF}$ product matrix. Although there are several well-known mathematical techniques (26) available for solving the eigenvalue problem expressed by Equation 2-5, they all involve the direct or indirect solution of a set of vibrational secular equations given by the determinant

$$| \underline{G}\,\underline{F} - \lambda_i \underline{E} | = 0 , \qquad (2\text{-}7)$$

where $\underline{E}$ is a (3N - 6) x (3N - 6) identity matrix. Once the eigenvalues have been determined, then the eigenvectors can be computed.

The formulation of the solution to the eigenvalue problem is straightforward, but in practice we may generally encounter a major difficulty. As explained by Mills (13, 27), the problem is that for most molecules we have more unknown force constants {approximately $\sum n_s(n_s + 1)/2$, where n_s is the number of coordinates of symmetry type S} than we have known λ_i 's. This situation renders the secular equation unsolvable unless we (1) constrain the force field, (2) assume values for the unknown force constants, or (3) obtain additional independent experimental data such as frequencies (λ_i's) from isotopically substituted molecules, Coriolis coupling constants, centrifugal distortion constants, or other data of this type. The point to be made is that if we constrain the force field or make a bad assumption for any unknown force constants, then these constraints and assumptions will be reflected in $\underline{L}$. In

short, an ill-defined force field yields an ill-defined set of normal coordinates. Thus, we cannot expect any subsequent calculations involving $\underline{L}$ to be any better than the set of force constants used to obtain $\underline{L}$. Up to this point, we have assumed that the geometry and the vibrational frequencies of the molecule are known. If there are errors in either of these experimental quantities, then as RNO have demonstrated (18), the normal coordinates will reflect them also. Generally this kind of lack of knowledge is not as serious a problem as the one to obtain the complete set of force constants.

We have outlined above the relation between the normal coordinate and a set of Cartesian displacement coordinates. The inverse transformations from the normal coordinates to the Cartesian displacement coordinates are outlined below.

The inverse $\underline{L}$ matrix is related to $\underline{L}$, $\underline{F}$, and $\underline{\Lambda}^{-1}$ by the relationship

$$\underline{L}^{-1} = \underline{\Lambda}^{-1}\underline{L}'\,\underline{F} \quad , \tag{2-8}$$

where $\underline{L}'$ is the transpose of $\underline{L}$ and $\underline{Q} = \underline{L}^{-1}\underline{S}$. The $\underline{\Lambda}^{-1}$ is easily evaluated since $\underline{\Lambda}$ is a diagonal matrix and $\underline{F}$ is known (after the normal coordinate calculations). The internal coordinates are obtained from the symmetry coordinates by

$$\underline{R} = \underline{U}'\,\underline{S} \quad , \tag{2-9}$$

since $\underline{U}$ is an orthogonal matrix ($\underline{U}^{-1} = \underline{U}'$). Since $\underline{B}$ is not a square matrix, we cannot evaluate $\underline{B}^{-1}$ by direct inversion.

Instead, we calculate the inverse transformation matrix $\underline{A}$ to carry the internal displacement coordinates back to a set of Cartesian displacement coordinates ($\underline{X} = \underline{A}\,\underline{R}$) by the following:

$$\underline{A} = \underline{M}^{-1}\,\underline{B}'\,\underline{G}^{-1} \quad . \tag{2-10}$$

Here $\underline{M}^{-1}$ is easily obtained since $\underline{M}$ is diagonal; $\underline{B}'$ is just the transpose of $\underline{B}$, and the inverse of $\underline{G}$ can be computed by:

$$\underline{G}^{-1} = (\underline{L}^{-1})'\,(\underline{L}^{-1}) \quad . \tag{2-11}$$

Thus we can write

$$\underline{X} = \underline{A}\,\underline{R} = \underline{A}\,\underline{U}'\underline{L}\,\underline{Q} \tag{2-12}$$

for the transformation from internal displacement coordinates to the Cartesian displacement coordinates.

There is a subtlety in this last coordinate transformation, however, that should be pointed out. $\underline{A}$ carries $\underline{R}$ into a set of molecule-fixed Cartesian displacement coordinates, whereas by using $\underline{B}$ in Equation 2-1 we transformed a set of space-fixed Cartesian displacement coordinates into a set of molecule-fixed internal displacement coordinates. Thus, the $\underline{X}$ vector of Equation 2-12 is not the same as the $\underline{X}$ vector we started with in Equation 2-1. This brings us back to the point mentioned earlier in this section about transforming from space-fixed to molecule-fixed coordinate systems, and we shall now explore this in a little more detail.

In order to transform a set of space-fixed Cartesian coordinates into a set of space-fixed internal coordinates,

the augmented $\underline{B}$ matrix is used:

$$\begin{pmatrix} \underline{R} \\ \cdots\cdots \\ \underline{\rho} \end{pmatrix} = \begin{pmatrix} \underline{B} \\ \cdots\cdots \\ \underline{\beta} \end{pmatrix} \underline{X} \quad , \tag{2-13}$$

where $\underline{R}$ is the (3N - 6) x 1 column vector of internal coordinates previously defined and $\underline{\rho}$ is a 6 x 1 column vector of the translations and rotations of the whole molecule. $\underline{B}$ is the transformation matrix defined previously and $\underline{\beta}$ is a 6 x 3N rotation matrix relating $\underline{\rho}$ to $\underline{X}$. The inclusion of the $\underline{\rho}$ (and $\underline{\beta}$) is an explicit expression of the Eckart conditions (28) for the space-fixed molecular coordinate frame. A typical $\underline{\beta}$ matrix for the αth atom is given below.

$$\begin{pmatrix} m_\alpha/M^{\frac{1}{2}} & 0 & 0 \\ 0 & m_\alpha/M^{\frac{1}{2}} & 0 \\ 0 & 0 & m_\alpha/M^{\frac{1}{2}} \\ 0 & -m_\alpha z_\alpha^{(e)}/I_x^{\frac{1}{2}} & m_\alpha y_\alpha^{(e)}/I_x^{\frac{1}{2}} \\ m_\alpha z_\alpha^{(e)}/I_y^{\frac{1}{2}} & 0 & -m_\alpha x_\alpha^{(e)}/I_y^{\frac{1}{2}} \\ -m_\alpha y_\alpha^{(e)}/I_z^{\frac{1}{2}} & m_\alpha x_\alpha^{(e)}/I_z^{\frac{1}{2}} & 0 \end{pmatrix} .$$

Here m_α is the mass of the α atom; M is the total mass of the molecule; I_x, I_y, and I_z are the moments of inertia about the equilibrium principal axes; $x_\alpha^{(e)}$, $y_\alpha^{(e)}$ and $z_\alpha^{(e)}$ are the coordinates of the α atom at equilibrium, measured from the origin at the center of mass, along the principal axes of

inertia (12). There are N such 6 x 3 matrices juxtaposed to form $\underline{\beta}$. The $\underline{\rho}$ vector is just $\underline{\beta}\ \underline{X}$. To transform a set of molecule-fixed internal displacement coordinates back to a set of space-fixed Cartesian displacement coordinates, the $\underline{\rho}$ vector and the augmented $\underline{A}$ matrix must be employed as shown in Equation 2-14:

$$\underline{X} = \left(\begin{array}{c:c} \underline{A} & \underline{\alpha} \end{array} \right) \left(\begin{array}{c} \underline{R} \\ \hdashline \underline{\rho} \end{array} \right) \quad . \tag{2-14}$$

$\underline{A}$, $\underline{R}$, and $\underline{\rho}$ have been defined and $\underline{\alpha} = \underline{M}^{-1}\ \underline{\beta}$. Thus,

$$\underline{X} = \underline{A}\ \underline{R} + \underline{\alpha\rho} \quad , \tag{2-15}$$

where $\underline{X}$ is now in terms of space-fixed Cartesian displacement coordinates equivalent to those in Equation 2-1. The product $\underline{\alpha\rho}$ forms the rotational and translational corrections necessary for transforming from the molecule-fixed reference frame to the space-fixed reference frame. A summary of the normal coordinate transformation notation used in this section is given in Table 2-1.

Atomic Polar Tensors

As we indicated in Chapter 1 (Equation 1-2), the integrated infrared band intensity of a normal vibrational mode is related to the square of the dipole moment derivative with respect to the normal coordinate ($\partial\vec{p}/\partial Q_i$) of the particular mode. In the following discussion, we shall derive the atomic polar tensors for a molecular system in terms of space-fixed Cartesian displacement coordinates starting with the experimentally determined $\partial\vec{p}/\partial Q_i$'s. For each normal coordinate, Q_i, we can write a 3 x 1 column vector in terms

TABLE 2-1

SUMMARY OF NOTATION FOR A NORMAL COORDINATE TRANSFORMATION

Matrix	Typical Element	Dimensions (Unweighted)
$\underline{X}$	x_i, y_i, z_i	(length)
$\underline{R}$, $\underline{S}$	r_i (s), s_i (s)[a]	(length)
	r_j (b). s_j (b)[b]	--
$\underline{B}$	b_{ij} (s)	--
	b_{kl} (b)	$(\text{length})^{-1}$
$\underline{M}^{-1}$	$1/m_i$	$(\text{mass})^{-1}$
$\underline{L}$	L_{ij} (s)	$(\text{mass})^{-\frac{1}{2}}$
	L_{kl} (b)	$(\text{mass})^{-\frac{1}{2}}$ $(\text{length})^{-1}$
$\underline{Q}$	Q_i	$(\text{mass})^{\frac{1}{2}}$ (length)
$\underline{G}$[c]	g_{ij} (s,s)	$(\text{mass})^{-1}$
	g_{ij} (s,b)	$(\text{mass})^{-1}$ $(\text{length})^{-1}$
	g_{jj} (b,b)	$(\text{mass})^{-1}$ $(\text{length})^{-2}$

Continued on next page

(Table 1-1 continued)

Matrix	Typical Element	Dimensions (Unweighted)
$\underline{F}^c$	f_{ii} (s,s)	(energy) $(\text{length})^{-2}$
	f_{ij} (s,b)	(energy) $(\text{length})^{-1}$
	f_{jj} (b,b)	(energy)
$\underline{\Lambda}$	λ_i	$(\text{time})^{-2}$

a. s indicates a bond stretching motion.
b. b indicates an angle bending motion.
c. We shall use a weighted G matrix so that the s-b and s-s elements are weighted by $\bar{d} = 1.0$ Å and $d = (1.0\text{Å})^2$ respectively, and the force constants have units of Mdynes/Å for all f_{ij} elements.

of the x, y, and z components of the dipole moment derivative as described by Morcillo and co-workers (5).

$$\underline{P}_{Q_i} = \begin{pmatrix} \sigma_i \, \partial p_x/\partial Q_i \\ \sigma_i \, \partial p_y/\partial Q_i \\ \sigma_i \, \partial p_z/\partial Q_i \end{pmatrix} \text{(charge)(mass)}^{-\frac{1}{2}} \qquad (2\text{-}16)$$

Here σ_i is the sign (+ or -) of the dipole moment derivative with respect to the ith normal coordinate and the subscripts x, y, and z refer to the respective components of the dipole moment change in the molecule-fixed Cartesian coordinate frame.

For molecules with reasonable symmetry, the dipole moment change will occur parallel to only one of the coordinate axes so that only one component, say $\partial p_x/\partial Q_i$, will be non-zero. For some molecular systems this may not be true and in such cases one would have to resolve the $\partial \vec{p}/\partial Q_i$ vector into its respective components. Unless the particular vibrational mode in question happens to be a degenerate mode, it is not at once obvious how the experimentally determined $\partial \vec{p}/\partial Q_i$ should be partitioned into its components ($\partial p_x/\partial Q_i$, $\partial p_y/\partial Q_i$, $\partial p_z/\partial Q_i$) and in such cases this may negate the advantages of the interpretation of infrared intensities by the polar tensor technique. For the molecules we shall discuss, and for a large number of other molecules, this is not a problem and in the following development of the polar tensors we shall assume that this is always true.

We can form a 3 x (3N - 6) matrix, $\underline{P}_Q$, by the juxtaposition of the 3N - 6 column vectors, $\underline{P}_{Q_i}$, so that

$$\underline{P}_Q = \{\underline{P}_{Q_1} \vdots \underline{P}_{Q_2} \vdots \underline{P}_{Q_3} \vdots \cdots\cdots \vdots \underline{P}_{Q_{3N-6}}\} \quad . \tag{2-17}$$

We can express the dipole moment derivatives in terms of symmetry coordinates by

$$\underline{P}_S = \underline{P}_Q \, \underline{L}^{-1} \text{ (charge)} \quad , \tag{2-18}$$

where $\underline{P}_S$ is a 3 x (3N - 6) matrix with elements of the form $\partial p_\tau / \partial S_j$. A typical element of $\underline{P}_S$ is given by

$$\begin{aligned} \underline{P}_{S(\tau,k)} = \partial p_\tau / \partial S_k &= \sum_{i=1}^{3N-6} \sigma_i (\partial p_\tau / \partial Q_i)(\partial Q_i / \partial S_k) \\ &= \sum_{i=1}^{3N-6} \sigma_i (\partial p_\tau / \partial Q_i) L^{-1}_{ik} \quad , \end{aligned} \tag{2-19}$$

where τ represents x, y, or z, and k = 1, 2, 3 ....3N - 6.

Transformation to dipole derivatives with respect to internal displacement coordinates is accomplished by the use of the transformation matrix $\underline{U}$.

$$\underline{P}_R = \underline{P}_S \, \underline{U} \quad . \tag{2-20}$$

$\underline{P}_R$ is a 3 x (3N - 6) matrix containing elements of the form $\partial p_\tau / \partial r_k$ and given by

$$\begin{aligned} \underline{P}_{R(\tau,k)} = \partial p_\tau / \partial r_k &= \sum_{j=1}^{3N-6} (\partial p_\tau / \partial S)_j (\partial S_j / \partial r_k) \\ &= \sum_{j=1}^{3N-6} \underline{P}_{S(\tau,j)} \, U_{jk} \quad . \end{aligned} \tag{2-21}$$

We should note that Equation 2-19 and 2-21 represent the reduction of the intensity data from the $\partial \vec{p} / \partial Q_i$'s that we

referred to in Chapter 1. The reduction of the data to $\partial\vec{p}/\partial S_j$'s (or $\partial\vec{p}/\partial R_k$'s) and their use for subsequent interpretation of the intensities has been discussed by Overend (3) and in the past, interpretation of infrared intensities has been based on $\underline{P}_S$ and/or on $\underline{P}_R$.

We can transform the $\underline{P}_R$ matrix to a 3 x 3N matrix containing the dipole moment derivatives with respect to molecule-fixed Cartesian displacement coordinates using the $\underline{B}$ matrix. This transformation is given by Equation 2-22:

$$\underline{V}_X = \underline{P}_R \, \underline{B}. \tag{2-22}$$

In general, we are more interested in the dipole moment change with respect to the space-fixed Cartesian coordinates and in order to transform to that coordinate system we must use the augmented $\underline{B}$ and $\underline{P}_\rho$ matrices as given by

$$\underline{P}_X = \left(\underline{P}_R \vdots \underline{P}_\rho \right) \left(\begin{array}{c} \cdots \\ \underline{B} \\ \cdots \\ \underline{\beta} \end{array} \right)$$

$$= \underline{P}_R \, \underline{B} + \underline{P}_\rho \, \underline{\beta} \quad . \tag{2-23}$$

Here $\underline{P}_\rho$ is a 3 x 6 matrix which gives the dipole moment change with respect to translations and rotations of the molecule. Since a translation of the molecule does not change the dipole moment, the translational terms in $\underline{P}_\rho$ are zero. Using the relationship described by Biarge, Herranz, and Morcillo (5) for computing $\partial\vec{p}/\partial\rho$, we find that the $\underline{P}_\rho$ matrix has the form

$$\underline{P}_{\rho} = \begin{pmatrix} 0 & 0 & 0 & 0 & p_z^0/I_y^{\frac{1}{2}} & -p_y^0/I_z^{\frac{1}{2}} \\ 0 & 0 & 0 & -p_z^0/I_x^{\frac{1}{2}} & 0 & p_x^0/I_z^{\frac{1}{2}} \\ 0 & 0 & 0 & p_y^0/I_x^{\frac{1}{2}} & -p_x^0/I_y^{\frac{1}{2}} & 0 \end{pmatrix} \qquad (2\text{-}24)$$

The quantities I_x, I_y, and I_z are the three principal moments of inertia assuming that x, y, and z are drawn to coincide with these principal axes, and p_x^0, p_y^0, and p_z^0 are the x, y, and z components of the permanent dipole moment. $\underline{P}_{\rho}\underline{\beta}$ constitutes the rotational correction to the dipole moment derivatives for the space-fixed coordinate frame (11). Notice that if the molecule contains no permanent dipole moment, $\underline{P}_{\rho}$ becomes the null matrix and no rotational correction is made.

A typical element of $\underline{P}_X$, $\partial p_\tau/\partial x_k$, is given by

$$\underline{P}_{X(\tau,k)} = \sum_{j=1}^{3N} (\partial p_\tau/\partial r_j)(\partial r_j/\partial x_k)$$

$$= \sum_{j=1}^{3N} P_{R(\tau,j)}\, b_{jk}\,; \; k = 1,2,3\ldots 3N \; . \qquad (2\text{-}25)$$

The $\underline{P}_X$ matrix can be partitioned into a set of N 3 x 3 matrices associated with each atom (designated by the superscript) so that

$$\underline{P}_X = \{\underline{P}_X^{(1)} \cdot \underline{P}_X^{(2)} \cdot \underline{P}_X^{(3)} \cdot \ldots\ldots \underline{P}_X^{(N)}\} \; . \qquad (2\text{-}26)$$

The submatrix, $\underline{P}_X^{(\alpha)}$, is the desired atomic polar tensor for

atom α and has the form

$$\underline{P}_X^{\alpha} = \begin{pmatrix} \partial p_x/\partial x_\alpha & \partial p_x/\partial y_\alpha & \partial p_x/\partial z_\alpha \\ \partial p_y/\partial x_\alpha & \partial p_y/\partial y_\alpha & \partial p_y/\partial z_\alpha \\ \partial p_z/\partial x_\alpha & \partial p_z/\partial y_\alpha & \partial p_z/\partial z_\alpha \end{pmatrix} . \qquad (2\text{-}27)$$

The rotational correction ($\underline{P}_\rho \ \underline{\beta}$) is not explicit in Equation 2-27 but is implied by our notation. In writing $\underline{P}_X^{\alpha}$ or $\underline{P}_X$ it is understood that we are referring to a space-fixed coordinate frame and the rotational corrections are implicitly included. Notice that the use of polar tensors carries the reduction of the data in the form of $\partial\vec{p}/\partial Q_i$ one step further than the traditional interpretation in terms of $\partial\vec{p}/\partial R_i$'s.

The inverse transformations from $\underline{P}_X$ to $\underline{P}_Q$ can be carried out by employing the inverse coordinate transformations given in the last section. Thus, $\underline{P}_R$ can be computed from $\underline{P}_X$ by right multiplying Equation 2-23 by the $\underline{A}$ matrix so that $(\underline{P}_R \ \underline{B} + \underline{P}_\rho \ \underline{\beta})\underline{A} = \underline{P}_X\underline{A}$. Notice that since $\underline{\beta} \ \underline{A} = 0$ (12) the rotational corrections drop out so that

$$\underline{P}_R = \underline{P}_X \ \underline{A} \ , \qquad (2\text{-}28)$$

and

$$\underline{P}_S = \underline{P}_R \ \underline{U}' \ . \qquad (2\text{-}29)$$

Finally, $\underline{P}_Q$ is given by

$$\underline{P}_Q = \underline{P}_S \ \underline{L} = \underline{P}_X \ \underline{A} \ \underline{U}' \underline{L} \ . \qquad (2\text{-}30)$$

In order to obtain meaningful atomic polar tensors we need accurate intensity measurements and a well defined force field; moreover, we need to know the signs (σ's) of the $\partial\vec{p}/\partial Q_i$'s. If the symmetry properties of the polar tensors are neglected and if rotational corrections are applied, there are $2^{(3N-6)}$ {or $2^{(3N-5)}$ if the direction of the permanent dipole moment is known} possible sign combinations possible for a set of (3N - 6) $\partial\vec{p}/\partial Q_i$'s. In reality, the symmetry properties of the tensors reduce this number considerably, as we shall demonstrate in the next chapter. In addition, other sets may be eliminated by use of Coriolis coupling data, intensities from isotopically substituted molecules, or chemical intuition (using the latter with a great deal of caution).

We alluded to the effective charge, ξ_α, for a given atom, α, in Chapter 1. In terms of the $\underline{P}_X^\alpha$ tensor, the effective charge is

$$\xi_\alpha = \{\mathrm{Tr}\ \underline{P}_X^\alpha\ (\underline{P}_X^\alpha)'\}^{\frac{1}{2}}\ , \qquad (2\text{-}31)$$

where Tr is the trace of the product matrix $\underline{P}_X^\alpha(\underline{P}_X^\alpha)'$ (12).

The associated vectors of the polar tensors, referred to earlier, are the dipole moment change vectors produced by a unit displacement of a given atom parallel to one of the Cartesian coordinate axes (x, y, or z). That is, they give the magnitude and direction of the dipole moment change produced by the motion of one atom in a single given direction. We shall denote these vectors by $(\Delta\vec{p})_\tau^\alpha$ where the superscript α indicates the atom and τ indicates the coordinate axis (x,

y, or z), along which atom α is moved. The $(\Delta\vec{p})^{\alpha}_{\tau}$ vectors are defined by

$$(\Delta\vec{p})^{\alpha}_{\tau} = \left(\begin{array}{l} (\partial p_x/\partial\tau)\ \hat{i},\hat{i} \\ (\partial p_y/\partial\tau)\ \hat{j},\hat{j} \\ (\partial p_z/\partial\tau)\ \hat{k},\hat{k} \end{array} \right) \cdot \hat{\tau}\ (\delta\tau) \ . \qquad (2\text{-}32)$$

τ = x, y, or z

The quantity in brackets is just the τth column of the αth tensor, and $\hat{i}$, $\hat{j}$, $\hat{k}$ are the unit vectors parallel to the x, y, or z coordinate axes, respectively. The quantity $\hat{\tau}$ takes on the values of $\hat{i}$, $\hat{j}$, or $\hat{k}$ depending on the axis under consideration and $(\delta\tau)$ is a unit displacement parallel to the τth axis. These vectors are shown in plots given in Chapter 4 for the methyl halides, and their direction and magnitude form a useful pictorial representation of the atomic polar tensors.

Another useful property of the polar tensors derived by Biarge, Herranz, and Morcillo (5) is

$$\sum_{\alpha} \underline{P}^{\alpha}_{X} = 0. \qquad (2\text{-}33)$$

Here $\underline{P}^{\alpha}_{X}$ is the polar tensor for the αth atom in the space-fixed coordinate frame (rotationally corrected polar tensor). This relationship is particularly useful since it shows that there are only N - 1 independent tensors (N is the total number of atoms in the molecule). For additional properties

and relationships of the polar tensors, the reader is referred to the papers by Biarge, Herranz, and Morcillo (5), or to Person and Newton (12).

Morcillo (5) has discussed the fact that if the bond moment hypothesis were true one would expect the polar tensors to be diagonal. That is

$$\underset{\sim}{P}_X^{\alpha} = \begin{pmatrix} \partial\vec{p}/\partial x_\alpha & 0 & 0 \\ 0 & \partial\vec{p}/\partial y_\alpha & 0 \\ 0 & 0 & \partial\vec{p}/\partial z_\alpha \end{pmatrix} ,$$

and the dipole moment changes would only be induced parallel to the direction of motion. As a consequence, if off-diagonal non-zero elements appear, they should be a reflection of the error involved in the bond moment hypothesis and, as we shall show in Chapter 4, this "error" seems to be quite sensitive to the polarizability of adjacent substituents and the resulting induced dipole moments.

Signs of $\partial\vec{p}/\partial Q_i$'s

At this point we must interject a word of warning concerning the arbitrary nature of the signs of the $\partial\vec{p}/\partial Q_i$'s. To illustrate this point, consider a triatomic molecule XY_2 of C_{2v} symmetry with internal displacement coordinates, r_1, r_2, and α, and a permanent dipole moment $\vec{p}^0$ as shown in Figure 2-1(a). We can construct two symmetry displacement coordinates, S_1 and S_2, corresponding to the totally symmetric vibrational modes. Two ways of constructing these symmetry coordinates (differing only in relative phase) are shown in

Figures 2-1(b) and 2-1(c). Either way of defining the symmetry coordinates is acceptable since the only criterion for these coordinates is that they transform according to the totally symmetric representation of the C_{2v} point group. Now assume that a normal coordinate, Q_i, exists that is composed of a certain percentage of S_1 and S_2 (the percentage contributions are unimportant here). Associated with the normal coordinate is a dipole moment change $\Delta\vec{p}$. The Q_i may be a linear combination of S_1^b and S_2^b, as shown in Figure 2-1(d). However, an equivalent statement of Q_i is shown in Figure 2-1(e) as a linear combination of S_1^c and S_2^c. Assuming that we know the direction of the equilibrium dipole moment as indicated, then the sense of $\partial\vec{p}/\partial Q_i$ is negative in Figure 2-1(e) if Q_i is positive in that figure; and the sense of $\partial\vec{p}/\partial Q_i$ is positive in Figure 2-1(d) if Q_i is positive in that figure. The problem is, how do we know whether Q_i is "positive" or "negative" since both representations of Q_i are equivalent except for a phase difference? There is no a priori reason to choose Figure 2-1(b) or Figure 2-1(c) as the "positive" displacement, but it is obvious that the resulting sign of $\partial\vec{p}/\partial Q_i$ will depend on just that choice. In reality, we are not at liberty to choose 2-1(b) or 2-1(c) as positive; the choice is made for us by the coordinate definitions and the resulting L matrix from the normal coordinate analysis. If indeed there is any meaning to the sign of $\partial\vec{p}/\partial Q_i$, it is only within the context of the particular coordinate definitions and that particular L matrix from the normal coordinate calcula-

Figure 2-1: Schematic diagram of two ways to define totally symmetric symmetry coordinates of an XY_2 molecule.

(a) Equilibrium configuration.

(b) and (c) Two definitions of the totally symmetric vibrations differing only in phase.

(d) and (e) The resulting two definitions of the normal coordinate.

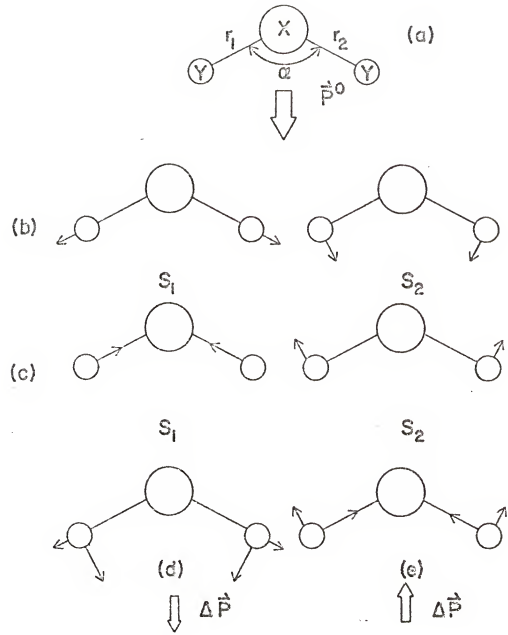
X
Y
Y
r_1
r_2
α
$\vec{P}^o$
(a)
(b)
S_1
S_2
(c)
S_1
S_2
(d)
(e)
$\Delta\vec{P}$
$\Delta\vec{P}$

tion. As a consequence of all this, if one speaks of the sign of a dipole moment derivative with respect to any set of coordinates ($\underline{X}$, $\underline{R}$, $\underline{S}$, or $\underline{Q}$), one cannot interpret the results unless the following definitions are known:

(1) the normal coordinate transformation matrix $\underline{L}$ or $\underline{L}^{-1}$,

(2) unambiguous definitions of the internal coordinates $\underline{R}$ and $\underline{S}$,

and (3) an unambiguous definition of the Cartesian coordinate axis and the direction of the dipole moment.

It is unfortunate that in many papers published on normal coordinate analyses, insufficient information is given on the actual coordinate definitions used. This means that one should be very cautious in using another's published normal coordinates for calculating dipole moment derivatives. In order to insure consistency in coordinate definitions, it is advisable for one person to do both the normal coordinate calculation and the dipole moment derivative calculation.

In addition, one must also be aware of the difficulties that may arise due to the arbitrary signs of the eigenvectors of $\underline{GF}$ (the columns of $\underline{L}$), particularly when comparisons are made between independent workers. These signs are quite arbitrary and depend on the diagonalization and normalization routines used in the normal coordinate analysis. As a consequence, even if two independent workers use identical coordinate definitions in the normal coordinate analysis, they may obtain an apparent inconsistency in the signs of the $\underline{GF}$ eigen-

vector when their results are compared. For example, we have found in this laboratory that we obtain different signs for the columns of $\underline{L}$ for the B_1 and B_2 symmetry blocks of F_2CO when we use two different normal coordinate analysis computer programs {program CHARLY from the University of Minnesota (19), and Schachtschneider's program GVIB (29)}, even though the input for each program was identical. This fact probably contributed to some of the difficulties encountered by McKean, Bruns, Person, and Segal (30) in their paper on F_2CO.

In order for the reader not to be misled, it is important to realize that the sign of Q_i or $\partial\vec{p}/\partial Q_i$ in itself is not important; what is important is the actual direction of the displacements associated with a given Q_i. This can be determined only in light of the previous history of the coordinate definitions used to define Q_i. In the next chapter, we shall dwell at length on the signs of dipole moment derivatives but keep in mind that the signs have meaning only with reference to the defined coordinate axis, the internal coordinate definitions, and $\underline{L}$.

CHAPTER 3

POLAR TENSORS FOR THE METHYL HALIDES

Introduction

In this chapter we present the atomic polar tensors for the hydrogen, carbon, and halogen atoms derived from the experimental intensity data for CH_3X and CD_3X molecules (X = F, Br, Cl, I) for all the possible choices for the signs of the $\partial\vec{p}/\partial Q_i$'s, together with the polar tensors for CH_3F and CH_3Cl calculated by the CNDO/2 method. We then extend the error propagation treatment given by RNO (18) to the polar tensors and follow by a discussion of our best estimate of the signs of the $\partial\vec{p}/\partial Q_i$'s.

We shall restrict our attention exclusively to the rotationally corrected tensors $\underline{P}_X^\alpha$ since, as Crawford has explained (11), rotational corrections are required before comparisons can be made between such intensity parameters ($\underline{P}_X^\alpha$, or $\partial\vec{p}/\partial R_j$'s) from different isotopically substituted molecules. Our neglect of the non-rotationally corrected tensors ($\underline{V}^\alpha$) is not meant to imply that the $\underline{V}^\alpha$'s are not useful for interpretative purposes. It is just that we wish to use the isotopic invariance to help in the determination of the correct signs of the $\partial\vec{p}/\partial Q_i$'s. We also neglect the $\underline{P}_S$ tensors ($\partial\vec{p}/\partial S_j$'s) since RNO have dealt with them in

detail (18). However, both the $\underline{V}^{\alpha}$ and $\underline{P}_S$ tensors for the methyl halide series have been computed but are not reported in this thesis.

In order to insure consistency in the definition of coordinates, we repeated the normal coordinate analyses for the entire CH_3X and CD_3X series using the more recent, and apparently more well defined, force field of Duncan (20). A complete summary of the results from the normal coordinate analyses is given in Appendix I.

Calculation of the Polar Tensors from Experimental Data

The integrated infrared band intensities for all the CH_3X and CD_3X molecules were taken from the summary of RNO (18) and the corresponding values of $|\partial\vec{p}/\partial Q_i|$'s, calculated by Equation 1-4, are given in Table 3-1. The $\underline{P}_S$ tensors are calculated from Table 3-1 and Equation 2-18, using the $\underline{L}^{-1}$ matrix given in Table AI-1 in Appendix I. From these, $\underline{V}_X$ is calculated using Equation 2-12. Applying the rotational corrections to $\underline{V}_X$ as shown in Equation 2-23, we calculated the $\underline{P}_X^{\alpha}$ tensors as shown in Equation 2-26. The data required for the calculation of the rotational corrections are given in Tables 3-2 and 3-3, and a diagram of the Cartesian coordinate axis used in the calculation of $\underline{P}_X$ is given in Figure 3-1. The permanent dipole moment is shown as a vector defined to be positive when it is pointing from - to +, parallel to the C-X bond axis, as shown. The calculation of $\underline{P}_X$ from $\underline{P}_Q$ was carried out in one calculation on the computer, using the program PVDTEN described in Appendix II.

TABLE 3-1

ABSOLUTE VALUES OF $\partial\vec{p}/\partial Q_i$'S FOR THE METHYL HALIDES[a]
(The Units Are $D\text{Å}^{-1}$ $amu^{\frac{1}{2}}$)

Mode \ Molecule	CH_3F	CD_3F	CH_3Cl	CD_3Cl	CH_3Br	CD_3Br	CH_3I	CD_3I
ν_1 (z)[b]	0.7643 (±.1718)[c]	0.7238 (±.0353)	0.7135 (±.0117)	0.5087 (±.0147)	0.6563 (±.0304)	0.5124 (±.0126)	0.5474 (±.0319)	0.4243 (±.0105)
ν_2 (z)	0.1454 (±.1119)	0.9974 (±.0488)	0.4008 (±.0140)	0.5080 (±.0248)	0.5741 (±.0105)	0.5202 (±.0105)	0.6985 (±.0160)	0.3317 (±.0145)
ν_3 (z)	1.4977 (±.0731)	1.3227 (±.0646)	0.7404 (±.0074)	0.6081 (±.0150)	0.4517 (±.0142)	0.4005 (±.0099)	0.2136 (±.0021)	0.1530 (±.0038)
ν_4 (x,y)	0.8490 (±.0707)	0.6835 (±.0337)	0.3381 (±.0096)	0.2493 (±.0062)	0.2324 (±.0037)	0.1622 (±.0040)	0.1596 (±.0050)	0.0912 (±.0044)

Continued on next page

(Table 3-1 continued)

Mode \ Molecule	CH_3F	CD_3F	CH_3Cl	CD_3Cl	CH_3Br	CD_3Br	CH_3I	CD_3I
ν_5 (x,y)	0.3202 (±.0367)	0.2383 (±.0987)	0.3810 (±.0073)	0.2881 (±.0186)	0.3760 (±.0027)	0.2912 (±.0093)	0.3532 (±.0054)	0.2738 (±.0068)
ν_6 (x,y)	0.1758 (±.0281)	0.0655 (±.0271)	0.2181 (±.0022)	0.1146 (±.0257)	0.2876 (±.0029)	0.1551 (±.0038)	0.3248 (±.0042)	0.1950 (±.0048)

a. Taken from Reference 18.
b. The normal vibration; the symbol in parentheses identifies the non-zero component of $\vec{p}$.
c. The errors reported in parentheses were calculated from the dispersions given in Reference 18. The four significant figures reported for the $\partial\vec{p}/\partial Q_i$'s are not indicative of the precision of the experimental measurements, as the errors show, but were used for computational consistency.

TABLE 3-2

CENTER OF MASS CARTESIAN COORDINATES[a] OF THE METHYL HALIDES (UNITS ARE Å)

	Atom #[b]	$x^{(e)}$	$y^{(e)}$	$z^{(e)}$
	1	0.000000	0.000000	-0.740982
	2	0.000000	0.000000	0.641018
CH_3F	3	-1.038888	0.000000	-1.087010
	4	0.519444	-0.899703	-1.087010
	5	0.519444	0.899703	-1.087010
	1	0.000000	0.000000	-0.652389
	2	0.000000	0.000000	0.729611
CD_3F	3	-1.038886	0.000000	-0.998420
	4	0.519444	-0.899703	-0.998420
	5	0.519444	0.899703	-0.998420
	1	0.000000	0.000000	-1.223346
	2	0.000000	0.000000	0.554654
CH_3Cl	3	-1.030521	0.000000	-1.559617
	4	0.515262	-0.892459	-1.559617
	5	0.515262	0.892459	-1.559617

Continued to next page

(Table 3-2 continued)

	Atom # [b]	x [(e)]	y [(e)]	z [(e)]
	1	0.000000	0.000000	-1.134529
	2	0.000000	0.000000	0.643471
CD_3Cl	3	-1.030521	0.000000	-1.470800
	4	0.515262	-0.892459	-1.470800
	5	0.515262	0.892459	-1.470800
	1	0.000000	0.000000	-1.615035
	2	0.000000	0.000000	0.319946
CH_3Br	3	-1.033611	0.000000	-1.941685
	4	0.516807	-0.895135	-1.941685
	5	0.516807	0.895135	-1.941685
	1	0.000000	0.000000	-1.554581
	2	0.000000	0.000000	0.380419
CD_3Br	3	-1.033611	0.000000	-1.881230
	4	0.516807	-0.895135	-1.881230
	5	0.516807	0.895135	-1.881230
	1	0.000000	0.000000	-1.903073
	2	0.000000	0.000000	0.232926
CH_3I	3	-1.034705	0.000000	-2.222871
	4	0.517353	-0.896082	-2.222871
	5	0.517353	0.896082	-2.222871

Continued to next page

(Table 3-2 continued)

	Atom # [b]	x (e)	y (e)	z (e)
	1	0.000000	0.000000	-1.856776
	2	0.000000	0.000000	0.279223
CD_3I	3	-1.034705	0.000000	-2.176575
	4	0.517353	-0.896082	-2.176575
	5	0.517353	0.896082	-2.176575

a. Calculated by program CART (J.H. Schachtschneider, "Vibrational Analysis of Polyatomic Molecules." V. Technical Report No. 231-64, Shell Development Co., Emeryville, California (1964), pp. 3-11). The center of mass for the isotopically substituted CH_3X molecules will shift on the z axis due to the difference in the masses of H and D.

b. Atom # refers to the atom sequence in Figure 3-1, as defined in Figure AI-1.

TABLE 3-3

PERMANENT DIPOLE MOMENTS AND PRINCIPAL MOMENTS OF INERTIA FOR THE METHYL HALIDES[a]

	$\lvert p^0 \rvert$ (D)[b]	$I_x = I_y$ amu(Å)^2	I_z amu(Å)^2
CH_3F	-1.855	19.599258	3.263191
CD_3F		24.504700	6.521367
CH_3Cl	-1.94	37.676437	3.210854
CD_3Cl		46.204346	6.416778
CH_3Br	-1.79	52.393448	3.230138
CD_3Br		65.033096	6.455317
CH_3I	-1.64	66.903107	3.236977
CD_3I		83.124970	6.468984

a. Since $\vec{p}^0$ is parallel to the z axis, only $\vec{p}_z^0$ is non-zero and $\vec{p}^0 = \vec{p}_z^0$.
b. Permanent dipole moments (in Debyes) were taken from R.D. Nelson, Jr., D.R. Lide, Jr., and A.A. Maryott, "Selected Values of Electric Dipole Moments for Molecules in the Gas Phase," NSRDS-NBS 10, National Bureau of Standards, Washington, D.C., 1967; and the principal moments of inertia were calculated by program CART (see reference at the bottom of Table 3-2), based on the center of mass Cartesian coordinates given in Table 3-2.

Figure 3-1: Definition of the coordinate axis used for the calculation of the polar tensors.

Atom 1 is carbon, atom 2 is halogen, and atoms 3, 4, and 5 are hydrogens. (See Figure AI-1.)

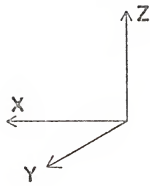
Z
X
Y

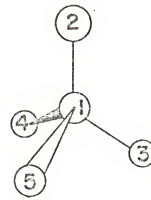
2
1
4
3
5

In general there are 2^9 possible sign combinations for the $\partial\vec{p}/\partial Q_i$'s for each methyl halide (if there were no constraints). However, since the $(\partial\vec{p}/\partial Q_i)_x$'s and $(\partial\vec{p}/\partial Q_i)_y$'s belong to the degenerate E class, the sign combination for these two rows must be identical. This reduced the total possible number of sign combinations to 2^6. In addition, for CH_3F and CD_3Cl, DiLauro and Mills (15) have shown that the signs of the $\partial\vec{p}/\partial Q_i$'s for ν_2 and ν_4 , as well as ν_3 and ν_6 , must be the same. This reduced the total number of possible sign combinations to 2^4. Although there are no experimental Coriolis data to indicate the relative signs for CH_3Br or CH_3I, we shall show later in this chapter that it is reasonable that the same relative signs are correct for them.

The experimental polar tensors for the CH_3X and CD_3X molecules are given in Tables 3-4 to 3-11 for all possible choices for the signs of the $\partial\vec{p}/\partial Q_i$'s consistent with the Coriolis data. The signs in the first column of the tables are arranged in order of the symmetry blocks. The first row of signs represent the chosen signs of the three $\partial\vec{p}/\partial Q_i$'s for the E_x degenerate vibrations; the second row of signs represent the chosen signs of the three $\partial\vec{p}/\partial Q_i$'s for the E_y degenerate vibrations; and the third row of signs is the sign choice for the three $\partial\vec{p}/\partial Q_i$'s of the $A_{1,z}$ vibrations. The sets of signs listed in the tables and identified by the letters (A-H) correspond to the signs in the order given below:

(turn to page 74)

TABLE 3-4

ATOMIC POLAR TENSORS FOR CH_3F

(Units are $D/\AA$)

Sign Set	Signs		P_x^H			P_x^F			P_x^C		
	---	E_x	0.660	0.000	0.327	-1.357	0.000	0.000	-0.066	0.000	0.000
A	---	E_y	0.000	0.289	0.000	0.000	-1.357	0.000	0.000	-0.066	0.000
	---	A_{1z}	0.475	0.000	0.286	0.000	0.000	-4.273	0.000	0.000	3.414
	+--	E_x	-0.591	0.000	-0.100	-1.335	0.000	0.000	1.758	0.000	0.000
B	+--	E_y	0.000	0.309	0.000	0.000	-1.335	0.000	0.000	1.758	0.000
	+--	A_{1z}	-0.326	0.000	-0.057	0.000	0.000	-4.202	0.000	0.000	4.373
	-+-	E_x	0.755	0.000	0.144	-1.288	0.000	0.000	0.423	0.000	0.000
C	-+-	E_y	0.000	-0.179	0.000	0.000	-1.298	0.000	0.000	0.423	0.000
	-+-	A_{1z}	0.404	0.000	0.429	0.000	0.000	-4.390	0.000	0.000	3.103

Continued on next page

(Table 3-4 continued)

Sign Set	Signs		p_x^H			p_x^F			p_x^C		
	--+	E_x	0.703	0.000	0.087	-1.039	0.000	0.000	-0.564	0.000	0.000
D	--+	E_y	0.000	0.365	0.000	0.000	-1.039	0.000	0.000	-0.564	0.000
	--+	A_{lz}	0.397	0.000	-0.086	0.000	0.000	4.319	0.000	0.000	-4.062
	+++	E_x	-0.452	0.000	-0.527	-0.949	0.000	0.000	1.749	0.000	0.000
E	+++	E_y	0.000	-0.081	0.000	0.000	-0.949	0.000	0.000	1.749	0.000
	+++	A_{lz}	-0.475	0.000	-0.286	0.000	0.000	4.273	0.000	0.000	-3.414
	-++	E_x	0.799	0.000	-0.098	-0.971	0.000	0.000	-0.075	0.000	0.000
F	-++	E_y	0.000	-0.102	0.000	0.000	-0.971	0.000	0.000	-0.075	0.000
	-++	A_{lz}	0.326	0.000	0.057	0.000	0.000	4.202	0.000	0.000	-4.373
	+-+	E_x	-0.548	0.000	-0.342	-1.017	0.000	0.000	1.260	0.000	0.000
G	+-+	E_y	0.000	0.386	0.000	0.000	-1.017	0.000	0.000	1.260	0.000
	+-+	A_{lz}	-0.404	0.000	-0.429	0.000	0.000	4.390	0.000	0.000	-3.103

Continued on next page

(Table 3-4 continued)

Sign Set	Signs		P_x^H			P_x^F			P_x^C		
	++-	E_x	-0.496	0.000	-0.286	-1.266	0.000	0.000	2.247	0.000	0.000
H	++-	E_y	0.000	-0.158	0.000	0.000	-1.266	0.000	0.000	2.247	0.000
	++-	A_{lz}	-0.397	0.000	0.086	0.000	0.000	-4.319	0.000	0.000	4.062
ERRORS		E_x	0.074	0.000	0.030	0.020	0.000	0.000	0.119	0.000	0.000
		E_y	0.000	0.025	0.000	0.000	0.020	0.000	0.000	0.119	0.000
		A_{lz}	0.136	0.000	0.095	0.000	0.000	0.388	0.000	0.000	0.481
CNDO		E_x	-0.57	0.00	-0.03	-1.41	0.00	0.00	2.19	0.00	0.00
		E_y	0.00	0.04	0.00	0.00	-1.41	0.00	0.00	2.19	0.00
		A_{lz}	-0.22	0.00	-0.13	0.00	0.00	-2.53	0.00	0.00	2.91
ROTATIONAL CORRECTIONS		E_x	0.104	0.000	-0.099	-1.153	0.000	0.000	0.842	0.000	0.000
		E_y	0.000	0.104	0.000	0.000	-1.153	0.000	0.000	0.842	0.000
		A_{lz}	0.000	0.000	0.000	0.000	0.000	0.000	0.000	0.000	0.000

TABLE 3-5

ATOMIC POLAR TENSORS FOR CD_3F

(Units are D/Å)

Sign Set	Signs		P_x^D			P_x^F			P_x^C		
	---	E_x	0.7573	0.000	0.1778	-1.1074	0.000	0.000	-0.6314	0.000	0.000
A	---	E_y	0.000	0.4018	0.000	0.000	-1.1074	0.000	0.000	-0.6314	0.000
	---	A_{lz}	0.7333	0.000	0.4488	0.000	0.000	-4.7634	0.000	0.000	3.4171
	+--	E_x	-0.597	0.000	-0.271	-1.114	0.000	0.000	1.423	0.000	0.000
B	+--	E_y	0.000	0.391	0.000	0.000	-1.114	0.000	0.000	1.423	0.000
	+--	A_{lz}	-0.307	0.000	-0.015	0.000	0.000	-4.768	0.000	0.000	4.813
	-+-	E_x	0.889	0.000	0.087	-1.140	0.000	0.000	-0.057	0.000	0.000
C	-+-	E_y	0.000	-0.091	0.000	0.000	-1.140	0.000	0.000	-0.097	0.000
	-+-	A_{lz}	-0.013	0.000	1.351	0.000	0.000	-2.883	0.000	0.000	-1.168

Continued on next page

(Table 3-5 continued)

Sign Set	Signs		p_x^D			p_x^F			p_x^C		
	--+	E_x	0.770	0.000	0.045	-0.951	0.000	0.000	-0.812	0.000	0.000
D	--+	E_y	0.000	0.406	0.000	0.000	-0.951	0.000	0.000	-0.812	0.000
	--+	A_{lz}	1.054	0.000	-0.887	0.000	0.000	2.888	0.000	0.000	-0.228
	+++	E_x	-0.453	0.000	-0.495	-0.991	0.000	0.000	1.817	0.000	0.000
E	+++	E_y	0.000	-0.097	0.000	0.000	-0.991	0.000	0.000	1.817	0.000
	+++	A_{lz}	-0.733	0.000	-0.449	0.000	0.000	4.763	0.000	0.000	-3.417
	-++	E_x	0.902	0.000	-0.046	-0.985	0.000	0.000	-0.238	0.000	0.000
F	-++	E_y	0.000	-0.087	0.000	0.000	-0.985	0.000	0.000	-0.238	0.000
	-++	A_{lz}	0.307	0.000	0.015	0.000	0.000	4.768	0.000	0.000	-4.813
	+-+	E_x	-0.584	0.000	-0.403	-0.958	0.000	0.000	1.242	0.000	0.000
G	+-+	E_y	0.000	0.395	0.000	0.000	-0.958	0.000	0.000	1.242	0.000
	+-+	A_{lz}	0.013	0.000	-1.351	0.000	0.000	2.883	0.000	0.000	1.168

Continued on next page

(Table 3-5 continued)

Sign Set	Signs		p_x^D			p_x^F			p_x^C		
	++-	E_x	-0.466	0.000	-0.362	-1.147	0.000	0.000	1.997	0.000	0.000
H	++-	E_y	0.000	-0.101	0.000	0.000	-1.147	0.000	0.000	1.997	0.000
	++-	A_{lz}	-1.053	0.000	0.887	0.000	0.000	-2.888	0.000	0.000	0.228
ERRORS		E_x	0.044	0.000	0.032	0.015	0.000	0.000	0.134	0.000	0.000
		E_y	0.000	0.085	0.000	0.000	0.015	0.000	0.000	0.134	0.000
		A_{lz}	0.043	0.000	0.071	0.000	0.000	0.325	0.000	0.000	0.390
ROTATIONAL CORRECTIONS		E_x	0.152	0.000	-0.158	-1.049	0.000	0.000	0.593	0.000	0.000
		E_y	0.000	0.152	0.000	0.000	-1.049	0.000	0.000	0.593	0.000
		A_{lz}	0.000	0.000	0.000	0.000	0.000	0.000	0.000	0.000	0.000

TABLE 3-6

ATOMIC POLAR TENSORS FOR CH_3Cl

(Units are D/Å)

Sign Set	Signs		P_x^H			P_x^{Cl}			P_x^C		
	---	E_x	0.249	0.000	0.298	-1.195	0.000	0.000	0.379	0.000	0.000
A	---	E_y	0.000	0.296	0.000	0.000	-1.195	0.000	0.000	0.379	0.000
	---	A_{1z}	0.484	0.000	0.040	0.000	0.000	-2.237	0.000	0.000	2.117
	+--	E_x	-0.252	0.000	0.138	-1.196	0.000	0.000	1.117	0.000	0.000
B	+--	E_y	0.000	0.305	0.000	0.000	-1.196	0.000	0.000	1.117	0.000
	+--	A_{1z}	-0.293	0.000	-0.215	0.000	0.000	-2.219	0.000	0.000	2.364
	-+-	E_x	0.361	0.000	0.060	-1.113	0.000	0.000	0.954	0.000	0.000
C	-+-	E_y	0.000	-0.254	0.000	0.000	-1.113	0.000	0.000	0.954	0.000
	-+-	A_{1z}	0.325	0.000	0.448	0.000	0.000	-2.547	0.000	0.000	1.203

Continued on next page

(Table 3-6 continued)

Sign Set	Signs		P_x^H			P_x^{Cl}			P_x^C		
	--+	E_x	0.302	0.000	-0.008	-0.883	0.000	0.000	-0.180	0.000	0.000
D	--+	E_y	0.000	0.406	0.000	0.000	-0.883	0.000	0.000	-0.180	0.000
	--+	A_{lz}	0.452	0.000	-0.193	0.000	0.000	2.529	0.000	0.000	-0.950
	+++	E_x	-0.087	0.000	-0.405	-0.802	0.000	0.000	1.133	0.000	0.000
E	+++	E_y	0.000	-0.134	0.000	0.000	-0.802	0.000	0.000	1.133	0.000
	+++	A_{lz}	-0.484	0.000	-0.040	0.000	0.000	2.237	0.000	0.000	-2.117
	-++	E_x	0.414	0.000	-0.245	-0.801	0.000	0.000	0.395	0.000	0.000
F	-++	E_y	0.000	-0.144	0.000	0.000	-0.801	0.000	0.000	0.395	0.000
	-++	A_{lz}	0.293	0.000	0.215	0.000	0.000	2.219	0.000	0.000	-2.864
	+-+	E_x	-0.199	0.000	-0.167	-0.884	0.000	0.000	0.558	0.000	0.000
G	+-+	E_y	0.000	0.416	0.000	0.000	-0.884	0.000	0.000	0.558	0.000
	+-+	A_{lz}	-0.325	0.000	-0.448	0.000	0.000	2.547	0.000	0.000	-1.204

Continued on next page

(Table 3-6 continued)

Sign Set	Signs		P_x^H			P_x^{Cl}			P_x^C		
	++-	E_x	-0.140	0.000	-0.099	-1.114	0.000	0.000	1.692	0.000	0.000
H	++-	E_y	0.000	-0.245	0.000	0.000	-1.114	0.000	0.000	1.692	0.000
	++-	A_{lz}	-0.452	0.000	0.193	0.000	0.000	-2.529	0.000	0.000	1.950
		E_x	0.008	0.000	0.010	0.009	0.000	0.000	0.118	0.000	0.000
ERRORS		E_y	0.000	0.006	0.000	0.000	0.009	0.000	0.000	0.118	0.000
		A_{lz}	0.010	0.000	0.008	0.000	0.000	0.086	0.000	0.000	0.481
CNDO		E_x	-0.100	0.000	-0.037	0.193	0.000	0.000	0.298	0.000	0.000
		E_y	0.000	0.037	0.000	0.000	0.193	0.000	0.000	0.289	0.000
		A_{lz}	-0.056	0.000	-0.058	0.000	0.000	0.102	0.000	0.000	0.071
ROTATIONAL CORRECTIONS		E_x	0.081	0.000	-0.054	-0.999	0.000	0.000	0.756	0.000	0.000
		E_y	0.000	0.081	0.000	0.000	-0.999	0.000	0.000	0.756	0.000
		A_{lz}	0.000	0.000	0.000	0.000	0.000	0.000	0.000	0.000	0.000

TABLE 3-7

ATOMIC POLAR TENSORS FOR CD_3Cl

(Units are D/Å)

Sign Set	Signs		P_x^D			P_x^{Cl}			P_x^C		
	---	E_x	0.282	0.000	0.203	-1.076	0.000	0.000	0.060	0.000	0.000
A	---	E_y	0.000	0.395	0.000	0.000	-1.076	0.000	0.000	0.060	0.000
	---	A_{1z}	0.618	0.000	0.065	0.000	0.000	-2.061	0.000	0.000	1.865
	+--	E_x	-0.214	0.000	0.048	-1.082	0.000	0.000	0.811	0.000	0.000
B	+--	E_y	0.000	0.394	0.000	0.000	-1.082	0.000	0.000	0.811	0.000
	+--	A_{1z}	-0.287	0.000	-0.243	0.000	0.000	-2.072	0.000	0.000	2.780
	-+-	E_x	0.444	0.000	0.012	-1.030	0.000	0.000	0.651	0.000	0.000
C	-+-	E_y	0.000	0.191	0.000	0.000	-1.030	0.000	0.000	0.651	0.000
	-+-	A_{1z}	0.296	0.000	0.698	0.000	0.000	-2.123	0.000	0.000	0.028

Continued on next page

(Table 3-7 continued)

Sign Set	Signs		P_x^D			P_x^{Cl}			P_x^C		
	--+	E_x	0.301	0.000	-0.030	-0.854	0.000	0.000	-0.260	0.000	0.000
D	--+	E_y	0.000	0.441	0.000	0.000	-0.854	0.000	0.000	-0.260	0.000
	--+	A_{lz}	0.609	0.000	-0.391	0.000	0.000	2.134	0.000	0.0-0	-0.963
	+++	E_x	-0.034	0.000	-0.378	-0.813	0.000	0.000	1.083	0.000	0.000
E	+++	E_y	0.000	-0.146	0.000	0.000	-0.813	0.000	0.000	1.083	0.000
	+++	A_{lz}	-0.618	0.000	-0.065	0.000	0.000	2.061	0.000	0.000	-1.805
	-++	E_x	0.463	0.000	-0.222	-0.808	0.000	0.000	0.332	0.000	0.000
F	-++	E_y	0.000	-0.145	0.000	0.000	-0.808	0.000	0.000	0.332	0.000
	-++	A_{lz}	0.287	0.000	0.243	0.000	0.000	2.072	0.000	0.000	-2.800
	+-+	E_x	-0.195	0.000	-0.186	-0.860	0.000	0.000	0.491	0.000	0.000
G	+-+	E_y	0.000	0.440	0.000	0.000	-0.860	0.000	0.000	0.491	0.000
	+-+	A_{lz}	-0.296	0.000	-0.698	0.000	0.000	2.123	0.000	0.000	-0.028

Continued on next page

(Table 3-7 continued)

Sign Set	Signs		P_x^D			P_x^{Cl}			P_x^C		
	++-	E_x	-0.053	0.000	-0.144	-1.036	0.000	0.000	1.403	0.000	0.000
H	++-	E_y	0.000	-0.192	0.000	0.000	-1.036	0.000	0.000	1.403	0.000
	++-	A_{lz}	-0.609	0.000	0.391	0.000	0.000	-2.134	0.000	0.000	0.903
ERRORS		E_x	0.008	0.000	0.015	0.014	0.000	0.000	0.031	0.000	0.000
		E_y	0.000	0.015	0.000	0.000	0.014	0.000	0.000	0.031	0.000
		A_{lz}	0.015	0.000	0.020	0.000	0.000	0.063	0.000	0.000	0.088
ROTATIONAL CORRECTIONS		E_x	0.124	0.000	-0.087	-0.945	0.000	0.000	0.571	0.000	0.000
		E_y	0.000	0.124	0.000	0.000	-0.945	0.000	0.000	0.571	0.000
		A_{lz}	0.000	0.000	0.000	0.000	0.000	0.000	0.000	0.000	0.000

TABLE 3-8

ATOMIC POLAR TENSORS FOR CH_3Br

(Units are D/Å)

Sign Set	Signs		P_x^H			P_x^{Br}			P_x^C		
	---	E_x	0.150	0.000	0.332	-1.084	0.000	0.000	0.451	0.000	0.000
A	---	E_y	0.000	0.272	0.000	0.000	-1.084	0.000	0.000	0.451	0.000
	---	A_{lz}	0.474	0.000	-0.100	0.000	0.000	-1.396	0.000	0.000	1.696
	+--	E_x	-0.195	0.000	0.224	-1.083	0.000	0.000	0.956	0.000	0.000
B	+--	E_y	0.000	0.280	0.000	0.000	-1.083	0.000	0.000	0.956	0.000
	+--	A_{lz}	-0.246	0.000	-0.318	0.000	0.000	-1.388	0.000	0.000	2.343
	-+-	E_x	0.253	0.000	0.118	-1.026	0.000	0.000	1.064	0.000	0.000
C	-+-	E_y	0.000	-0.278	0.000	0.000	-1.026	0.000	0.000	1.064	0.000
	-+-	A_{lz}	0.262	0.000	0.488	0.000	0.000	-1.806	0.000	0.000	0.342

Continued on next page

(Table 3-8 continued)

Sign Set	Signs		P_x^H			P_x^{Br}			P_x^C		
	--+	E_x	0.226	0.000	-0.082	-0.700	0.000	0.000	-0.243	0.000	0.000
D	--+	E_y	0.000	0.404	0.000	0.000	-0.700	0.000	0.000	-0.243	0.000
	--+	A_{lz}	0.458	0.000	-0.270	0.000	0.000	1.798	0.000	0.000	-0.989
	+++	E_x	-0.016	0.000	-0.403	-0.641	0.000	0.000	0.873	0.000	0.000
E	+++	E_y	0.000	-0.138	0.000	0.000	-0.641	0.000	0.000	0.873	0.000
	+++	A_{lz}	-0.474	0.000	0.100	0.000	0.000	1.396	0.000	0.000	-1.696
	-++	E_x	0.329	0.000	-0.245	-0.642	0.000	0.000	0.369	0.000	0.000
F	-++	E_y	0.000	-0.147	0.000	0.000	-0.642	0.000	0.000	0.369	0.000
	-++	A_{lz}	0.246	0.000	0.318	0.000	0.000	1.388	0.000	0.000	-2.343
	+-+	E_x	-0.120	0.000	-0.190	-0.699	0.000	0.000	0.261	0.000	0.000
G	+-+	E_y	0.000	0.412	0.000	0.000	-0.699	0.000	0.000	0.261	0.000
	+-+	A_{lz}	-0.262	0.000	-0.488	0.000	0.000	1.806	0.000	0.000	-0.342

Continued on next page

(Table 3-8 continued)

Sign Set	Signs		P_x^H			P_x^{Br}			P_x^C		
	++-	E_x	-0.092	0.000	0.010	-1.025	0.000	0.000	1.568	0.000	0.000
H	++-	E_y	0.000	-0.270	0.000	0.000	-1.025	0.000	0.000	1.568	0.000
	++-	A_{lz}	-0.458	0.000	0.270	0.000	0.000	-1.798	0.000	0.000	0.989
ERRORS		E_x	0.005	0.000	0.009	0.007	0.000	0.000	0.015	0.000	0.000
		E_y	0.000	0.004	0.000	0.000	0.007	0.000	0.000	0.015	0.000
		A_{lz}	0.021	0.000	0.009	0.000	0.000	0.118	0.000	0.000	0.127
ROTATIONAL CORRECTIONS		E_x	0.067	0.000	-0.036	-0.863	0.000	0.000	0.662	0.000	0.000
		E_y	0.000	0.067	0.000	0.000	-0.863	0.000	0.000	0.662	0.000
		A_{lz}	0.000	0.000	0.000	0.000	0.000	0.000	0.000	0.000	0.000

TABLE 3-9

ATOMIC POLAR TENSORS FOR CD_3Br

(Units are D/Å)

Sign Set	Signs		P_x^D			P_x^{Br}			P_x^C		
	---	E_x	0.172	0.000	0.243	-0.982	0.000	0.000	0.165	0.000	0.000
A	---	E_y	0.000	0.373	0.000	0.000	-0.982	0.000	0.000	0.165	0.000
	---	A_{lz}	0.549	0.000	-0.043	0.000	0.000	-1.475	0.000	0.000	1.603
	+--	E_x	-0.152	0.000	0.143	-0.983	0.000	0.000	0.650	0.000	0.000
B	+--	E_y	0.000	0.374	0.000	0.000	-0.983	0.000	0.000	0.650	0.000
	+--	A_{lz}	-0.234	0.000	-0.288	0.000	0.000	-1.487	0.000	0.000	2.351
	-+-	E_x	0.330	0.000	0.066	-0.951	0.000	0.000	0.790	0.000	0.000
C	-+-	E_y	0.000	-0.222	0.000	0.000	-0.951	0.000	0.000	0.790	0.000
	-+-	A_{lz}	0.242	0.000	0.618	0.000	0.000	-1.581	0.000	0.000	-0.272

Continued on next page

(Table 3-9 continued

Sign Set	Signs		P_x^D			P_x^{Br}			P_x^C		
	--+	E_x	0.203	0.000	-0.080	-0.701	0.000	0.000	-0.248	0.000	0.000
D	--+	E_y	0.000	0.430	0.000	0.000	-0.701	0.000	0.000	-0.248	0.000
	--+	A_{lz}	0.541	0.000	-0.373	0.000	0.000	1.593	0.000	0.000	-0.475
	+++	E_x	0.037	0.000	-0.358	-0.671	0.000	0.000	-0.862	0.000	0.000
E	+++	E_y	0.000	-0.165	0.000	0.000	-0.671	0.000	0.000	0.862	0.000
	+++	A_{lz}	-0.549	0.000	0.043	0.000	0.000	1.475	0.000	0.000	-1.603
	-++	E_x	0.361	0.000	-0.258	-0.669	0.000	0.000	0.377	0.000	0.000
F	-++	E_y	0.000	-0.166	0.000	0.000	-0.669	0.000	0.000	0.377	0.000
	-++	A_{lz}	0.234	0.000	0.288	0.000	0.000	1.487	0.000	0.000	-2.351
	+-+	E_x	-0.121	0.000	-0.180	-0.702	0.000	0.000	0.237	0.000	0.000
G	+-+	E_y	0.000	0.341	0.000	0.000	-0.702	0.000	0.000	0.237	0.000
	+-+	A_{lz}	-0.242	0.000	-0.618	0.000	0.000	1.581	0.000	0.000	0.272

Continued on next page

Table 3-9 continued)

Sign Set	Signs		P_x^D			P_x^{Br}			P_x^C		
	++-	E_x	0.006	0.000	-0.035	-0.952	0.000	0.000	1.275	0.000	0.000
H	++-	E_y	0.000	-0.221	0.000	0.000	-0.952	0.000	0.000	1.275	0.000
	++-	A_{lz}	-0.541	0.000	0.373	0.000	0.000	-1.593	0.000	0.000	0.475
		E_x	0.005	0.000	0.004	0.002	0.000	0.000	0.013	0.000	0.000
ERRORS		E_y	0.000	0.008	0.000	0.000	0.002	0.000	0.000	0.013	0.000
		A_{lz}	0.011	0.000	0.011	0.000	0.000	0.040	0.000	0.000	0.053
ROTATIONAL CORRECTIONS		E_x	0.104	0.000	-0.057	-0.826	0.000	0.000	0.513	0.000	0.000
		E_y	0.000	0.104	0.000	0.000	-0.826	0.000	0.000	0.513	0.000
		A_{lz}	0.000	0.000	0.000	0.000	0.000	0.000	0.000	0.000	0.000

TABLE 3-10

ATOMIC POLAR TENSORS FOR CH_3I

(Units are D/Å)

Sign Set	Signs		P_x^H			P_x^I			P_x^C		
	---	E_x	0.078	0.000	0.343	-0.946	0.000	0.000	0.467	0.000	0.000
A	---	E_y	0.000	0.240	0.000	0.000	-0.946	0.000	0.000	0.467	0.000
	---	A_{lz}	0.427	0.000	-0.233	0.000	0.000	-0.537	0.000	0.000	1.235
	+--	E_x	-0.158	0.000	0.268	-0.943	0.000	0.000	0.812	0.000	0.000
B	+--	E_y	0.000	0.246	0.000	0.000	-0.943	0.000	0.000	0.812	0.000
	+--	A_{lz}	-0.178	0.000	-0.403	0.000	0.000	-0.537	0.000	0.000	1.745
	-+-	E_x	0.176	0.000	0.152	-0.902	0.000	0.000	1.057	0.000	0.000
C	-+-	E_y	0.000	-0.279	0.000	0.000	-0.902	0.000	0.000	1.057	0.000
	-+-	A_{lz}	0.185	0.000	0.487	0.000	0.000	-1.022	0.000	0.000	-0.439

Continued on next page

(Table 3-10 continued)

Sign Set	Signs		P_x^H			P_x^I			P_x^C		
	--+	E_x	0.171	0.000	-0.128	-0.550	0.000	0.000	-0.282	0.000	0.000
D	--+	E_y	0.000	0.384	0.000	0.000	-0.550	0.000	0.000	-0.282	0.000
	--+	A_{lz}	0.420	0.000	-0.317	0.000	0.000	1.022	0.000	0.000	-0.071
	+++	E_x	0.031	0.000	-0.395	-0.503	0.000	0.000	0.652	0.000	0.000
E	+++	E_y	0.000	-0.130	0.000	0.000	-0.503	0.000	0.000	0.652	0.000
	+++	A_{lz}	-0.427	0.000	0.233	0.000	0.000	0.537	0.000	0.000	-1.235
	-++	E_x	0.268	0.000	-0.319	-0.506	0.000	0.000	0.308	0.000	0.000
F	-++	E_y	0.000	-0.136	0.000	0.000	-0.506	0.000	0.000	0.308	0.000
	-++	A_{lz}	0.178	0.000	0.403	0.000	0.000	0.537	0.000	0.000	-1.745
	+-+	E_x	-0.066	0.000	-0.203	-0.547	0.000	0.000	0.063	0.000	0.000
G	+-+	E_y	0.000	0.389	0.000	0.000	-0.547	0.000	0.000	0.063	0.000
	+-+	A_{lz}	-0.185	0.000	-0.487	0.000	0.000	1.022	0.000	0.000	0.439

Continued on next page

(Table 3-10 continued)

Sign Set	Signs		p^H_x			p^I_x			p^C_x		
	++-	E_x	-0.061	0.000	0.077	-0.899	0.000	0.000	1.401	0.000	0.000
H	++-	E_y	0.000	-0.274	0.000	0.000	-0.899	0.000	0.000	1.401	0.000
	++-	A_{lz}	-0.420	0.000	0.317	0.000	0.000	-1.022	0.000	0.000	0.071
		E_x	0.006	0.000	0.009	0.007	0.000	0.000	0.015	0.000	0.000
ERRORS		E_y	0.000	0.005	0.000	0.000	0.007	0.000	0.000	0.015	0.000
		A_{lz}	0.020	0.000	0.011	0.000	0.000	0.138	0.000	0.000	0.141
		E_x	0.055	0.000	-0.026	-0.725	0.000	0.000	0.559	0.000	0.000
ROTATIONAL CORRECTIONS		E_y	0.000	0.055	0.000	0.000	-0.725	0.000	0.000	0.559	0.000
		A_{lz}	0.000	0.000	0.000	0.000	0.000	0.000	0.000	0.000	0.000

TABLE 3-11

ATOMIC POLAR TENSORS FOR CD_3I

(Units are D/Å)

Sign Set	Signs		P_x^D			P_x^I			P_x^C		
	---	E_x	0.070	0.000	0.274	-0.875	0.000	0.000	0.260	0.000	0.000
A	---	E_y	0.000	0.330	0.000	0.000	-0.875	0.000	0.000	0.260	0.000
	---	A_{lz}	0.421	0.000	-0.055	0.000	0.000	-0.552	0.000	0.000	0.717
	+--	E_x	-0.102	0.000	0.217	-0.874	0.000	0.000	0.531	0.000	0.000
B	+--	E_y	0.000	0.331	0.000	0.000	-0.874	0.000	0.000	0.531	0.000
	+--	A_{lz}	-0.234	0.000	-0.245	0.000	0.000	-0.564	0.000	0.000	1.298
	-+-	E_x	0.229	0.000	0.110	-0.848	0.000	0.000	0.851	0.000	0.000
C	-+-	E_y	0.000	-0.231	0.000	0.000	-0.848	0.000	0.000	0.851	0.000
	-+-	A_{lz}	0.238	0.000	0.373	0.000	0.000	-0.651	0.000	0.000	-0.469

Continued on next page

(Table 3-11 continued)

Sign Set	Signs		P_x^D			P_x^I			P_x^C		
	--+	E_x	0.126	0.000	-0.135	-0.551	0.000	0.000	-0.242	0.000	0.000
D	--+	E_y	0.000	0.403	0.000	0.000	-0.551	0.000	0.000	-0.242	0.000
	--+	A_{lz}	0.417	0.000	-0.184	0.000	0.0-0	0.664	0.000	0.000	-0.113
	+++	E_x	0.093	0.000	-0.357	-0.523	0.000	0.000	0.619	0.000	0.000
E	+++	E_y	0.000	-0.157	0.000	0.000	-0.523	0.000	0.000	0.619	0.000
	+++	A_{lz}	-0.421	0.000	0.055	0.000	0.000	0.552	0.000	0.000	-0.717
	-++	E_x	0.275	0.000	-0.299	-0.524	0.000	0.000	0.348	0.000	0.000
F	-++	E_y	0.000	-0.158	0.000	0.000	-0.524	0.000	0.000	0.348	0.000
	-++	A_{lz}	0.234	0.000	0.245	0.000	0.000	0.564	0.000	0.000	-1.298
	+-+	E_x	-0.056	0.000	-0.192	-0.550	0.000	0.000	0.029	0.000	0.000
G	+-+	E_y	0.000	0.404	0.000	0.000	-0.550	0.000	0.000	0.029	0.000
	+-+	A_{lz}	-0.238	0.000	-0.373	0.000	0.000	0.651	0.000	0.000	0.409

Continued on next page

(Table 3-11 continued)

Sign Set	Signs		P^D_x			P^I_x			P^C_x		
	++-	E_x	0.047	0.000	0.052	-0.847	0.000	0.000	1.122	0.000	0.000
H	++-	E_y	0.000	-0.230	0.000	0.000	-0.847	0.000	0.000	1.122	0.000
	++-	A_{lz}	-0.417	0.000	0.184	0.000	0.000	-0.664	0.000	0.000	0.113
		E_x	0.005	0.000	0.004	0.003	0.000	0.000	0.011	0.000	0.000
ERRORS		E_y	0.000	0.006	0.000	0.000	0.003	0.000	0.000	0.011	0.000
		A_{lz}	0.008	0.000	0.005	0.000	0.000	0.015	0.000	0.000	0.022
ROTATIONAL CORRECTIONS		E_x	0.087	0.000	-0.041	-0.699	0.000	0.000	0.440	0.000	0.000
		E_y	0.000	0.087	0.000	0.000	-0.699	0.000	0.000	0.440	0.000
		A_{lz}	0.000	0.000	0.000	0.000	0.000	0.000	0.000	0.000	0.000

$$\begin{pmatrix} \partial\vec{p}/\partial Q_4 & \partial\vec{p}/\partial Q_5 & \partial\vec{p}/\partial Q_{6\ x} \\ \partial\vec{p}/\partial Q_4 & \partial\vec{p}/\partial Q_5 & \partial\vec{p}/\partial Q_{6\ y} \\ \partial\vec{p}/\partial Q_1 & \partial\vec{p}/\partial Q_2 & \partial\vec{p}/\partial Q_{3\ z} \end{pmatrix}.$$

We reported only eight possible sign combinations in the tables, and by considering the Coriolis data we can construct eight additional acceptable sign sets, all subject to the two constraints just mentioned. These additional sets will later be designated by a double letter notation given by: AB, BA, CH, HC, DG, GD, EF, FG. By this notation we mean that the E_x and E_y rows of the set indicated by the first letter is combined with the $A_{1,z}$ row of the set indicated by the second letter. Thus, for the tensor indicated by set AB, we mean the tensor formed by combining the E_x and E_y rows of set A with the $A_{1,z}$ row of set B.

Calculation of the Polar Tensor for CH_3F and CH_3Cl by CNDO/2 Methods

The CNDO/2 approximate quantum mechanical technique has been described in detail by Pople and Beveridge (31). The calculations of the polar tensors were made using the IBM 370/165 computer with Segal's CNDO program from QCPE (32). The $\underline{P}_X^{\alpha}$ tensors for CH_3F and CH_3Cl were calculated by

$$(\partial p/\partial x)^{\alpha} \simeq (\Delta p/\Delta x)^{\alpha} = (P_\tau^+ - P_\tau^-)/2.0(\tau^+ - \tau^-) \ . \qquad (3\text{-}1)$$

$$\tau = x, y, \text{ or } z.$$

Here P_τ^+ and P_τ^- are the calculated permanent dipole moment

components for the displacement of the αth atom along the positive and negative τth axis on either side of the equilibrium position of the atom. The quantities τ^+ and τ^- are the actual displacements (0.01A and -0.01A, respectively) along the τth axes. Thus, we approximated $(\partial\vec{p}/\partial x)$ by averaging the permanent dipole moments calculated from displacement on either side of the equilibrium position of the αth atom. The atomic displacements were made relative to the experimental geometries as suggested by Schwendeman, who found that from the point of view of the spectroscopist, the experimental equilibrium geometry is acceptable since the theoretically calculated minimum geometry "...may lead to errors in the spectroscopic parameters which are larger than those due to all other causes combined" (33).

The calculated polar tensors $(\underline{P}_X^{\alpha})$ for CH_3F and CH_3Cl are given at the bottom of Tables 3-4 and 3-6, respectively.

Error Propagation

In RNO's analysis of the propagation of the experimental errors for the $\partial\vec{p}/\partial S_j$'s, the contributions from the random errors in the experimental intensities, force constants, molecular geometries, and in the harmonic frequencies were taken into account. We used RNO's estimated errors in the $\partial\vec{p}/\partial S_j$'s of the methyl halides as a starting point for the estimation of the uncertainties in the atomic polar tensors.

An element of $\underline{P}_X^{\alpha}$ can be expressed in terms of the $\partial\vec{p}/\partial S_j$'s (the $\underline{P}_S$ tensor elements) as

$$\partial p/\partial x_i = \sum_j (\partial \vec{p}/\partial S_j)\, b_{ji} \quad , \qquad (3\text{-}2)$$

where b_{ji} is the jith element of the symmetrized B matrix and the sum is over all symmetry coordinates in a given symmetry block. Since RNO have shown that the errors in the molecular geometries are negligible, then the only errors contributing to the $\partial p/\partial x_i$ are those associated with the $\partial \vec{p}/\partial S_j$'s. We used the dispersions listed by RNO as the estimated errors in the $\partial \vec{p}/\partial S_j$ elements and calculated the standard deviation, ε_i^α, for each polar tensor element by

$$\varepsilon_i^\alpha = \{ \sum_j \delta(\partial \vec{p}/\partial S_j)^2 (b_{ji})^2 \}^{\frac{1}{2}} \quad . \qquad (3\text{-}3)$$

This value, ε_i^α, is the quantity we used as a measure of the errors in the αth atomic polar tensor element (i).

Since the propagated errors are independent of the sign choices for the $\partial \vec{p}/\partial Q_i$'s (18), only one propagation calculation of the standard deviations for each polar tensor is required and the results are reported in Tables 3-4 to 3-11 for each CH_3X and CD_3X atomic polar tensor.

We did not use the force fields given by RNO for the calculation (see Appendix I) of normal coordinates of the methyl halides, but rather the force fields of Duncan. Since the latter force field has smaller dispersions (Chapter 1), the propagated errors in our L matrix are expected to be smaller so that errors given in the polar tensors (and derived from the error in L given by RNO) may be slightly overestimated. It was not our intent to carry out an exact error

analysis, but just to obtain an estimate of the reliability of the elements listed for the atomic polar tensors.

Sign Choice of the $\partial\vec{p}/\partial Q_i$'s

Although eight of the sixteen possible sign combinations of the $\partial\vec{p}/\partial Q_i$'s were eliminated by RNO, they were not able to make a unique choice as to the correct sign combination preferred for the methyl halides. Their criterion for selecting the most probable sign combination was based on the isotopic invariance principle (11). According to that criterion, if the differences in the $\partial\vec{p}/\partial S$'s for CH_3X and for CD_3X exceeded the sums of the errors in the $\partial\vec{p}/\partial S$'s for CH_3X and for CD_3X for a given sign combination of the $\partial\vec{p}/\partial Q_i$'s, then that sign choice was unacceptable. However, the eight remaining sign sets were consistent with the Coriolis data (15) discussed earlier in this chapter. They were unable to choose the best set from these eight.

We employed an additional criterion to allow rejection of seven other sign sets; namely, agreement of the experimental polar tensors with the CNDO-calculated tensors.

For the criterion of isotopic invariance, we calculated two statistical parameters $\sigma(\alpha)$ and $d^{\alpha}_{D,H}$ for each atomic tensor. The quantity $\sigma(\alpha)$ is an average standard deviation of the propagated errors in the αth tensor elements for the whole tensor and is defined as

$$\sigma(\alpha) = 1/n \{\sum_{j}^{n}(|\varepsilon^{\alpha}_{j,D}|^2 + |\varepsilon^{\alpha}_{j,H}|^2)\}^{\frac{1}{2}} , \qquad (3\text{-}4)$$

where n is the number of non-zero elements in the αth tensor and the sum is over all non-zero elements. The quantity $\varepsilon^{\alpha}_{j,D}$ and $\varepsilon^{\alpha}_{j,H}$ are the propagated errors computed by Equation 3-3 for the jth elements of the αth tensor for CD_3X and CH_3X, respectively. Thus, $\sigma(\alpha)$ gives an estimate of the total error in the αth atomic tensor for CH_3X and CD_3X due to errors in the experimental intensities, force constants, geometries and harmonic frequencies based on RNO's error analysis.

The second statistical parameter, $d^{\alpha}_{H,D}$ is the root-mean-squared difference of the αth tensor of CD_3X and CH_3X defined as

$$d^{\alpha}_{D,H} = 1/n \quad \{\sum_j |P^{\alpha}_j(D) - P^{\alpha}_j(H)|^2\}^{\frac{1}{2}} , \qquad (3\text{-}5)$$

where $P^{\alpha}_j(D)$ and $P^{\alpha}_j(H)$ are the jth element of the αth tensor for CD_3X and CH_3X, respectively, for a positive sign choice, and n and j are the same as in Equation 3-4. The quantity $d_{D,H}$ gives a measure of the difference between the αth tensor from CD_3X and that from CH_3X. These two quantities, $\sigma(\alpha)$ and $d^{\alpha}_{D,H}$, are characteristic of the tensor as a whole so that the isotopic invariance criterion is based on a tensor-by-tensor comparison rather than on an element-by-element comparison. We picked the tensor comparison because it seemed to be straightforward and effective for the intensity parameters involving the entire αth atoms. We have restricted our analysis to the $\underline{P}^{H}_{X}$ (or $\underline{P}^{D}_{X}$) and $\underline{P}^{X}_{X}$ tensors, neglecting the carbon tensors, since the $\underline{P}^{C}_{X}$ tensor can be found from

the others. Notice that $d^{\alpha}_{D,H}$ should be zero within experimental error measured by $\sigma(\alpha)$, if the correct signs of the $\partial\vec{p}/\partial Q_i$'s were used in computing the tensors.

For a given methyl halide, we computed the sum of $\sigma(H) + \sigma(X)$, designated as σ_T, which is a measure of the total experimental error for that methyl halide and its trideuterated isotope. We then computed $d^{H}_{D,H} + d^{X}_{D,H}$, designated as d_T for the same methyl halide for each sign set of $\partial\vec{p}/\partial Q_i$'s; if d_T was greater than twice the sum of the average standard deviation ($2\sigma_T$) for any sign set, we considered that the isotopic invariance principle was not satisfied and eliminated that sign set from further consideration.

The second criterion is based on the quality of agreement between the experimental $\underline{P}^{\alpha}_{X}$ tensors and the $\underline{P}^{\alpha}_{X}$ tensors calculated by the CNDO technique. For comparison of the experimental tensors to the CNDO tensors, we calculated a root-mean-squared difference ($\bar{d}^{H}_{T}$) between the two, similar to Equation 3-5, for the CH_3X tensors by replacing the $\underline{P}^{\alpha}_{i}(D)$ tensor in Equation 3-1 with the CNDO calculated tensor element $\underline{P}^{\alpha}_{i}(CNDO)$. In like manner, we calculated $d^{\alpha}_{D,CNDO}$ for each tensor element of the CH_3X molecule by replacing the $\underline{P}^{\alpha}_{i}(H)$ tensor element by the CNDO calculated tensor element. The sums $d^{H}_{H,CNDO} + d^{X}_{H,CNDO}$ designated as $\bar{d}^{-H}_{T}$, and $d^{D}_{D,CNDO} + d^{X}_{H,CNDO}$, designated as d^{-D}_{T}, were calculated for the eight sign sets remaining after applying the first criterion. We chose as the most probable sign set that set for which the d^{-D}_{T} and $\bar{d}^{-H}_{T}$ were smallest.

Selection of the Signs of the $\partial\vec{p}/\partial Q_i$'s for CH_3F

The $\underline{P}_X$ tensors for CH_3F and CD_3F are given in Table 3-4 and 3-5 for all possible sign choices of the $\partial\vec{p}/\partial Q_i$'s consistent with the Coriolis data. The statistical data, described in the previous section, used for the selection of the sign set for the $\partial\vec{p}/\partial Q_i$'s are given in Table 3-12. By using criterion 1 (isotopic invariance), we eliminated sets C, D, G, H, CH, HC, DG, and GD. RNO arrived at the same conclusions with respect to non-acceptable sign combinations with, however, one exception. They found that they could reject the --- combination for the E modes. As shown in Table 3-12, we cannot reject this sign choice (which appears in sets A and AB) based solely on isotopic invariance. Of the remaining sign sets (A, B, E, AB, BA, EF, and FE), set B gives a minimum for both $\bar{d}_T^H$ and $\bar{d}_T^D$, and therefore is our preferred sign set for CH_3F.

Restricting our attention to the sets not ruled out by the first criterion (sets A, B, AB, BA, EF, and FE), we should point out a fact that is implicit in the numbers in Table 3-12, but perhaps not obvious. If we examine the $A_{1,z}$ rows of the E and F sign sets in Table 3-4 (or Table 3-5) for the $\underline{P}_X^F$ tensor, we see that the experimental C-F bond moment derivative is a relatively large positive number. This result is intuitively unreasonable, since it implies that the fluorine atom "effective charge" $\partial p_z^F/\partial z$ is positive. Previous studies of fluorine containing compounds (such as CF_4, F_2CO, and C_6F_6) support the intuitive idea that this C-F

TABLE 3-12

CRITERIA FOR REJECTION OF SIGN SETS
FOR METHYL FLUORIDE[a]

Sign Set	Reason for Rejection[c]	$d^{H}_{D,H}$	$d^{F}_{H,H}$	d_{T}	$d^{H}_{H,CNDO}$	$d^{F}_{H,CNDO}$	d^{-H}_{T}	$d^{H}_{D,CNDO}$	$d^{F}_{D,CNDO}$	d^{-D}_{T}
A	2	.07	.20	.27	.31	.58	.81	.37	.76	1.13
B[b]		.04	.20	.24	.06	.56	.62	.09	.76	.85
C	1	.21	.51	.72	--	--	--	--	--	--
D	1	.21	.48	.69	--	--	--	--	--	--
E	2	.06	.17	.23	.12	2.28	2.40	.16	2.44	2.50
F	2	.03	.19	.22	.29	2.25	2.54	.32	2.44	2.76
G	1	.20	.50	.70	--	--	--	--	--	--
H	1	.21	.48	.69	--	--	--	--	--	--
AB	2	.04	.22	.26	.26	.58	.84	.28	.76	1.04
BA	2	.07	.19	.26	.18	.54	.72	.24	.76	1.00
CH	1	.21	.48	.69	--	--	--	--	--	--

Continued on next page

(Table 3-12 continued)

Sign Set	Reason for Rejection[c]	$d^H_{D,H}$	$d^F_{H,H}$	d_T	$d^H_{H,CNDO}$	$d^F_{H,CNDO}$	$\bar{d}^H_T$	$d^H_{D,CNDO}$	$d^F_{D,CNDO}$	$\bar{d}^D_T$
HC	1	.20	.51	.71	--	--	--	--	--	--
DG	1	.20	.50	.70	--	--	--	--	--	--
GD	1	.21	.48	.69	--	--	--	--	--	--
EF	2	.02	.07	.09	.16	2.25	2.41	.15	2.44	2.59
FG	2	.20	.13	.33	.28	2.28	2.56	.32	2.44	2.76

$\sigma(H) = 0.06$

$\sigma(F) = 0.24$

$2\{\sigma(H) + \sigma(F)\} = 2\sigma_T = 0.60$

a. See text for explanation of symbols in this table, and their use.
b. Our preferred set of signs.
c. 1 means isotopic invariance principle, and 2 means agreement with the CNDO/2 calculated tensors.

bond moment parameter is negative (4). As a consequence, we feel that sign sets E and F should be eliminated from consideration. This conclusion requires that the sign sets EF, and FE, also, be discarded, since any sign set from the E_x and E_y rows of set E or F must be restricted with a set of signs from the $A_{1,z}$ rows consistent with the Coriolis data. By means of this pragmatic argument, only sets A, B, AB, and BA must still be considered possible. Examination of $\bar{d}_T^H$ and $\bar{d}_T^D$ in Table 3-12 for these sets shows little difference between the four sets. If, however, we examine only the $\underline{P}_X^H$ (or $\underline{P}_X^D$) tensor of set A (in Table 3-4), we see that the first element of the E_x row, $\partial p_x/\partial x$, has a relatively large positive value although CNDO/2 predicts an equally large negative value; also the first element of the $A_{1,z}$ row, $\partial p_z/\partial x$, for set A is a relatively large positive number and CNDO/2 predicts a negative value for that element. However, the signs of these elements from set B are consistent with the CNDO/2-predicted signs. (Note that the $\underline{P}_X^F$ tensors for both set A and set B are very similar and we do not gain any additional information by examining these tensors.)

Determination of the Signs of $\partial\vec{p}/\partial Q_i$ for CH_3Cl

The polar tensors for CH_3Cl and CD_3Cl for all possible sign choices of the $\partial\vec{p}/\partial Q_i$'s are given in Tables 3-6 and 3-7. As in the case of CH_3F, DiLauro and Mills (15) have shown that the signs of the $\partial\vec{p}/\partial Q_i$'s for ν_2 and ν_3 , as well as for ν_4 and ν_6 , must be identical, and as a consequence, CH_3Cl has the same number of possible sign sets as CH_3F.

Following a similar procedure as for CH_3F (as described below), set B is found to be the preferred set of signs for CH_3Cl and CD_3Cl. The data used in making this choice are given in Table 3-13.

We have used the same criteria (isotopic invariance and CNDO-calculated tensors) for selecting a preferred sign set for CH_3Cl as was used for CH_3F with, however, a modification of the CNDO criterion. From Table 3-6 we see that the CNDO/2-calculated bond moment parameter $\partial p_z/\partial z$ for the C-Cl bond is positive. We feel that this is clearly an error on the part of the CNDO/2 calculation for chlorine, based on the same reasoning given for rejection of corresponding positive C-F bond moment parameters. Hence, we used only the $\underline{P}_X^H$ and $\underline{P}_X^D$ tensors to compute $d_{H,CNDO}^H$ and $d_{D,CNDO}^D$, even though the inability of CNDO/2 to predict the C-Cl bond moment sign introduces a larger degree of uncertainty in the entire calculation.

Using the isotopic invariance criterion, we eliminated sets C, D, G, H, CH, HC, GD, and DG. Of the remaining sets (A, B, E, F, AB, BA, EF, and FE), set B gives the minimum value for $d_{D,CNDO}^H$ and $d_{H,CNDO}^D$.

Determination of the Signs of $\partial\vec{p}/\partial Q_i$'s for CH_3Br and CH_3I

The polar tensors for CH_3Br, CD_3Br, CH_3I, and CD_3I are given in Tables 3-8 to 3-11 for all possible sign combinations of the $\partial\vec{p}/\partial Q_i$'s. We will treat these molecules collectively since the problem of determination of the signs of the $\partial\vec{p}/\partial Q_i$'s are common for both CH_3Br and CH_3I.

TABLE 3-13

CRITERIA FOR REJECTION OF SIGN SETS FOR CH_3Cl

Sign Set	Reason for Rejection[a]	$d^H_{H,D}$	$d^{Cl}_{H,D}$	d_T	$d^{H}_{H,CNDO}$[b]	$d^{D}_{D,CNDO}$[b]
A	2	.039	.081	.120	.24	.26
B[c]		.037	.073	.100	.08	.08
C	1	.104	.147	.251	.27	.29
D	1	.051	.132	.183	.22	.24
E	2	.030	.059	.089	.13	.14
F	2	.012	.049	.061	.24	.25
G	1	.051	.142	.193	.08	.11
H	1	.055	.137	.192	.15	.19
AB	2	.029	.074	.103	.18	.18
BA	2	.038	.080	.118	.18	.21
CH	1	.104	.137	.241	.22	.24

Continued to next page

(TABLE 3-13 continued)

Sign Set	Reason for Rejection[a]	$d^{H}_{H,D}$	$d^{Cl}_{H,D}$	d_{T}	$d^{H}_{H,CNDO}$[b]	$d^{D}_{D,CNDO}$[b]
HC	1	.055	.146	.201	.22	.25
DG	1	.051	.132	.183	.17	.19
GD	1	.051	.132	.183	.16	.19
EF	2	.013	.049	.062	.19	.19
FE	2	.029	.059	.088	.20	.22

$\sigma(H) = 0.010$

$\sigma(Cl) = 0.051$

$2 \times \{\sigma(H) + \sigma(Cl)\} = 0.122$

a. 1 means the isotopic invariance principle, and 2 means agreement with the CNDO/2 calculated tensors.

b. We omitted $d^{H}_{Cl,CNDO}$ and $d^{D}_{Cl,CNDO}$ since we believe the C-X bond moment as calculated by CNDO/2 was incorrect (see text). We used only $d^{H}_{H,CNDO}$ and $d^{D}_{D,CNDO}$ for our statistical parameters.

c. Our preferred sign set.

We were unable to eliminate any of the possible sign sets for CH_3Br using the isotopic criterion. For each sign set, $d^{H}_{H,D} + d^{Br}_{H,D}$ was smaller than twice the sum of the standard deviation as shown in Table 3-14; however, a less rigorous criterion (that $d^{H} + d^{Br}$ be less than σ) would eliminate all sets except E, F, EF, and FE.

Since we do not have a CNDO/2 calculation of the polar tensors for molecules containing atoms outside the first and second row elements, it appears that all sign sets for CH_3Br might have to be considered. In addition, there is no direct experimental evidence (for example, Coriolis data) that requires $\partial\vec{p}/\partial Q_2$ and $\partial\vec{p}/\partial Q_5$, or $\partial\vec{p}/\partial Q_3$ and $\partial\vec{p}/\partial Q_6$, to have the same signs, as was the case for CH_3Cl and CH_3F. If this requirement is removed, then we should consider an additional forty-eight sign sets.

In the case of CH_3I, we were able to reduce the number of possible sign sets by the isotopic invariance criterion. The same sets as were eliminated for CH_3F and CH_3Cl are eliminated for CH_3I, using the same criterion. The statistical data are given in Table 3-15. As in the case of CH_3Br there are no Coriolis data available to determine whether the relative signs of $\partial\vec{p}/\partial Q_2$ and $\partial\vec{p}/\partial Q_5$ or $\partial\vec{p}/\partial Q_3$ and $\partial\vec{p}/\partial Q_6$ are the same. Without this information, there are eight more possible sign combinations that should be considered, in addition to those listed in Table 3-15 for CH_3I.

It is apparent that without the Coriolis data and CNDO/2 data for CH_3Br and CH_3I we have a rather large number of

TABLE 3-14

CRITERIA FOR REJECTION OF SIGN SETS FOR CH_3Br

Set	Reason for Rejection[a]	$d^{H}_{D,H}$	$d^{Br}_{D,H}$	d_T
A		.033	.055	.088
B		.027	.058	.085
C		.034	.083	.117
D		.027	.068	.095
E		.024	.030	.054
F		.010	.035	.045
G		.031	.075	.106
H		.036	.077	.113
AB		.028	.058	.086
BA		.032	.054	.086
CH		.034	.077	.111
HC		.035	.083	.118
DG		.027	.075	.102

Continued on next page

(Table 3-14 continued)

Set	Reason for Rejection[a]	$d^{H}_{D,H}$	$d^{Br}_{D,H}$	d_{T}
GH		.030	.068	.098
EF		.014	.033	.047
FE		.020	.029	.049

$\sigma(H) = .0085$

$\sigma(Br) = .0530$

$2 \times\{\sigma(H) + \sigma(Br)\} = 2\sigma_{T} = .123$

a. For CH_3Br we were unable to reject any sets of signs for the $\partial\vec{p}/\partial Q_i$'s by the isotopic invariance criteria (see text), and the CNDO/2 technique has not been used here for elements outside the second row of the periodic chart.

TABLE 3-15

CRITERIA FOR REJECTION OF SIGN SETS FOR CH_3I

Set	Reason for Rejection[a]	$d^H_{H,D}$	$d^I_{H,D}$	d_T
A		.034	.042	.076
B		.034	.041	.075
C	1	.126	.030	.156
D	1	.119	.028	.147
E		.011	.039	.060
F		.012	.034	.046
G	1	.124	.025	.149
H	1	.121	.036	.157
AB		.035	.040	.075
BA		.033	.042	.075
CH	1	.122	.031	.153
HC	1	.126	.035	.161
DG	1	.124	.027	.151

Continued on next page

(Table 3-15 continued)

Set	Reason for Rejection[a]	$d^{H}_{H,D}$	$d^{I}_{H,D}$	d_T
GH	1	.119	.027	.126
EF		.013	.037	.050
FE		.010	.036	.046

$\sigma(H) = .0075$

$\sigma(I) = .0511$

$2\{\sigma(H) + \sigma(I)\} = 2\sigma_T = 0.117$

a. 1 means the isotopic invariance principle.

possible sign sets that should be considered. It appears to be impossible at this point to make an objective choice. However, it is quite reasonable to assume for CH_3Br and CH_3I that we can proceed by analogy with the CH_3F and CH_3Cl sign choice. This argument is based on the fact that the methyl halides are structurally similar and that intuitively one would expect to find a smooth trent in the physical properties. We observed no anomalous behavior in the normal coordinates or the force fields (Appendix I) for the series.

The requirement that the relative signs of the dipole moment derivatives of ν_2 and ν_5 , and ν_3 and ν_6 be the same for CH_3Cl and CH_3F is based on the knowledge (from a normal coordinate analysis) of the absolute sign of the Coriolis coupling constant, $\zeta_{R,S}$, and the sign (determined from the Coriolis effect) of the product $\zeta^{Y}_{R,S}$ $(\partial\vec{p}/\partial Q_R \times \partial\vec{p}/\partial Q_S)$ (see Reference 34). If the product is positive, then there is a positive perturbation between the ν_R and ν_S modes $(\nu_R > \nu_S)$ which produces an enhancement of the R branch and depletion of the P branch of the low frequency mode (ν_S) and the enhancement of the P branch and depletion of the R branch of the high frequency mode (ν_R). If the product is negative, then there is a negative perturbation between the coupled modes and the intensity perturbation in the P and R branches are just reversed. In principle, by simple inspection of the gas phase infrared spectrum, one can determine whether the perturbation is positive or negative and a knowledge of

the sign of $\zeta^{Y}_{R,S}$ allows us to infer the relative signs of the derivatives. In practice, however, a complete band shape analysis (34, 35) as a function of $\zeta^{Y}_{R,S}$ would have to be carried out.

We calculated $\zeta^{Y}_{2,5}$ and $\zeta^{Y}_{3,6}$ for the CH_3X series (see Appendix III) in order to see if the ζ^{Y}'s changed signs for any member of the series. We found the calculated values of ζ^{Y}'s do not change signs; moreover, their magnitudes were surprisingly constant or varied smoothly through the series. This fact is encouraging in that it suggests that there is no anomalous behavior through the series with respect to the Coriolis constants for the modes in question. Since we found no anomalies in the calculated ζ constants, we predict that there will be no anomalies in the signs of the dipole moment derivatives for CH_3Br and CH_3I. We do not mean to imply that the calculated signs for the ζ's are proof that the relative signs of the $\partial\vec{p}/\partial Q_i$'s of ν_2 and ν_5, and ν_3 and ν_6 are really the same in CH_3Br and CH_3I, but rather offer the calculation as evidence to support our prediction of similar behavior through the CH_3X series.

We believe that it is reasonable to assume that the same type of Coriolis perturbations found in CH_3F and CH_3Cl will also occur for CH_3Br and CH_3I. Based on this expected similarity, we have selected sign set B, by analogy with CH_3F and CH_3Cl, as our preferred set of signs for CH_3Br and CH_3I, also.

Summary

We have assumed that the total number of possible sign sets is the same for each of the CH_3X molecules. As we have explained, this assumption is based on the idea that there should be a close similarity in the Coriolis perturbations through the series; an argument was presented to support this assumption, based on calculated ζ constants. We were able to eliminate several of the possible sign sets for CH_3F, CH_3Cl, and CH_3I based on the isotopic invariance principle. For the remaining sets (A, B, E, F, AB, BA, EF, and FE) we ruled out sets E, F, EF, FE for CH_3F and CH_3Cl because of their lack of agreement with the CNDO/2 results (and because of the pragmatic argument based on the sign of the C-X bond moments). The bond moment argument may also be used to eliminate the same sign sets for CH_3Br and CH_3I. We feel that one of the remaining sets (A, B, AB, and BA) is the most probable sign set for the series, and we chose set B for CH_3F and CH_3Cl based on its agreement with the CNDO/2 calculations. By analogy, we picked the same set to be the most probable sign set for CH_3Br and CH_3I.

We believe that the isotopic invariance criterion is fairly sound, although it is applied subject to the errors in the experimental intensity measurements; for ν_1 and ν_2 of CH_3F, these errors are quite large (18). The argument concerning the relative signs of $\partial\vec{p}/\partial Q_2$ and $\partial\vec{p}/\partial Q_5$, and $\partial\vec{p}/\partial Q_3$ and $\partial\vec{p}/\partial Q_6$ for CH_3Br and CH_3I is intuitive, but we believe it is justified. What is needed experimentally in

this regard is a thorough examination of the Coriolis perturbations in CH_3Br and CH_3I (or the deuterated isotopes). We should point out that there is also Coriolis coupling between the ν_1 and ν_4 modes of the CH_3X series and we believe these intensity perturbations have not been investigated. This information could provide an additional check on our choice of sign sets. In regard to the CNDO/2 criterion, we recognize the approximate nature of the calculations, but a high degree of confidence in its ability to predict the signs of dipole moment derivatives for molecules made up of first row elements has been expressed (4). As a consequence, we have a fairly high degree of confidence in our preferred sign choices for CH_3F and CH_3Cl.

To summarize, we collect our preferred polar tensors for the CH_3X series in Table 3-16. The tensor elements reported in the table are the average of the CH_3X and CD_3X tensor elements for sign set B in Tables 3-4 to 3-11, with the difference between the CH_3X and CD_3X tensor elements as a measure of the experimental error in a given element, reported in the table. (We should point out that the errors reported in Table 3-16 are generally smaller than the errors propagated through from the $\partial\vec{p}/\partial S$ values. This might suggest that we did overestimate the errors in the original error analysis.)

TABLE 3-16

THE AVERAGE OF THE CH_3X AND CD_3X TENSORS FOR THE PREFERRED SIGN SET (B) OF THE $\partial\vec{p}/\partial Q_i$'S
(Units are D/Å)

Molecule	Signs		P^H_X			P^F_X			P^C_X		
CH_3F	+--	E_x	-0.594 ±.003	0.000	-0.186 ±.086	-1.225 ±.111	0.000	0.000	1.591 ±.168	0.000	0.000
	+--	E_y	0.000	0.350 ±.041	0.000	0.000	-1.225 ±.111	0.000	0.000	1.591 ±.168	0.000
	+--	A_{1z}	-0.317 ±.010	0.000	-0.036 ±.021	0.000	0.000	-4.485 ±.283	0.000	0.000	4.593 ±.220
	+--	E_x	0.233 ±.019	0.000	0.093 ±.045	-1.139 ±.057	0.000	0.000	0.964 ±.153	0.000	0.000
CH_3Cl	+--	E_y	0.000	0.350 ±.045	0.000	0.000	-1.139 ±.057	0.000	0.000	0.964 ±.153	0.000
	+--	A_{1z}	-0.290 ±.003	0.000	-0.229 ±.014	0.000	0.000	-2.146 ±.074	0.000	0.000	2.572 ±.208

Continued on next page

(Table 3-16 continued)

Molecule	Signs		$\underline{P}^{H}_{X}$			$\underline{P}^{F}_{X}$			$\underline{P}^{C}_{X}$		
	+--	E_x	-0.174 ±.022	0.000	0.184 ±.041	-1.033 ±.050	0.000	0.000	0.803 ±.153	0.000	0.000
CH_3Br	+--	E_y	0.000	0.327 ±.047	0.000	0.000	-1.033 ±.050	0.000	0.000	0.803 ±.153	0.000
	+--	A_{1z}	-0.240 ±.006	0.000	-0.273 ±.045	0.000	0.000	-1.438 ±.050	0.000	0.000	2.347 ±.004
	+--	E_x	-0.130 ±.028	0.000	0.243 ±.026	-0.909 ±.035	0.000	0.000	0.672 ±.140	0.000	0.000
CH_3I	+--	E_y	0.000	0.289 ±.043	0.000	0.000	-0.909 ±.035	0.000	0.000	0.672 ±.140	0.000
	+--	A_{1z}	-0.206 ±.028	0.000	-0.324 ±.079	0.000	0.000	-0.551 ±.013	0.000	0.000	1.522 ±.224

CHAPTER 4

DISCUSSION OF RESULTS

Introduction

In this chapter we shall examine the atomic polar tensors for the halogen and hydrogen atoms for the preferred sign choice given in Table 3-16. For the following discussion, we have changed the units of the tensor elements from D/Å to the number of electronic charges (e) (1 D/Å = 0.208 e) in order to conform more closely to recommendations (4) based on SI units. The preferred polar tensors given in Table 3-16 are given again in Table 4-1 in these units.

We shall be primarily concerned with the total dipole moment change induced in the molecule due to a unit displacement, δx, etc., for the αth atom parallel to the Cartesian coordinate axis (x, y, or z) as given by Equation 2-32. For a unit displacement (in Å) of the αth atom parallel to the τth Cartesian axis, the dipole moment change vectors, $(\Delta P)_\tau^\alpha$, have the units of e Å.

We shall first discuss the $\underline{P}_X^X$ tensors and the trends observed in the $(\Delta P)_\tau^X$ vectors as the X atom is changed, followed by a discussion of the $\underline{P}_X^H$ tensors and their associated dipole moment change vectors, $(\Delta P)_\tau^H$.

The P_X^X Tensors

In this section we shall devote our attention to the halogen atom polar tensors given in Table 4-1. The P_X^X tensors are diagonal so the magnitudes of the $(\Delta P)_\tau^X$ vectors are just the magnitudes of the diagonal elements.

For motion of the X atoms parallel to the C-X bond (the z axis), there is a steady decrease in the magnitude of $(\Delta P)_z^X$ as the halogen atom changes from F to I. Each displacement vector $(\Delta P)_z^X$ is directed along the C-X bond pointing from the negative X atom to the positive carbon atom. The $(\Delta P)_z^X$ vectors are shown plotted to scale (decreasing in length from F to I) in Figure 4-1. The $(\Delta P)_x^X$ displacement vectors for motion of the X atom perpendicular to the C-X bond along the x axis are shown in Figure 4-2. The most striking feature of the $(\Delta P)_x^X$ vectors is that there is so little change in magnitude as X is changed from F to I.

Because of the cylindrical symmetry, the dipole vector displacements $(\Delta P)_y^X$ for motion along the y axis have the same magnitudes as the $(\Delta P)_x^X$ vectors, but are oriented along y. Note that the direction of all the dipole displacement vectors is consistent with movement of a negatively charged halogen atom. Movement of the F atom, which is expected by electronegativity conditions to have the highest negative charge in a C-X bond is consistent with this idea of motion along z. (However, the relatively constant values of $(\Delta P)_x^X$ and $(\Delta P)_y^X$ for all the CH_3X compounds suggests that this idea is too naive.)

Figure 4-1: The $(\Delta P)_z^X$ vectors for the displacement of X parallel to the z axis for the methyl halides.

The displacement relative to the molecular frame is shown by the bold arrow labelled as δz. The direction of the permanent dipole moment, $\vec{p}^o$, is also shown by a bold arrow.

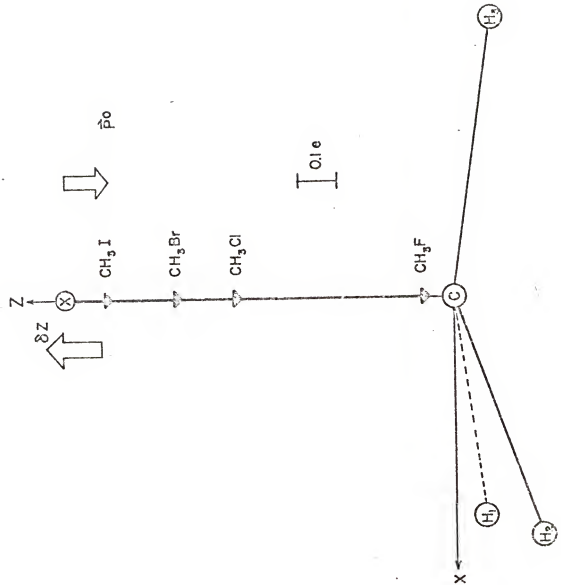
Z
δZ
CH3I
CH3Br
CH3Cl
CH3F
p̄o
0.1 e
C
H1
H2
H3
X

Figure 4-2: The $(\Delta P)^{X}_{x}$ vectors for the displacement of X parallel to the x axis for the methyl halides.

The X atom displacement relative to the molecular frame is shown by the bold arrow labelled δx. The direction of the dipole moment, $\vec{p}^{o}$, is also shown.

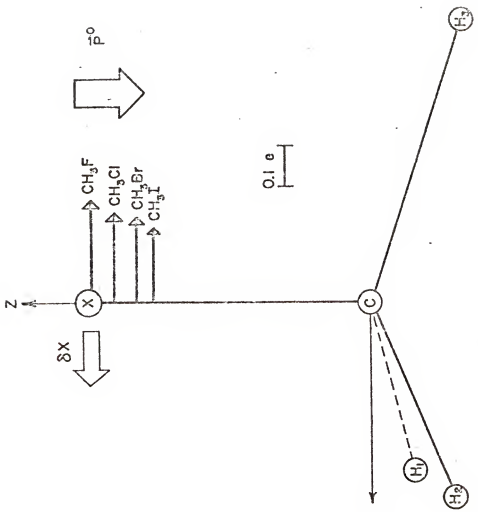
$\vec{p}^{o}$
CH_3F
CH_3Cl
CH_3Br
CH_3I
0.1 e
Z
X
δX
C
H^1
H^2
H^3
X

TABLE 4-1

AVERAGE POLAR TENSORS FOR CH_3X
EXPRESSED IN ELECTRONS[a] FOR PREFERRED[b] SIGN CHOICE B

		P_x^H			P_x^X			P_x^C	
	-0.123 ± .001	0.000	-0.039 ± .018	-0.255 ± .018	0.000	0.000	0.331 ± .035	0.000	0.000
CH_3F	0.000	0.073 ± .009	0.000	0.000	-0.255 ± .023	0.000	0.000	0.331 ± .035	0.000
	-0.066 ± .002	0.000	-0.007 ± .004	0.000	0.000	-0.933 ± .059	0.000	0.000	0.955 ± .046
	-0.048 ± .004	0.000	0.019 ± .009	-0.234 ± .012	0.000	0.000	0.201 ± .032	0.000	0.000
CH_3Cl	0.000	0.073 ± .009	0.000	0.000	-0.234 ± .012	0.000	0.000	0.201 ± .032	0.000
	-0.060 ± .001	0.000	-0.048 ± .003	0.000	0.000	-0.446 ± .015	0.000	0.000	0.535 ± .043

Continued on next page

(Table 4-1 continued)

	P_x^H			P_x^X			P_x^C		
	-0.036 ± .004	0.000	0.038 ± .008	-0.215 ± .010	0.000	0.000	0.167 ± .032	0.000	0.000
CH_3Br	0.000	0.068 ± .009	0.000	0.000	-0.215 ± .010	0.000	0.000	0.167 ± .032	0.000
	-0.050 ± .001	0.000	-0.063 ± .003	0.000	0.000	-0.299 ± .010	0.000	0.000	0.488 ± .001
	-0.027 ± .006	0.000	0.050 ± .005	-0.189 ± .007	0.000	0.000	0.141 ± .030	0.000	0.000
CH_3I	0.000	0.060 ± .009	0.000	0.000	-0.189 ± .007	0.000	0.000	0.141 ± .030	0.000
	-0.043 ± .006	0.000	-0.067 ± .016	0.000	0.000	-0.115 ± .003	0.000	0.000	0.316 ± .046
CNDO									
	-0.119	0.000	-0.006	-0.293	0.000	0.000	0.456	0.000	0.000
CH_3F	0.000	0.008	0.000	0.000	-0.293	0.000	0.000	0.456	0.000
	-0.046	0.000	-0.027	0.000	0.000	-0.526	0.000	0.000	0.605

Continued on next page

(Table 4-1 continued)

CNDO		p_x^H		p_x^X			p_x^C		
	-0.100	0.000	-0.037	-0.193	0.000	0.000	0.289	0.000	0.000
CH_3Cl	0.000	0.037	0.000	0.000	-0.193	0.000	0,000	0.289	0.000
	-0.056	0.000	-0.058	0.000	0.000	0.102	0.000	0.000	0.071

a. 1 D/Å = 0.208 e.
b. The preferred sign choice is +-- for each symmetry block.

Tensor Rotation

For the analysis of the hydrogen atom polar tensors, $\underline{P}^{H}_{X}$, it is more convenient and informative to rotate the Cartesian coordinate system from that (x, y, z) shown in Figure 4-1 to one (x', y', z') with the z' axis parallel to a C-H bond, shown in Figure 4-3. This tensor is more directly related to the intensities of the C-H bond stretching and C-H bending motions. The corresponding $\underline{T}'$ tensor in the new coordinate system has elements related to the old tensor by:

$$T'_{k,\ell} = \sum_{i=1}^{3} \sum_{j=1}^{3} a_{k,i}\, a_{\ell,j}\, T_{i,j} \quad . \qquad (4\text{-}1)$$

$$k,\ell = 1, 2, 3.$$

Here 1, 2, and 3 correspond to $\underline{i}'$, $\underline{j}'$ and $\underline{k}'$ respectively in the new coordinate system, and $a_{k,i}$ is the k,ith dot product of the unit vectors; for example, $a_{1,2}$ is $\underline{i}' \cdot \underline{j}$, etc. Thus the $a_{k,i}$ coefficients are the cosines of the angles between the original Cartesian axes and the rotated axes. $T_{i,j}$ is the i, jth element of the original tensors, and $T'_{k,\ell}$ is the k, ℓth element of the rotated tensor (36).

We shall designate the rotated tensors by $\underline{P}^{\alpha}_{X'}$, where the subscript X' indicated the polar tensors in the rotated $P^{\alpha}_{X'}$ coordinate system. We chose to rotate about the y axis, so that the z' axis lies along the C-H bond in the zx plane, as shown in Figure 4-3. The resulting $\underline{P}^{H}_{X'}$ tensors given in Table 4-2 were calculated from the $\underline{P}^{H}_{X}$ tensors in Table 4-1 by the computer program TRANSC described in Appendix II.

Figure 4-3: Definition of the x', y', z' coordinate system for the methyl halides.

Here z' is along the C-H bond and x' is in the XCH plane, and y' is the old y axis.

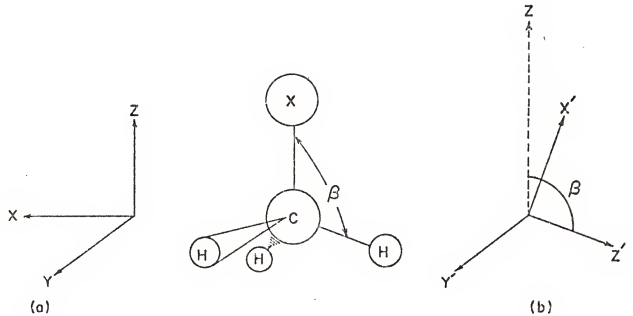

(a) Original Coordinate System

(b) Coordinate System Rotated Through Angle β About Y

TABLE 4-2

AVERAGE OF THE $\underline{P}^{H}_{X}$, TENSORS[a] OF CH_3X AND CD_3X FOR THE PREFERRED SIGN CHOICE OF $\partial\vec{p}/\partial Q$'S[b]
(Units are e)

	0.012 ±.009	0.000	0.021 ±.005
CH_3F	0.000	0.073 ±.009	0.000
	-0.007 ±.015	0.000	-0.143 ±.005
	-0.036 ±.0004	0.000	0.056 ±.0006
CH_3Cl	0.000	0.073 ±.009	0.000
	-0.024 ±.011	0.000	-0.061 ±.0008
	-0.057 ±.005	0.000	0.057 ±.002
CH_3Br	0.000	0.068 ±.010	0.000
	-0.031 ±.008	0.000	-0.042 ±.002

Continued on next page

(Table 4-2 continued)

	-0.066 ±.019	0.000	0.055 ±.002
CH_3I	0.000	0.060 ±.010	0.000
	-0.038 ±.001	0.000	-0.028 ±.004

a. As defined in Figure 4-3.
b. 1 D/Å = 0.208 e.

The $\underline{P}^H_{x'}$ Tensors

We shall first examine the dipole displacement vectors, $(\Delta P)^H_{z'}$, for motion of the hydrogen atom parallel to z'. We see from the last column of each tensor in Table 4-2 that these vectors have both x' and z' components. This means, of course, that $(\Delta P)^H_{z'}$ is not parallel to the C-H bond as was required by symmetry for the halogen atom tensors in the other coordinate system. If the bond moment hypothesis (as described in Chapter 1) were true, we should expect these $\underline{P}^H_{x'}$ tensors to be diagonal. The fact that $\underline{P}^H_{x'}$ is not diagonal is indicative of the "error" in the bond moment hypothesis; in particular, in the assumption that the dipole moment change is generated in the direction of motion of the atoms.

The magnitudes of the $(\Delta P)^H_{z'}$ vectors are given in Table 4-3 along with the angles θ_z, that the vectors make with the C-H bond axis. The positive sense of θ_z is defined as a clockwise rotation from the C-H bond when looking down towards the origin along the positive y' axis. A pictorial representation is given in Figure 4-4.

The errors given in Table 4-3 were computed by

$$(\delta P)^H_{z'} = \{(\partial r/\partial P_{x'})^2 \sigma^2_{P_{x'}} + (\partial r/\partial P_{z'})^2 \sigma^2_{P_{z'}}\}^{\frac{1}{2}} \quad (4\text{-}2)$$

for the errors in $(\Delta P)^H_{z'}$, and

$$\delta(\theta) = \{(\partial\theta_z/\partial P_{x'})^2 \sigma^2_{P_{x'}} + (\partial\theta_z/\partial P_{z'})^2 \sigma_{P_{z'}}\}^{\frac{1}{2}} \quad (4\text{-}3)$$

for the errors in θ_z. In Equation 4-2, r is the absolute

TABLE 4-3

THE $(\Delta P)^{H}_{z'}$ VECTORS AND ANGLE θ_z
FOR THE MOTION OF H PARALLEL TO THE z' AXIS

	$(\Delta P)^{H}_{z'}$ (e Å)	θ^{a}_{z} (degrees)
CH_3F	0.145 ± .005	8.2 ± 1.9
CH_3Cl	0.083 ± .001	42.9 ± 0.5
CH_3Br	0.071 ± .002	53.5 ± 1.8
CH_3I	0.062 ± .003	62.7 ± 3.2

a. θ_z is measured as a clockwise rotation of $(\Delta P)^{H}_{z'}$ from the C-H bond axis as seen by looking down the positive y' axis centered on the H atom.

Figure 4-4: The $(\Delta P)^{H}_{z'}$ vectors for the displacement of H parallel to the z' axis for the methyl halides.

The H atom displacement relative to the molecular frame is shown by the bold arrow labelled $\delta z'$. The direction of the permanent dipole moment, $\vec{p}^{o}$, is also shown.

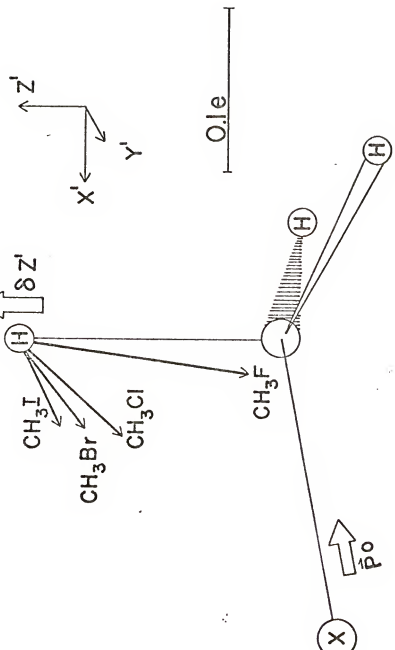
Z'
Y'
X'
0.1e
δZ'
H
CH_3I
CH_3Br
CH_3Cl
CH_3F
H
H
X
$\vec{p}_0$

magnitude of the $(\Delta P)^{X}_{z'}$, given by $r = (P^{2}_{x'} + P^{2}_{z'})$, where $P_{x'}$ and $P_{z'}$ are the x' and z' components of $(\Delta P)^{H}_{z'}$ given in Table 4-2; σ_{P_x} and σ_{P_z} are the experimental errors in $P_{x'}$ and $P_{z'}$ as derived from the difference in tensor elements of CH_3X and CD_3X as given in Table 4-2. The partial derivatives of θ_z in Equation 4-3 were computed from $\theta_z = \cos^{-1}(r/P_{z'})$.

There are two trends in the $(\Delta P)^{H}_{z'}$ vectors shown in Figure 4-4. As found in the case of the $(\Delta P)^{X}_{z}$ vectors, there is a smooth decrease in the magnitude of the $(\Delta P)^{H}_{z'}$ vectors when the halogen atoms are changed through the series from F to I. In addition, the angle θ_z increases through the series. An examination of the value of θ_z demonstrates quite dramatically the error involved in the bond moment hypothesis assumption that $(\Delta P)^{H}_{z'}$ should be along the C-H bond. Figure 4-4 implies that the "error" increases as the polarizability of the adjacent substituent (in this case, the halogen atom) increases, or as its electronegativity decreases. Note in Figure 4-4 that the direction of $(\Delta P)^{H}_{z'}$ implies a negative effective charge on H for this $\delta z'$ displacement.

The $(\Delta P)^{H}_{y'}$ vectors in Table 4-2 for the motion of H parallel to y' are allowed by symmetry to have only one component, $P_{y'}$, , parallel to the y' axis and pointing in the positive y' direction, suggesting a positive effective charge on H for this $\delta y'$ displacement. The $(\Delta P)^{H}_{y'}$ are pictured in Figure 4-5, and are the same within experimental error for this "out-of-plane" motion of the hydrogen in all four CH_3X compounds.

Figure 4-5: The $(\Delta P)^{H}_{y'}$ vectors for the displacement of H parallel to the y' axis for the methyl halides.

The H atom displacement relative to the molecular frame is shown by the bold arrow labelled $\delta y'$. The direction of the permanent dipole moment is also shown. (Note that $\vec{p}^{o}$ originates behind the paper at X and comes toward the C atom in the plane of the paper.)

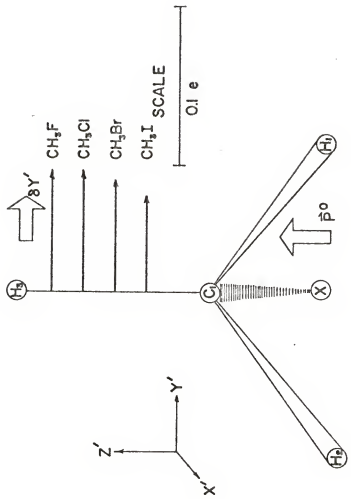
H
δY'
CH₃F
CH₃Cl
CH₃Br
CH₃I
SCALE
0.1 e
C
X
H
p₀
H
Y'
Z'
X'

The $(\Delta P)^{H}_{x'}$ vectors for the motion of the hydrogen atom perpendicular to the C-H bond and parallel to the x' axis also have non-zero x' and z' components. Like the $(\Delta P)^{H}_{z'}$ vectors, the $(\Delta P)^{H}_{x'}$ vectors are not parallel to the coordinate axis and indicate a negative effective charge on H for this motion. The vectors and the angle θ_x {defined as in the $(\Delta P)^{H}_{z'}$ case} are given in Table 4-4. A diagram of the vectors is shown in Figure 4-6.

The large error in $(\Delta P)^{H}_{x'}$ for CH_3F and in the associated angle θ_x makes this vector essentially undetermined; nevertheless, there is a discernible trend in the magnitudes of the vectors as the halogen atom is changed. It is interesting that this trend is in the opposite direction from the trend found for the $(\Delta P)^{H}_{z'}$ vectors. As the polarizability (or electronegativity) of the halogen decreases, the magnitude of $(\Delta P)^{H}_{x'}$ increases; whereas, for $(\Delta P)^{H}_{z'}$, the opposite occurred. Note that (except for CH_3F when it is undetermined) the value of θ_x is essentially constant for the CH_3X molecules.

Correlations with Electronegativity

Since the electronic character of the halogen atoms and substituents is represented qualitatively by their electronegativities, this parameter is a logical choice for correlating with the $(\Delta P)^{\alpha}_{\tau}$ vectors. The trends in the $(\Delta P)^{X}_{\tau}$ and $(\Delta P)^{H}_{\tau}$ vectors with changing X shown in the last section correlate quite well with the electronegativities (EN) of the halogen atoms. Figure 4-7 shows a plot of the $(\Delta P)^{X}_{\tau}$ vectors *vs.* EN for the halogen atoms. As the EN of the X atom

TABLE 4-4

THE $(\Delta P)^{H}_{x'}$ VECTORS AND ANGLE θ^{x} FOR THE MOTION OF H PARALLEL TO THE X' AXIS[a]

	$(\Delta P)^{H}_{x'}$ (e A)	θ^{b}_{x} (degrees)
CH_3F	0.014 ± .011	61.5 ± 55.8
CH_3Cl	0.043 ± .006	303.3 ± 11.9
CH_3Br	0.065 ± .006	298.7 ± 6.6
CH_3I	0.076 ± .016	300.2 ± 7.1

a. The errors were computed as described previously for the $(\Delta P)^{H}_{z'}$ vectors.
b. θ is measured as a clockwise rotation from the CH bond axis to $(\Delta P)^{H}_{x'}$, as seen by looking down the positive y' axis centered on the H atom.

Figure 4-6: The $(\Delta P)^{H}_{\text{parallel}^{x'}}$ vectors for the displacement of H parallel to the x' axis for the methyl halides.

The H atom displacement relative to the molecular frame is shown by the bold arrow labelled $\delta x'$. The direction of the permanent dipole moment is also shown.

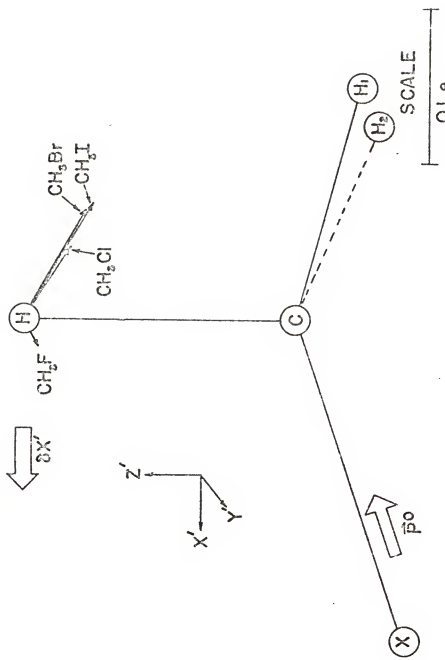
H
C
X
H1
H2
CH2F
CH2Cl
CH2Br
CH2I
δX'
p0
Z'
X'
Y'
SCALE
0.1 e

Figure 4-7: A plot of the magnitude of the $(\Delta P)_r^X$ vectors against the electronegativity of the halogen atoms.

The electronegativity values of the halogen atoms were taken from M.C. Day and J. Selbin, Theoretical Inorganic Chemistry (Rienhold Publishing Company, New York, 1962), p. 114.

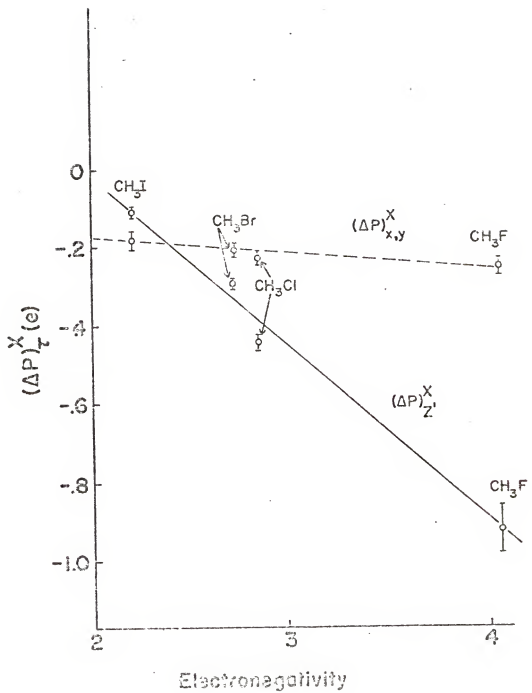
0
-.2
-.4
-.6
-.8
-1.0
$(\Delta P)^X_Z$ (e)
CH_3I
CH_3Br
CH_3Cl
CH_3F
$(\Delta P)^X_{x,y}$
$(\Delta P)^X_{Z'}$
CH_3F
2
3
4
Electronegativity

increases, the magnitude $|(\Delta P)^X_z|$ increases, with quite a steep slope (nearly 0.7). On the other hand, the magnitudes $|(\Delta P)^X_x|$ and $|(\Delta P)^X_y|$, are almost independent of the EN changes (see Figure 4-7).

By applying the simple model for the dipole moment change developed by Bruns and Person (37) for the diatomic hydrides, HY, (Y = B, C, N, O, and F), we can attempt to separate different contributions to the $(\Delta P)^X_z$ vectors and to rationalize the observed trends in the $(\Delta P)^X_z$ vectors with EN. In order to do so, we make two additional assumptions. The first assumption is that the "out-of-plane" $(\Delta P)^X_y$ vectors reflect only the dipole moment change generated by moving the fixed charge on the halogen atoms out of the plane, to give $(\Delta P)_1$. (Bruns and Person refer to this as q_1.) This assumption is reasonable since this vector is essentially constant, indicating that the fixed (equilibrium) charge on X is nearly the same for each halogen for the series; furthermore, one would not expect the rehybridization moment to contribute an appreciable amount to this motion. The second assumption involves the rehybridization term $(\Delta P)_{sp}$ (called q_{sp} by Bruns and Person). We shall assume that this term is constant for the CH_3X series, by analogy with the HY series; moreover, we shall assume the same constant value for $(\Delta P)_{sp}$ as Bruns and Person calculated for the HY series {$(\Delta P)_{sp}$ = +0.20 e}. The model, based on the CNDO/2 breakdown of contributions to the total dipole moment (14), assumes that the contributions to the dipole moment change vectors, $(\Delta P)^\alpha_\tau$, come from three

different terms:

$$(\Delta P)^{\alpha}_{\tau} = (\Delta P)^{\alpha}_{1} + (\Delta P)^{\alpha}_{2} + (\Delta P)^{\alpha}_{hyb} \quad , \qquad (4\text{-}4)$$

where $(\Delta P)^{\alpha}_{1}$ is the dipole moment change due to the equilibrium charge on each atom, and $(\Delta P)^{\alpha}_{2}$, called q_2 by Bruns and Person, is the dipole moment change due to the change in the charge when the C-X bond is stretched. The $(\Delta P)^{\alpha}_{hyb}$ term contains the contribution to the dipole moment change due to the rehybridization (or polarization) during bond stretching. For the first row elements $(\Delta P)^{\alpha}_{hyb}$ consists only of sp contributions, $(\Delta P)_{sp}$, but for second row elements, both sp and pd contributions are present $\{(\Delta P)_{hyb} = (\Delta P)_{sp} + (\Delta P)_{pd}\}$. In Table 4-5, the resulting breakdown into the different contributions is given. If the model is correct, the observed trend in $(\Delta P)^{X}_{z}$ is due to the trend for the $(\Delta P)_2$ and/or the $(\Delta P)_{pd}$ terms. At this point, we cannot further separate the $(\Delta P)_2$ and $(\Delta P)_{pd}$ terms, for it is not clear whether one dominates, or what is the percentage that each term contributes to the total $\{(\Delta P)^{X}_{2} + (\Delta P)^{X}_{pd})\}$.

These results can be contrasted with those obtained from the HY series (37). In that series, the $(\Delta P)_1$ vectors varied as Y is changed across the periodic table with increasing atomic number (and presumably EN), while the $(\Delta P)_2$ vectors were constant. For the CH_3X series, variation of X down the column of the periodic table (Z constant but EN changes) changes $(\Delta P)_2$ but not $(\Delta P)_1$.

TABLE 4-5

MAGNITUDE OF THE DIFFERENT CONTRIBUTIONS TO THE HALOGEN $(\Delta P)_z^X$ VECTORS

(Units are e·Å)

Molecule	$(\Delta P)_z^{X\,a}$	$(\Delta P)_2^X + (\Delta P)_{hyb}^{X\,b}$	$(\Delta P)_2^X + (\Delta P)_{pd}^{X\,c}$
CH_3F	-0.93	-0.70	-0.90[d]
CH_3Cl	-0.45	-0.22	-0.42
CH_3Br	-0.30	-0.07	-0.27
CH_3I	-0.12	+0.11	-0.09

a. Taken from Table 4-1.
b. The values of $(\Delta P)_y^X$ for the CH_3X series were averaged to give $(\Delta P)_1^X = -0.23$ e·Å; this number is subtracted from the $(\Delta P)_z^X$ values to obtain the number in this column.
c. These numbers were obtained by subtracting the constant value of $(\Delta P)_{sp} = +0.20$ e·Å, given by Bruns and Person (37), from numbers in the second column.
d. The value of $(\Delta P)_{pd}^F$ is expected to be negligible.

The magnitudes of the $(\Delta P)^{H}_{z'}$ vectors are plotted against EN in Figure 4-8. Again we find a fairly good linear relationship between $(\Delta P)^{H}_{z'}$ (and also $\theta_{z'}$) and EN. A similar plot for the $(\Delta P)^{H}_{x'}$ vectors is shown in Figure 4-9. Here the errors are quite large, but the same trend is discernible. The angles $\theta_{x'}$ for the $(\Delta P)^{H}_{x'}$ vectors are almost independent of EN within the uncertainties in $\theta_{x'}$. It is interesting to note that $(\Delta P)^{H}_{z'}$ increases, while $(\Delta P)^{H}_{x'}$ decreases by almost the same amount, with increasing EN.

The magnitude $|(\Delta P)^{H}_{y'}|$ is independent of EN within experimental error, as shown in Figure 4-10. This "out-of-plane" motion is quite insensitive to a change in the halogen atom and appears to be quite transferrable in the series.

Assuming that the $(\Delta P)^{H}_{y'}$ vectors measure the contribution from motion of the static charge, as we did in discussing the $(\Delta P)^{X}_{z}$ vectors, we calculated the contributions to the hydrogen vectors $(\Delta P)^{H}_{z'}$ and $(\Delta P)^{H}_{x'}$ that come from $(\Delta P)_2$ and $(\Delta P)_{hyb}$. We did not attempt an additional breakdown of $(\Delta P)_{hyb}$ into $(\Delta P)_{sp}$ and $(\Delta P)_{pd}$ since the motion of the hydrogen atoms was not expected to result in an appreciable contribution from $(\Delta P)_{hyb}$. We note that $(\Delta P)_1$ is a vector parallel to the displacement $\delta x'$ or $\delta z'$. The data for $(\Delta P)^{H}_{z'}$ and for $(\Delta P)^{H}_{x'}$, are given in Tables 4-6 and 4-7, respectively.

As Tables 4-6 and 4-7 indicate, the observed trends (Figures 4-8, 4-9) are due to the change in the $(\Delta P)_2$ + $(\Delta P)_{hyb}$ vectors as the electronegativity changes. If the $(\Delta P)_{hyb}$ term is nearly constant down the series of halogens,

Figure 4-8: A plot of the magnitude of the $(\Delta P)_z^H$ vectors against the electronegativity of the halogen atoms.

See the reference in Figure 4-7 for the electronegativity data.

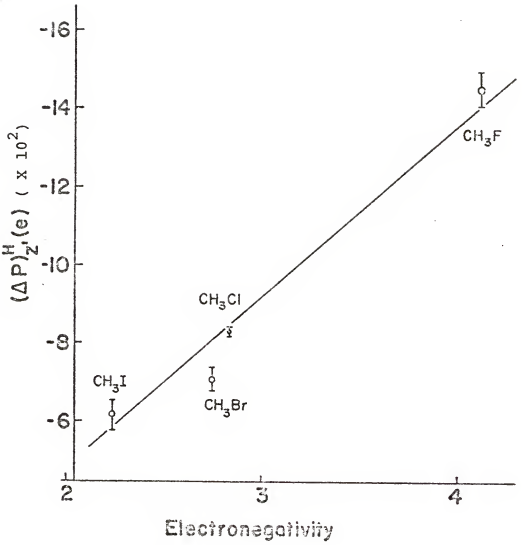
-16
-14
-12
-10
-8
-6
$(\Delta P)^{H}_{Z'}(e)$ (x 10^2)
CH_3F
CH_3Cl
CH_3I
CH_3Br
2
3
4
Electronegativity

Figure 4-9: A plot of the magnitudes of the $(\Delta P)^{H}_{X}$, vectors against the electronegativity of the halogen atoms.

See the reference in Figure 4-7 for the electronegativity data.

Figure 4-10: A plot of the magnitude of the $(\Delta P)^{H}_{y}$, vectors against the electronegativity of the halogen atoms.

See reference in Figure 4-7 for the electronegativity data.

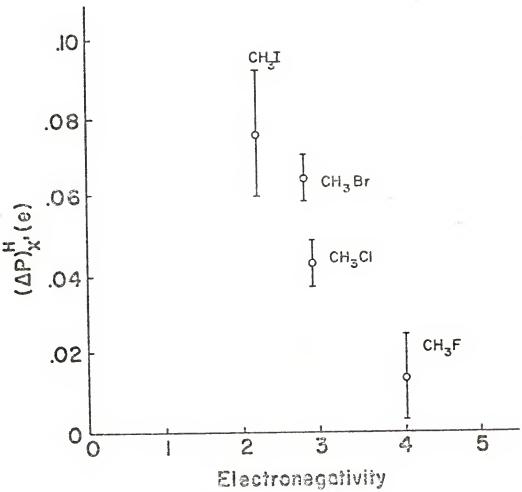
.10
.08
.06
.04
.02
0
$(\Delta P)^H_X$, (e)
CH_3I
CH_3Br
CH_3Cl
CH_3F
0
1
2
3
4
5
Electronegativity

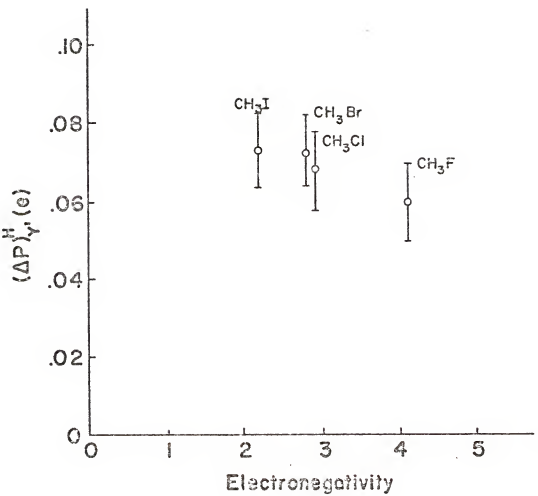
.10
.08
.06
.04
.02
0
$(\Delta P)^H_{\gamma'}$ (e)
CH_3I
CH_3Br
CH_3Cl
CH_3F
0
1
2
3
4
5
Electronegativity

TABLE 4-6

MAGNITUDE OF THE DIFFERENT CONTRIBUTIONS TO THE HYDROGEN $(\Delta P)^H_z$, TERMS
(Units are e·Å)

	$(\Delta P^H_{z'})_{z'}$ [a]	$(\Delta P^H_{z'})_{x'}$ [b]	$\{(\Delta P_2 + (\Delta P)_{hyb}\}_{z'}$ [c]	$\{(\Delta P_2 + (\Delta P)_{hyb}\}$ [d]
CH_3F	-0.143	+0.021	-0.213	+0.021
CH_3Cl	-0.061	+0.056	-0.131	+0.056
CH_3Br	-0.042	+0.057	-0.112	+0.057
CH_3I	-0.028	+0.055	-0.098	+0.055

a. These values are z' components of $(\Delta P^H_{z'})$, or the $\partial p^H_z/\partial z'$ tensor elements given in Table 4-2.
b. These are the x' components of $(\Delta P^H_{z'})$, or the values of $\partial p_{x'}/\partial z'$ from the tensor elements of Table 4-2.
c. These values were computed from the first column by averaging the $(\Delta P)^H_y$, vectors in Table 4-2 for the CH_3X series, assuming $(\Delta P)_1 = +0.070$ and subtracting this value from the first column.
d. These are the x' components of $(\Delta P)_2 + (\Delta P)_{hyb}$.

TABLE 4-7

MAGNITUDES OF THE DIFFERENT CONTRIBUTIONS TO THE HYDROGEN $(\Delta P)^{H}_{x',a}$ TERMS
(Units are e·Å)

	$(\Delta P^{H}_{x',})^{a}_{x'}$	$(\Delta P^{H}_{x',})^{b}_{z'}$	$\{(\Delta P)_2 + (\Delta P)_{hyb}\}^{c}_{x'}$	$\{(\Delta P)_2 + (\Delta P)_{hyb}\}^{d}_{z'}$
CH_3F	0.012	-0.007	-0.058	-0.007
CH_3Cl	-0.036	-0.024	-0.106	-0.024
CH_3Br	-0.057	-0.031	-0.127	-0.031
CH_3I	-0.066	-0.038	-0.136	-0.038

a. These values are the x' components of $(\Delta P)^{H}_{x',a}$ or the values of $\partial p_x/\partial x'$ taken from Table 4-2.
b. These values are the z' components of $(\Delta P)^{H}_{x',a}$ or the values of $\partial p_{z'}/\partial x'$ taken from Table 4-2.
c. These values are the x' components, computed from the first column as in Table 4-6.
d. These values are the z' components, computed as before (in Table 4-6).

$(\Delta P)_2$ must be causing the trend. We see that $(\Delta P)_2$ for the $\delta x'$ displacement becomes more negative by nearly a factor of two down the series from CH_3F to CH_3I, while $(\Delta P)_2$ for the $\delta z'$ displacement becomes less negative by about the same factor.

This discussion has suggested one possible approach to rationalizing the trends found empirically in examining the vectors giving the dipole moment changes. In Chapter 5, we shall return to this simple approach and compare the results with contributions calculated by the CNDO/2 procedure, and show that our model is, perhaps, too simple.

There are other effects that could contribute to the observed trends in the $(\Delta P)_\tau^\alpha$ vectors which we have not considered explicitly. For example, we did not specifically include in our model the effect of dipole-dipole, charge-dipole, and charge-charge induction effects on the dipole moment changes, and these effects should be considered in any quantitative explanation of the observed trends. There may or may not be a cause-and-effect relationship between EN and the observed trends in the $(\Delta P)_\tau^\alpha$ vectors, although our results suggest that the EN of the halogen is an important factor. Keep in mind, however, that EN correlated with many fundamental quantities such as atomic number, or electron density, so that a correlation with EN may reflect a correlation with a more fundamental and theoretically sound principle that is hidden in the qualitative EN numbers (38).

The significance of the correlation of the $(\Delta P)_\tau^\alpha$ vectors

with EN is that there is a smooth trend that may be useful for predicting polar tensors of these atoms in other molecules. The insensitivity of the $(\Delta P)^H_y$, and $(\Delta P)^X_y$, vectors to EN certainly suggests that these quantities may be quite transferable.

Correlations with Atomic Polarizability

The atomic polarizability, α_x, of the halogen atoms is another parameter that might be expected to correlate with the $(\Delta P)^H_\tau$ vectors. The atomic polarizability of X may affect $(\Delta P)^H_\tau$ because the moment induced in X by the oscillating dipole from the motion of the hydrogen atom may add a term to the intrinsic values of $(\Delta P^0)^H_\tau$ that is proportional to α. This induced moment is expected to contribute to the deviation of the direction of $(\Delta P)^H_z$, or $(\Delta P)^H_x$, from the direction of motion since the induced moment $(\Delta P)_{ind}$ is not parallel to the direction of motion, and $(\Delta P)^H_\tau = (\Delta P^0)^H_\tau + (\Delta P)_{ind}$.

A plot of $(\Delta P)^H_z$ *vs.* the atomic polarizabilities of the halogen atoms is shown in Figure 4-11. The magnitude $(\Delta P)^H_z$, decreases smoothly as the polarizability of X increases, implying an induced moment that opposes the direction of the intrinsic moment. A plot of θ_z *vs.* the atomic polarizabilities is shown in Figure 4-12; as the polarizability of X increases, θ is found to increase smoothly in qualitative agreement with the preceding.

A plot of $(\Delta P)^H_x$, *vs.* the atomic polarizability is given in Figure 4-13. Within experimental error, there is a linear

Figure 4-11: A plot of the magnitude of the $(\Delta P)^{H}_{z'}$ vectors against the atomic polarizabilities of the halogen atoms.

The atomic polarizabilities of the halogen atoms were taken from Reference 39.

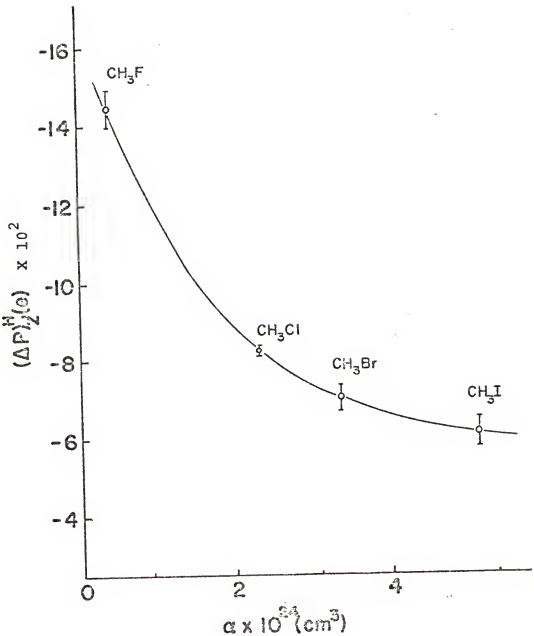
-16
-14
-12
-10
-8
-6
-4
$(\Delta P)^{H}_{l,l}(a)$ x 10^2
CH_3F
CH_3Cl
CH_3Br
CH_3I
0
2
4
$a \times 10^{24}(cm^3)$

Figure 4-12: A plot of the angle θ_z against atomic polarizability of the halogen atoms for displacement of H along z'.

See Reference 39 for atomic polarizability data.

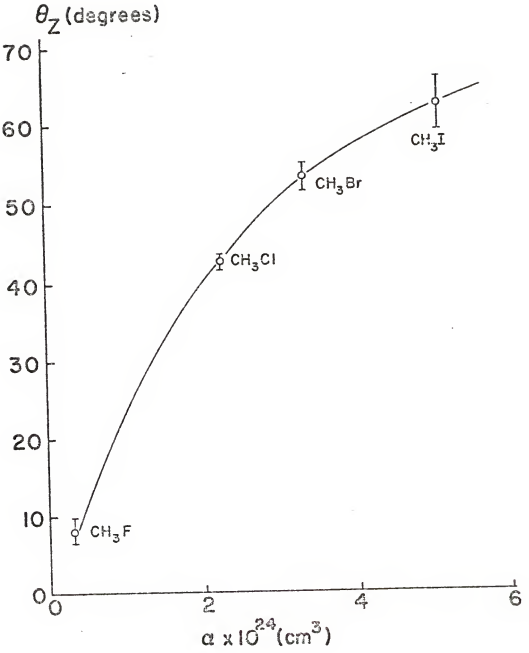
θ_Z (degrees)
70
60
50
40
30
20
10
0
0
2
4
6
$\alpha \times 10^{24}$ (cm^3)
CH_3F
CH_3Cl
CH_3Br
CH_3I

Figure 4-13: A plot of the magnitude of the $(\Delta P)^{H}_{x'}$ vectors against the atomic polarizability of the halogen atoms.

See Reference 39 for atomic polarizability data.

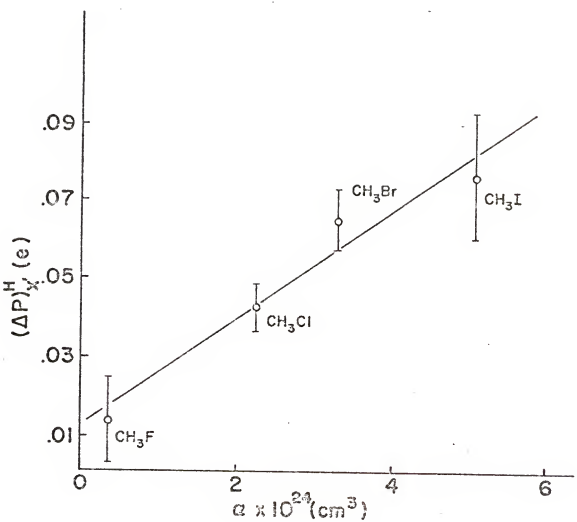
.09
.07
.05
.03
.01
$(\Delta P)^H_{\chi'}$ (e)
CH_3Br
CH_3I
CH_3Cl
CH_3F
0
2
4
6
$\alpha \times 10^{24}(cm^3)$

correlation between $(\Delta P)^{H}_{x'}$ and the polarizability of the halogen atoms, in contrast with the curve found for $(\Delta P)^{H}_{z'}$. There is no change in θ_x with a change in the X atom within experimental error, except possibly for CH_3F.

The $(\Delta P)^{H}_{y'}$ vectors are parallel to y'. A plot of the $(\Delta P)^{H}_{y'}$ vectors vs. the atomic polarizabilities of the X atoms is given in Figure 4-14. The $(\Delta P)^{H}_{y'}$ vectors are constant within experimental error and independent of changes in the polarizability of the X atom.

In order to determine whether the contribution from the induced moments in the halogen atoms are expected to be as large as required to explain these results (see discussion above), we carried out the following simple calculation. We assumed that an oscillating point dipole with a magnitude and direction equal to that of the z' component of $(\Delta P)^{H}_{z'}$ (and to that of the x' component for $(\Delta P)^{H}_{x'}$,) was located at the hydrogen atom. Using the atomic polarizability, α, of the halogen atoms (39), we calculated the polar coordinate components of the dipole induced at the halogen atom, $\vec{\mu}_r$ and $\vec{\mu}_\Phi$ (40) using

$$\vec{\mu}_r = 2\alpha\, P^{H}_{\tau}\, (\cos\Phi/r^3) \qquad (4\text{-}5)$$

and

$$\vec{\mu}_\Phi = \alpha P^{H}_{\tau}\, (\sin\Phi/r^3) \quad . \qquad (4\text{-}6)$$

Here P^{H}_{τ}, the components of the $(\Delta P)^{H}$ vectors, are co-linear with the direction of motion of the H atom along the τ axis; (τ = z' or x'); r is the distance from the point dipole to

Figure 4-14: A plot of the magnitudes of the $(\Delta P)^{H}_{y'}$ vectors against the atomic polarizability of the halogen atoms.

See Reference 39 for the atomic polarizability data.

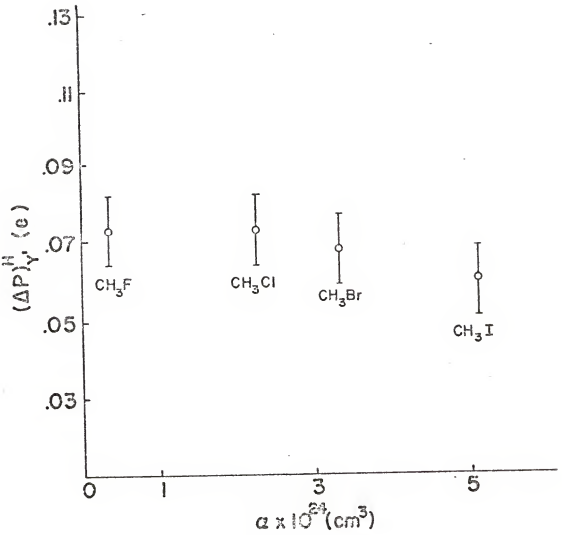
.13
.11
.09
.07
.05
.03
$(\Delta P)^{H}_{V'}$ (e)
CH_3F
CH_3Cl
CH_3Br
CH_3I
0
1
3
5
$\alpha \times 10^{24}$ (cm^3)

the polarizable halogen atom and Φ is the angle between the axis of the dipole and the $\vec{r}$ vector, as defined in Figure 4-15.

The $\vec{\mu}_r$ component of the induced moment is positive in the same sense as $\vec{r}$, and the $\vec{\mu}_\Phi$ component is perpendicular to $\vec{r}$ and has the same directional sense as Φ, defined in Figure 4-15. The resulting induced moment $\vec{\mu}_i$ is just the vector sum of the two components. With a knowledge of the molecular geometry and of these calculated values of $\vec{\mu}_r$ and $\vec{\mu}_\Phi$, $\vec{\mu}_i$ can be transformed back to the rotated Cartesian coordinate axes (x', y' z') to find the contribution from $\vec{\mu}_i$ to $(\Delta P)^H_{z'}$. The data required to calculate $\vec{\mu}_i$ for each methyl halide are given in Table 4-8, as are the calculated induced components $\vec{\mu}_r$ and $\vec{\mu}_\Phi$. These values are converted to the resultant induced moment $\vec{\mu}_i$ and the calculated contributions to $(\Delta P)^H_{z'}$ are compared with experimental values.

We see in Table 4-8 that the dipole induced on the halogen atom due to the dipole in the C-H bond generated when the H atom is displaced by $\delta z'$ is calculated to have a qualitative resemblance to the experimental behavior of $(\Delta P^H_{z'})$. This can be seen by comparing the calculated x' components of $\vec{\mu}_i$ with the experimental values of $(\Delta P^H_{z'})_{x'}$ shown in Table 4-8 in parentheses. We see that this estimated induced moment, if added vectorially to an intrinsic moment $(\Delta \vec{P}^0)^\alpha_\tau$ directed along the C-H bond, gives a resultant value of $(\Delta P)^H_{z'}$, $\{= (\Delta \vec{P}^0)^\alpha_\tau + \vec{\mu}_i\}$ that behaves qualitatively like the observed value, in terms of its trend with changing

Figure 4-15: A schematic diagram of the model used for calculating the induced moments in the halogen atoms assuming an oscillating unit dipole at the hydrogen atom parallel to the C-H bond.

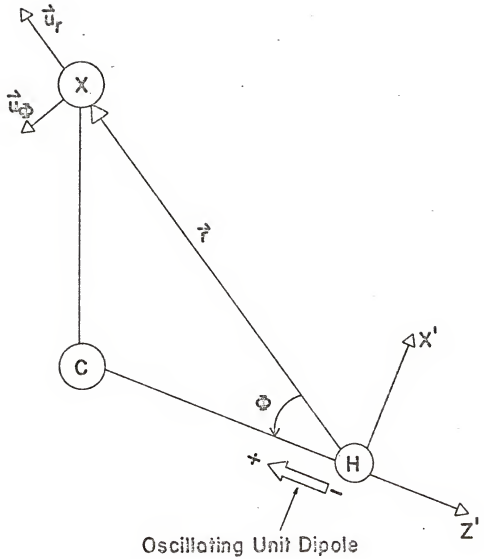
X
C
H
X'
Z'
Oscillating Unit Dipole

TABLE 4-8

DATA AND RESULTS FOR THE CALCULATION OF THE INDUCED MOMENT IN X FOR THE MOTION OF H PARALLEL TO Z'

	α[a] ($\times 10^{24}$ cm^3)	r[b] (Å)	ϕ[b] (deg.)	$\lvert\vec{\mu}_r\rvert$ (e·Å)	$\lvert\vec{\mu}_\phi\rvert$ (e·Å)	$\lvert\vec{\mu}_i\rvert$ (e·Å)	$(\Delta P^H_{z'})_{x'}$ (e·Å)	$(\Delta P^H_{z'})_{z'}$ (e·Å)	γ[c] (deg.)	$\theta_{z'}$ (deg.)
CH_3F	0.38	2.02	40.6	0.010	0.004	0.011	0.010 (+0.021)[d]	-0.005	26.3	3.8 (8.2)[e]
CH_3Cl	2.28	2.35	45.9	0.015	0.008	0.017	0.016 (+0.056)	-0.005	16.7	13.7 (42.9)
CH_3Br	3.34	2.49	47.9	0.012	0.007	0.014	0.014 (+0.057	-0.003	13.1	16.8 (53.5)
CH_3I	5.11	2.66	50.0	0.010	0.006	0.011	0.011 (+0.055)	-0.002	9.2	20.5 (62.7)

a. Taken from Reference 39.
b. Calculated from geometry of the molecule as given in Table AI-2.
c. The angle γ is defined as the angle between the C-H bond axis (z') and the $\vec{\mu}_i$ vector, and has the sense of a clockwise direction of rotation from the C-H bond when looking down the y' axis centered on the H atom.
d. Values in parentheses are experimental values from Table 4-6.
e. Values in parentheses are experimental values of $\theta_{z'}$ from Table 4-3.

X. This trend is shown in Figure 4-16, which pictures the vector addition, showing the apparent increase in $\theta_{z'}$, with decreasing EN as the magnitude (and direction) of $\vec{\mu}_i$ changes relative to the intrinsic moment ($\Delta\vec{P}_0$).

We note that the magnitude of the z' component of the induced moment is estimated to be so small as to be negligible, compared to the z' component of the intrinsic moments.

In conclusion, the induced dipole may contribute somewhat to the apparent "rotation" of $(\Delta P)^H_{z'}$, with changing X, since the effect of the induced moment is qualitatively in agreement with the observed behavior. However, the magnitude calculated for this effect is much smaller than observed, so that we must conclude that the induced moment makes only a very small contribution to the observed effect. (See the comparison between calculated and experimental $\theta_{z'}$ values.)

The calculation of the induced moment due to the oscillating dipole parallel to the x' axis and the associated angles is presented in Table 4-9. The coordinates are defined in Figure 4-17. From the table we see that generally the dipole induced moment is smaller for the $(\Delta P)^H_{x'}$ vectors than for the $(\Delta P)^H_{z'}$ vectors in Table 4-8. In the case of the x' components of $\vec{\mu}_i$, the errors in the experimental values are about the same as the calculated induced moment components. These calculated z' components of $\vec{\mu}_i$ are a little larger than the x' components, but are still quite small. One must conclude again that the effect due to the induced moment is small, and that it does not explain the observed trends.

Figure 4-16: The resultant vectors for the addition of $\vec{\mu}_i$ and $(\Delta P^o)^H_{z'}$.

The intrinsic dipole moment change vector, $(\Delta P^o)^H_{z'}$, is assumed to be equal to the z' component of the $(\Delta P)^H_{z'}$ vector. The angle θ_z is measured from the C-H bond axis.

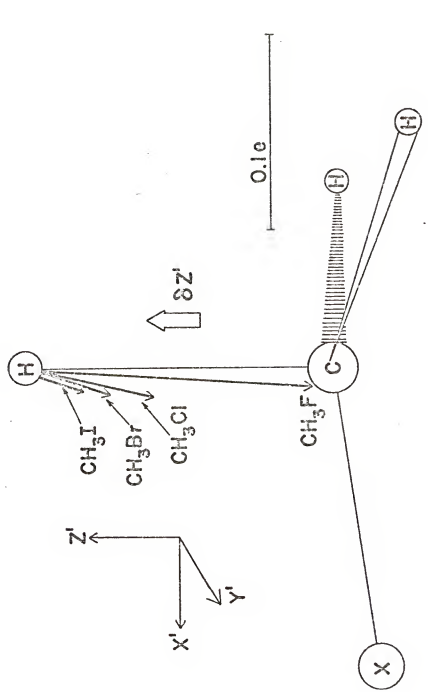
H
C
H
H
X
CH_3F
CH_3Cl
CH_3Br
CH_3I
$\delta Z'$
0.1e
Z'
Y'
X'

TABLE 4-9

DATA AND RESULTS FOR THE CALCULATION OF THE INDUCED MOMENT IN X FOR THE MOTION OF H PARALLEL TO X'

	$\lvert\vec{\mu}_r\rvert$ (e·Å)	$\lvert\vec{\mu}_\phi\rvert$ (e·Å)	$\lvert\vec{\mu}_i\rvert$ (e·Å)	$(\vec{\mu}_i)_{x'}$[a] (e·Å)	$(\vec{\mu}_i)_{z'}$[a] (e·Å)	γ[b] (degrees)	$\theta_{x'}$[c] (degrees)
CH_3F	0.0007	0.004	0.0008	0.000 (0.012)	0.001 (-0.007)	10.3	86.1 (61.5)
CH_3Cl	-0.009	-0.004	0.0010	-0.003 (-0.036)	+0.009 (-0.024)	-20.1	256.5 (303.3)
CH_3Br	-0.018	-0.008	0.0200	+0.008 (-0.057)	+0.018 (-0.031)	-23.6	254.1 (298.7)
CH_3I	-0.027	-0.011	0.0296	-0.014 (-0.066)	+0.026 (-0.038)	-27.2	251.7 (300.2)

a. The experimental values of $(\Delta P^H_{x'})_{x'}$ and $(\Delta P^H_{x'})_{z'}$, , respectively.
b. The angle γ is defined as the angle between the C-H bond axis (z') and the $\vec{\mu}_i$ vector, and has the sense of a clockwise direction of rotation from the C-H bond when looking down the y' axis centered on the H atom.
c. θ is the angle between +z' and $\vec{\mu}_\phi$, and is defined as a clockwise rotation of $\vec{\mu}_\phi$ from +z' as seen by looking down the +z' axis centered on the H atom.

Figure 4-17: A schematic diagram of the model used for calculating the induced moments in the halogen atoms assuming an oscillating unit dipole at the hydrogen atom perpendicular to the C-H bond.

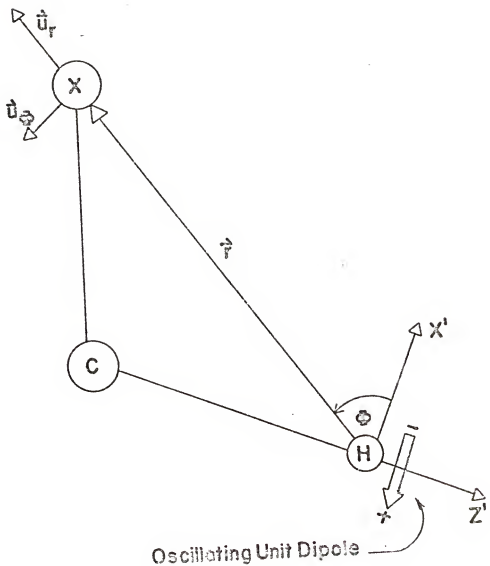
$\hat{U}_r$
X
$\hat{U}_\phi$
$\vec{r}$
C
X'
H
$\vec{l}$
Z'
Oscillating Unit Dipole

The dipole induced moment for the motion of H parallel to y' can be calculated using the model discussed above. In this instance, however, there is only one non-zero component of $\vec{\mu}_i$; namely, the $\vec{\mu}_\Phi$ component. Since $\Phi = 90^o$, Equation 4-5 becomes zero and Equation 4-6 reduces to

$$\vec{\mu}_\Phi = (\Delta P_{y'}/r^3) \cdot \alpha \quad . \tag{4-7}$$

The dipole induced moments are parallel to the y' axis and in the opposite direction to the $(\Delta P)^H_{y'}$ vectors. The induced moments are given in Table 4-10. For CH_3Cl, CH_3Br, and CH_3I, the calculated induced moment is essentially constant, as Equation 4-7 suggests. The magnitudes of $\vec{\mu}_i$ are comparable to the errors in $(\Delta P)^H_{y'}$, which seems to support our earlier hypothesis that the dipole moment change for this "out-of-plane" motion is due only to the motion of the fixed charge on the hydrogen atom.

The simple calculation of the induced moment in the halogen atom has qualitatively reproduced some of the observed trends in the experimental results; however, the model is by no means quantitative. We have neglected some effects which may be just as important as the induced moments. For example, we completely neglected the charge effect of the hydrogen, halogen, and the methyl carbon in our simple approach.

As was the case in the correlations with EN, the trends exhibited by the experimental vectors are the important features. The simple model of the induced dipole effect was

TABLE 4-10

THE DIPOLE INDUCED MOMENT FOR MOTION OF H PARALLEL TO Y'

	$\vec{\mu}_i$ [a] (electrons)
CH_3F	-0.003 (0.073)
CH_3Cl	-0.013 (0.073)
CH_3Br	-0.015 (0.068)
CH_3I	-0.016 (0.060)

a. The values in parentheses are the experimental $(\Delta P)^H_{Y'}$ vectors.

suggested as one possible effect that should contribute to the observed trends. The calculations suggest that it is actually of minor importance.

Effective Charges

King, Mast and Blanchette (KMB) (10) first introduced the concept of effective charge of the αth atom, ξ_α , relating it to the intensity sum rule of Crawford (11). They found for hydrocarbons with symmetrically equivalent hydrogen atoms that:

$$(n_H/m_H)\,\xi_H^2 + (n_C/m_C)\,\xi_C^2 = K\sum A_i + \Omega \ . \qquad (4\text{-}8)$$

Here n_α and m_α are the number of atoms of type α and their masses, Ω is the rotational correction. If data for the completely deuterated isotopes are available, a corresponding equation can be written for the isotopically substituted species (with $\xi_H = \xi_D$, $n_H = n_D$) and the two equations solved for the resulting ξ_H value. By this procedure, KMB obtained a set of ξ_H values from the various hydrocarbons whose intensities had been studied; the values of ξ_H were surprisingly constant for the entire series and appeared to be quite transferrable for the molecules for which data were available.

For the CH_3X compounds, KMB calculated the effective charge ξ_H on the hydrogen atoms from the intensity sums for CH_3X and CD_3X, as described for the hydrocarbons, but they were not able to resolve the effective charge for the CX group into the atomic effective charges, ξ_C and ξ_X. Instead, they determined an apparent effective charge for the CX group:

$$\xi_{CX}^2 = (\mu_C \xi_C^2 + \mu_X \xi_X^2)/(\mu_C + \mu_X) \quad . \tag{4-9}$$

From the point of view of the atomic polar tensors, the effective charge is given by Equation 2-31. Using that equation, we see that ξ_α is an important invariant of the atomic polar tensors. It is clear that $\xi_\alpha = |\partial\vec{P}/\partial\vec{R}_\alpha|$, so that ξ_α is the magnitude of the gradient of the dipole moment. Furthermore, this gradient is given by the vector sum of the ΔP^α vectors defined above:

$$\partial\vec{P}/\partial\vec{R}_\alpha = \Delta P_x^\alpha + \Delta P_y^\alpha + \Delta P_z^\alpha \quad . \tag{4-10}$$

The effective charges, ξ_H , ξ_X , and ξ_C for the atoms in the methyl halide molecules are given in Table 4-11, along with the values computed by KMB from the intensity sums of CH_3X and CD_3X. The agreement between the values for ξ_H and ξ_{CX} found by KMB and the values we found is probably about as good as can be expected, considering the rather large errors in the infrared intensity sums. KMB estimated that the propagated error in ξ_C is nearly as large as ξ_C itself; the propagated errors in ξ_H are smaller, however, and nearly the same as the differences here between the ξ_H values.

Examining Table 4-11, we see that the values of ξ_H for the methyl halides from our analysis are nearly the same (within experimental error) as the average value for ξ_H in hydrocarbons ($\xi_H = 0.15$ e), thus supporting the suggestion by KMB that these quantities may be transferable. In order to examine this question further, we include in Table 4-11 values

TABLE 4-11

EFFECTIVE CHARGES (IN e) FOR THE ATOMS IN SOME CH_3X AND CX_4 MOLECULES

Compound	ξ_H[a] (this work)	ξ_H[b] (KMB)	ξ_X[a] (this work)	ξ_X[b] (KMB)	ξ_C[a] (this work)
CH_4	---	0.172	---		---
CH_3F	0.164 ±0.007	---	1.000 ±0.004	---	1.063 ±0.417
CH_3Cl	0.119 ±0.003	0.129	0.557 ±0.002	0.55	0.588 ±0.060
CH_3Br	0.119 ±0.001	0.132	0.426 ±0.003	0.43	0.542 ±0.022
CH_3I	0.117 ±0.006	0.132	0.291 ±0.003	0.30	0.374 ±0.061
CF_4[c]	---	---	1.043	---	2.98
CCl_4[c]	---	---	0.64 (or 0.72)[d]	---	2.06 (or 2.02)[d]

(continued to next page)

(Table 4-11, continued)

a. The errors were estimated by taking the absolute difference between the effective charge of CH_3X and CD_3X.
b. Taken from Reference 10. For CH_3X compounds we list ξ_X from KMB.
c. Estimated from the intensity sums (see text).
d. Alternate value of $\partial\vec{p}/\partial R$ used here.

of effective charges calculated from the intensity sums for CF_4 and CCl_4. We use equation 4-11:

$$K\sum A_i = (4.0\ \xi_x^2\ \ \mu_x + \xi_C^2\ \mu_C)\ , \qquad (4\text{-}11)$$

since $\Omega = 0$ for these non-polar molecules. Here K is $(1.537 \times 10^{-2}/4.8)^2$ (41), μ_X and μ_C are the inverse masses (amu) of the X and C atoms, and $\sum A_i$ is the intensity sum (cm mmole^{-1}) of the infrared-active fundamental modes of vibration.

In order to separate ξ_F and ξ_C in CF_4, we recall that for tetrahedral symmetry with z along the CF bond:

$$P_X^F = \begin{pmatrix} \partial p_x/\partial x_F & 0 & 0 \\ 0 & \partial p_y/\partial y_F & 0 \\ 0 & 0 & \partial p_z/\partial z_F \end{pmatrix} .$$

Here $(\partial p_x/\partial x_F) = (\partial p_y/\partial y_F)$, and it is reasonable to assume that it is the same value (- 0.25 e) as found for the CF bond in CH_3F. We can estimate $(\partial p_z/\partial z_F)$ in several ways -- for example, assume that ξ_F is the same in CF_4 as in CH_3F and then obtain $\partial p_z/\partial z_F$ from Equation 4-10. Alternatively, we can obtain $\partial p_z/\partial z_F$ from the value given by Levin and Lewis (42) for $\partial \vec{p}/\partial R_{CF}$, realizing that $\partial \vec{p}/\partial R_{CF} = \partial p_z/\partial z_F$. Since the latter is readily available, we obtain $\partial p/\partial z_F$ from $\partial p_z/\partial R_z = -0.984$ e. From this value, and the value above for $\partial p_x/\partial x_F$ (- 0.25 e),

we calculate $\xi_F = 1.043$. Then, using Equation 4-11, we find $\xi_C = 2.98\ \underline{e}$. The values for CCl_4 are obtained in a similar fashion, using the value of $-0.544\ \underline{e}$ (or $-0.628\ \underline{e}$) for $\partial\vec{p}/\partial R_{CCl}$ from Lindsay and Schatz (43).

From the results given in Table 4-11 for ξ_F from CH_3F and CF_4, and for ξ_{Cl} from CH_3Cl and CCl_4, we conclude that ξ_F and ξ_{Cl} are nearly transferable, as is ξ_H. The average effective charge found by KMB for the hydrocarbons ($\xi_H = 0.15\ \underline{e}$) was somewhat larger than the average given in Table 4-11 for the four methyl halides. This difference in values is only slightly larger than experimental error; in fact, we believe the values are probably the same within experimental error, although it is possible that ξ_H may depend somewhat on the substituent X groups in X-C-H molecules.

Notice that ξ_C is nearly exactly equal to ξ_X for the CH_3X compounds. {We remember that $\partial\vec{p}/\partial R_C$ must have a sign opposite (positive here) that for $\partial\vec{p}/\partial R_F$ (negative here).} This equality implies that the vector sum of the gradients $(\partial\vec{p}/\partial R_H)$ for the three H atoms is zero for each one of the methyl halides.

The value of ξ_C for the C atom in CF_4, for example, is related to ξ_F, since (see Equation 2-33):

$$\sum_{\alpha} P_x^{\alpha} = 0.$$

For the Cartesian coordinate systems we have been considering (CF_1 bond defines the z axis), $(\Delta P)_x^C$ is diagonal and the tetrahedral symmetry requires that $\partial p_x/\partial x_C = \partial p_y/\partial y_C = \partial p_z/\partial z_C$.

Furthermore,

$$\partial p_x/\partial x_C = -\sum_i \partial p_x/\partial x_{F_i} \quad , \qquad (4\text{-}12)$$

from Equation 2-33. The polar tensor elements for the different F atoms are related to each other by Equation 4-1. For these tetrahedral molecules (44):

$$\partial p_x/\partial x_C = \partial p_y/\partial y_C = \partial p_z/\partial z_C = 4/3(2T_{11} + T_{33}). \qquad (4\text{-}13)$$

Here $T_{11} = \partial p_x/\partial x_F = T_{22} = \partial p_y/\partial y_F$ and $T_{33} = \partial p_z/\partial z_F$. Hence,

$$\xi_C^2 = 3\{16/9(2T_{11} + T_{33})^2\} \quad . \qquad (4\text{-}14)$$

For CF_4 , Equation 4-14 yields 3.43 $\underline{e}$ and 2.34 $\underline{e}$ (or 2.56 $\underline{e}$, depending on the $\partial p/\partial R$ chosen) for CCl_4. The discrepancies between these numbers and those in Table 4-11 (2.98 $\underline{e}$ for CF_4 and 2.06 $\underline{e}$ or 2.02 $\underline{e}$ for CCl_4) are probably within the errors due to the intensity measurements.

Finally it is of interest to plot the effective charges (ξ_X) as a function of the electronegativity of X in CH_3X, in Figure 4-18. As we saw in the case of the $(\Delta P)_z^X$ vectors (Figure 4-1), so also does ξ_X increase linearly with the increase in electronegativity. In fact, the linearity of this plot is remarkable.

In order to test the possible predictive power of this correlation, we have included in Figure 4-18 the effective charge for oxygen (ξ_O), calculated from formaldehyde by Person and Newton (12), and ξ_H for hydrogen from the hydro-

Figure 4-18: Plot of the effective charge of the X atoms against their electronegativity.

The two points marked by the X are for hydrogen and oxygen (see text).

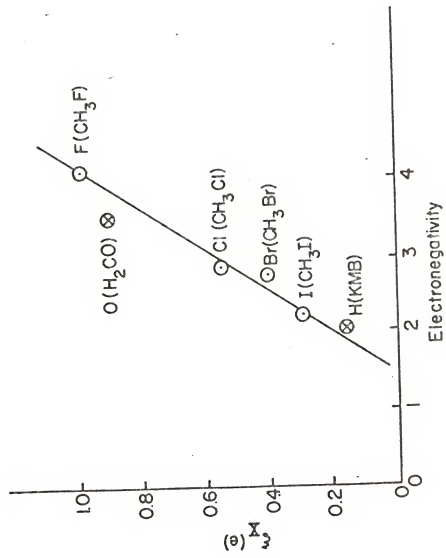
F(CH3F)
O(H2CO)
Cl(CH3Cl)
Br(CH3Br)
I(CH3I)
H(KMB)
1.0
0.8
0.6
0.4
0.2
0
0
1
2
3
4
Electronegativity
ξ(e)

carbon series of KMB. The agreement of these two extra points with the values predicted by the linear correlation is surprisingly good, especially when we consider that oxygen in H_2CO is double-bonded to an sp^2 carbon and is expected to have a different effective electronegativity relative to oxygen bonded to an sp^3 carbon (45).

It is apparent that we could have predicted quite accurately the values of ξ_X for CH_3Cl and CH_3Br if we had known the values for CH_3F and CH_3I. This ability to predict infrared intensities of molecules from values obtained for related molecules is expected to be of considerable value in future work.

Predicted Intensities

A more general form of Equation 4-8 is (5, 12):

$$K \sum_i A_i + \Omega = \sum_\alpha \xi_\alpha^2 (1/m_\alpha) \quad . \qquad (4\text{-}15)$$

Here, the index "i" runs over all infrared active fundamentals and "α" runs over all atoms in the molecule. The quantities K, A_i, Ω, ξ_α, and m_α have been previously defined (see Equation 4-8 and Equation 4-11).

The intensity sum and ξ_α^2 sum for the CH_3X molecules are compared in Table 4-12. The small discrepancy between the intensity sum and the squared effective charge sum is due to the fact that the ξ_α's used for the computations are average values computed for the CH_3X and CD_3X molecules (taken from Table 4-11).

In the previous section we predicted the ξ_C value of CF_4

TABLE 4-12

COMPARISON OF THE INTENSITY SUMS TO THE SUM OF THE SQUARED EFFECTIVE CHARGES FOR THE METHYL HALIDES

(Units are $e^2 \cdot amu^{-1}$)

	$\sum_\alpha \xi_\alpha^2 (1/m_\alpha)$ [a]	$K\sum A_i^b + \Omega$	Ω [c]
CH_3F	0.23	0.21	0.015
CH_3Cl	0.079	0.078	0.0089
CH_3Br	0.069	0.072	0.0053
CH_3I	0.053	0.062	0.0035

a. ξ_α values taken from Table 4-11.
b. Experimental intensities were taken from Reference 18.
c. The rotational corrections, Ω, were computed using the data in Table 3-3.

to be 3.43 e (by Equation 4-12) from the values we found for the CH_3F fluorine tensor and the experimental bond moment of the C-F bond in CF_4.

In the following table we have predicted the ξ_C values of CH_4, CHF_3 and CH_2F_2 based on the values for CH_3F and CF_4 in Table 4-11 by plotting ξ_C as a function of the number of fluorine atoms using CH_3F and CF_4 as reference points. The intercept (to give the value of ξ_C for CH_4) is $\xi_C^{CH_4} = 4/3\ \xi_C^{CH_3F} - 1/3\ \xi_C^{CF_4} = 0.274$ e. This value is very close to the experimental value (0.293 e) reported by KMB (see Table 4-11), increasing our confidence in the procedure.

Using the ξ_C values given in Table 4-13 and the ξ_H and ξ_F values calculated for the CH_3F molecule in Table 4-11 (first and third column, respectively), we attempted to predict the total intensity of the CH_4, CH_2F_2 and CHF_3 molecules using Equation 4-15. The results are given in Table 4-14.

The predicted intensity sums for CH_4 and for CH_2F_2 are in excellent agreement with the experimental values. The predicted value of $\sum A_i$ for CHF_3 is somewhat smaller than the experimental value, but there is reason to think that the experimental value reported in Table 4-14 is somewhat too high (46). The predicted value for CF_4 is somewhat higher than the most recent experimental value (0.971 e) (42). However, the average of the four values reported in Table 4-14 is 1.09 ± 0.14 e, which agrees with the predicted value (1.19 e) within the experimental scatter.

TABLE 4-13

PREDICTED ξ_C VALUES FOR CH_4, CH_3F, AND CH_2F_2
(Units are e)[a]

	CH_4	CH_3F[b]	CH_2F_2	CHF_3	CF_4[c]
ξ_C	0.274	1.063	1.85	2.64	3.43

a. These values are predicted by assuming a linear relationship between ξ_C and the number of fluorine atoms in the molecule, based on the CH_3F and CF_4 values given in Table 4-11.
b. CH_3F and CF_4 are taken as reference points. The ξ_C value for CH_3F was taken from Table 4-11.
c. The ξ_C value was calculated by Equation 4-12 (see text).

TABLE 4-14

A COMPARISON OF THE PREDICTED INTENSITY SUM ($\sum A_i$)
OF CH_4, CH_2F_2, CHF_3 AND CF_4
AND THE EXPERIMENTAL TOTAL INTENSITIES
(Units are e^2)

	$\sum_\alpha \xi_\alpha^2 (1/m_\alpha)$ (predicted)[a]	$K\sum_i A_i + \Omega$ (experimental)[b]	Ω
CH_4	0.113	0.110[c]	0.0
CH_2F_2	0.444	0.450[d] (0.405)[e]	0.0066
CHF_3	0.765	1.03[f]	0.0068
CF_4	1.19	0.971[g] (1.39)[h] (1.05)[i] (.956)[j]	0.0

a. The predicted values are calculated from Table 4-11 and 4-13, using Equation 4-14.
b. The data required for Ω (I_x , I_y) are based on the geometry reported in "Tables of Inter-Atomic Distances and Configurations of Molecules and Ions," Vol. 1, Special Publication No. 11, The Chemical Society, London, 1958, and the $\vec{p}^o$ values reported in "Selected Values of Electric Dipole Moments for Molecules in the Gas Phase," R.D. Nelson, Jr., D.L. Lide, Jr., and Moryott, eds., NSRDS-NBS 10, 1967.
c. Experimental intensities taken from E.T. Ruf, M.S. Thesis, University of Minnesota, 1959.
d. Experimental data taken from Reference 7.
e. Experimental data from private communication (S. Kondo and S. Saëki).

(Continued to next page)

(Table 4-14, continued)

f. Experimental data from J. Morcillo, J. Herranz, J.F. Biarge, Spectrochim. Acta, 15, 110 (1959).
g. Experimental data taken from I.W. Levin and T.P. Lewis (Reference 42).
h. B. Schurin, J. Chem. Phys., 30, 1 (1959).
i. A.A. Chalmers and D.C. McKean, Spectrochim. Acta, 22, 251 (1966).
j. R.W. Hannah, Ph.D. Thesis, Purdue University, 1957, as reported in Reference 47.

The preceding exercise in predicting intensity sums demonstrates quite well the transferability of ξ values through this series of compounds, and suggests the usefulness of the concept.

CHAPTER 5

DISCUSSION OF THE CNDO RESULTS

In Chapter 3 we used the CNDO/2 calculated tensors to help select the signs of the $\partial p/\partial Q$'s. In this chapter, we shall compare in some detail the tensors, the associated $(\Delta P)_\tau^\alpha$ vectors, and effective charges obtained from CNDO with the experimental values for CH_3F and CH_3Cl. For easy reference we summarize in Table 5-1 the experimental and CNDO tensor elements for CH_3F and CH_3Cl that had been given previously in Table 4-1.

As we have seen previously, the CNDO-calculated tensor elements are in fairly good agreement with the experimental values, especially for CH_3F. There are, however, notable exceptions. In the case of the $\underline{p}_x^F$ tensor, the CNDO values for $\partial p_x/\partial x$ and $\partial p_y/\partial y$ agree with the observed values almost within experimental error, but the calculated value of $\partial p_z/\partial_z$ is far outside the observed error limit. It appears that for this motion of the F atom (C-F bond stretching), the CNDO technique has underestimated the charge on the F atom. The CNDO calculation breaks down the total calculated dipole moment into contributions from two terms: the density term and the sp (and pd for second row elements) rehybridization (hybridization-polarization) term (14). It is of some interest

TABLE 5-1

CNDO[a] AND EXPERIMENTAL $P_{\underline{x}}^{X}$ AND $P_{\underline{x}}^{H}$ TENSORS[b]
FOR CH_3F AND CH_3Cl
(All Units Are Electrons)

$P_{\underline{x}}^{X}$

CH_3F

$$\begin{pmatrix} -0.255\pm.023\ (-0.293) & 0 & 0 \\ 0 & -0.255\pm.023\ (-0.293) & 0 \\ 0 & 0 & -0.933\pm.050\ (-0.526) \end{pmatrix}$$

CH_3Cl

$$\begin{pmatrix} -0.234\pm.012\ (-0.193) & 0 & 0 \\ 0 & -0.234\pm.012\ (-0.193) & 0 \\ 0 & 0 & -0.446\pm.015\ (+0.102) \end{pmatrix}$$

$P_{\underline{x}}^{H}$

CH_3F

$$\begin{pmatrix} 0.012\pm.009\ (-0.020) & 0 & 0.021\pm.005\ (+0.013) \\ 0 & 0.073\pm.009\ (+0.009) & 0 \\ -0.007\pm.015\ (-0.025) & 0 & -0.143\pm.005\ (-0.125) \end{pmatrix}$$

CH_3Cl

$$\begin{pmatrix} -0.036\pm.0004\ (-0.034) & 0 & 0.056\pm.0006\ (+0.034) \\ 0 & 0.073\pm.009\ (+0.037) & 0 \\ -0.024\pm.011\ (+0.017) & 0 & -0.061\pm.0008\ (-0.123) \end{pmatrix}$$

a. The CNDO values are in parentheses.
b. Axes defined with z along the CX bond.

to examine these different contributions to the polar tensors, in somewhat more detail than given previously in Chapter 4, where we examined the experimental data. The contributions to the tensor elements from the electron density term and from the sp rehybridization term for $\underset{\sim}{P}^{F}_{x}$ are given in Table 5-2, along with the contribution from the static charge $(\Delta P_1)^{\alpha}_{\tau}$. Notice that the contribution to $\partial p_z/\partial z$ from the sp term is quite small and that the density term predominates. For $\partial p_x/\partial x$ and $\partial p_y/\partial y$ the contribution from the sp terms is still small, but relatively larger than for $\partial p_z/\partial z$. It is apparent from Tables 5-1 and 5-2 that the CNDO procedure has underestimated either the density contribution or the rehybridization contribution (or both) for the $\partial p_z/\partial z$ element, but has only very slightly overestimated one or the other (or both) contribution to the $\partial p_x/\partial x$ and $\partial p_y/\partial y$ elements. However, since the sp rehybridization term is so small it can apparently be neglected in considering the contribution to the polar tensors for the F atom.

A breakdown of the CNDO $\underset{\sim}{P}^{H}_{x}$, tensor into contributions from the density and sp rehybridization terms is given in Table 5-3. In the first column of tensors, the sp and density terms oppose each other, but the resultants (Table 5-1) are in fairly good agreement with the experimental values (within the fairly large experimental errors). In the second column, the sp and density terms also oppose each other; the resultant CNDO-calculated value is far outside experimental error. Notice that in the last column the sp and density terms both have the same sign, and the agreement between the resultant CNDO tensor elements and the experimental values is fairly good.

TABLE 5-2

BREAKDOWN OF THE CNDO $\underline{P}_x^F$ TENSOR INTO
ELECTRON DENSITY AND SP REHYBRIDIZATION TERMS
(Units Are Electrons)

$$\underline{P}_x^F \text{ (density)} \quad \begin{pmatrix} -0.220 & 0.0 & 0.0 \\ 0.0 & -0.220 & 0.0 \\ 0.0 & 0.0 & -0.517 \end{pmatrix}$$

$$\underline{P}_x^F \text{ (sp)} \quad \begin{pmatrix} -0.072 & 0.0 & 0.0 \\ 0.0 & -0.072 & 0.0 \\ 0.0 & 0.0 & -0.009 \end{pmatrix}$$

$$(\Delta P_l)_x^{F\,a} \quad \begin{pmatrix} -0.194 & 0.0 & 0.0 \\ 0.0 & -0.194 & 0.0 \\ 0.0 & -0.0 & -0.194 \end{pmatrix}$$

a. Calculated from CNDO equilibrium charge on F.

TABLE 5-3

BREAKDOWN OF THE CNDO $\underline{P}^H_x$, TENSOR FOR CH_3F
INTO ELECTRON DENSITY AND $\underline{SP}$ REHYBRIDIZATION TERMS
(All Units Are Electrons)

$\underline{P}^H_x$, (density)	-0.053	0.0	0.0053
	0.0	-0.066	0.0
	0.019	0.0	-0.076
$\underline{P}^H_x$, ($\underline{sp}$)	0.033	0.0	0.0077
	0.0	0.075	0.0
	-0.045	0.0	-0.048
$(\Delta P)^{H\,a}_x$,	0.005	0.0	0.0
	0.0	0.005	0.0
	0.0	0.0	0.005

a. Calculated from CNDO equilibrium charge on H.

CH_3Cl

The contributions from the density and from the sp and pd rehybridization terms calculated (CNDO) for the $\underline{P}_x^{Cl}$ tensors and $(\Delta P)_x^{Cl}$ are given in Table 5-4. In the $\partial p_x/\partial x$ and $\partial p_y/\partial y$ elements, the density and sp terms both have the same sign, but the pd term has the opposite sign. The density contribution is essentially cancelled by the pd term. For the $\partial p_z/\partial z$ element, the sp and pd terms are both large and positive, as opposed to the negative density term so that the net result is calculated to be positive. This calculated positive sign is contrary to our expectations and is the major reason for our suspicion concerning the reliability of the calculation for this tensor alluded to earlier. It appears that the CNDO procedure grossly overestimates the contribution for the sp and pd terms and/or underestimates the contribution from the density term. We believe the latter term is underestimated because even if we neglect the positive sp and pd terms completely, we still calculate only a relatively small negative density term contribution to $\partial p_z/\partial z$.

The breakdown of the $\underline{P}_x^H$ CNDO calculated tensor for CH_3Cl into its respective terms is given in Table 5-5. There does not seem to be any systematic explanation in terms of the density, sp or pd terms that correlates with the agreement (or lack of agreement) between the CNDO-calculated tensor elements and the experimental tensor elements.

It is generally conceded that if the CNDO-calculated values for the contributions to the dipole moments are rela-

TABLE 5-4

BREAKDOWN OF THE CNDO $\underline{P}_{x'}^{Cl}$ TENSOR INTO ELECTRON DENSITY AND SP AND PD REHYBRIDIZATION TERMS
(All Units Are Electrons)

$\underline{P}_{x'}^{Cl}$ (density)

$$\begin{pmatrix} -0.072 & 0.0 & 0.0 \\ 0.0 & -0.072 & 0.0 \\ 0.0 & 0.0 & -0.193 \end{pmatrix}$$

$\underline{P}_{x'}^{Cl}$ (sp)

$$\begin{pmatrix} -0.190 & 0.0 & 0.0 \\ 0.0 & -0.190 & 0.0 \\ 0.0 & 0.0 & 0.142 \end{pmatrix}$$

$\underline{P}_{x'}^{Cl}$ (pd)

$$\begin{pmatrix} 0.067 & 0.0 & 0.0 \\ 0.0 & 0.067 & 0.0 \\ 0.0 & 0.0 & 0.153 \end{pmatrix}$$

(Continued on next page)

(Table 5-4 continued)

$$(\Delta P_{1}{}^{Cl^{a}}_{x'} \quad \begin{pmatrix} -0.050 & 0.0 & 0.0 \\ 0.0 & -0.050 & 0.0 \\ 0.0 & 0.0 & -0.050 \end{pmatrix}$$

a. Calculated from the CNDO equilibrium charge on Cl.

TABLE 5-5

BREAKDOWN OF THE CNDO $P^H_{x'}$ TENSORS FOR CH_3Cl INTO CONTRIBUTIONS FROM THE ELECTRON DENSITY AND SP AND PD REHYBRIDIZATION TERMS
(Units Are Electrons)

$$P^H_{x'}\ \text{(density)} \quad \begin{pmatrix} -0.089 & 0.0 & 0.021 \\ 0.0 & -0.047 & 0.0 \\ 0.027 & 0.0 & -0.087 \end{pmatrix}$$

$$P^H_{x'}\ (\underline{sp}) \quad \begin{pmatrix} 0.070 & 0.0 & 0.001 \\ 0.0 & 0.078 & 0.0 \\ -0.047 & 0.0 & -0.030 \end{pmatrix}$$

$$P^H_{x'}\ (\underline{pd}) \quad \begin{pmatrix} -0.015 & 0.0 & 0.012 \\ 0.0 & 0.006 & 0.0 \\ 0.038 & 0.0 & -0.006 \end{pmatrix}$$

$$(\Delta P_l)^{H\,a}_{x'} \quad \begin{pmatrix} 0.012 & 0.0 & 0.0 \\ 0.0 & 0.012 & 0.0 \\ 0.0 & 0.0 & 0.012 \end{pmatrix}$$

a. Calculated from the CNDO equilibrium charge on H.

tively large, with opposing signs, any conclusions about the sign of that dipole moment derivative are even more suspect than they would be otherwise (47). Our results for the F and CL tensors support this idea, but in the case of the H tensor (Tables 5-3 and 5-5) it is not clear what effect these opposing terms may actually have.

Recall in Chapter 4 that we broke down the polar tensors into contributions from the equilibrium static charge, $(\Delta P)_1^{\alpha}$, the charge reorientation, $(\Delta P)_2^{\alpha}$, and the term due to rehybridization, $(\Delta P)_{hyb}^{\alpha}$. In addition, we assumed that the "out-of-plane" motion of the halogen and the hydrogen atoms reflected the static charge contribution, $(\Delta P)_1^{\alpha}$.

Restricting our attention to the halogen tensors, we see from Table 5-2 that the calculated $(\Delta P)_1^F$ value is in good agreement with the -0.23 e value assumed in Chapter 4. However, in Table 5-4 we see that for $(\Delta P)_1^{Cl}$ the calculated value is -0.05 e, whereas in Chapter 4 we assumed it to be -0.23 e as for the $(\Delta P)_1^F$ value. Since the value of $(\Delta P)_1^X$ appears to be fairly constant (≈0.23 e) for all the halogens, it appears reasonable to assume that the calculated $(\Delta P)_1^{Cl}$ value in Table 5-4 is in error and the CNDO procedure has underestimated the equilibrium static charge contribution to the dipole moment change for motion of the chlorine atom in CH_3Cl.

In Chapter 4 we also assumed that the $(\Delta P)_{sp}^X$ term for the halogen atoms was constant at 0.20 e as predicted by Bruns and Person (37) based on the analysis of the diatomic

hydrides. In Tables 5-2 and 5-4, we see that the $(\Delta P)_{sp}$ terms are -0.009 e and +0.142 e for fluorine and chlorine, respectively. This discrepancy is not understood, but may be due to failure of the simple model used in Chapter 4.

Notice also that the $(\Delta P)_2^X$ terms can be calculated from the $\underline{P}_x^X$ (density) terms and the equilibrium static charge term $(\Delta P)_1^\alpha$ since the sum, $(\Delta P)_1^\alpha$ and $(\Delta P)_2^\alpha$, must equal the total density contribution. Notice that in the case of the diatomic hydrides, $(\Delta P)_1$ was constant, and $(\Delta P)_2$ varied as Z. In our case, however, the calculations seem to indicate that neither $(\Delta P)_1^X$ nor $(\Delta P)_2^X$ for the halogens is constant.

Turning our attention to the hydrogen tensors, we recall that in Chapter 4 we assumed a value of 0.070 e for the $(\Delta P)_1^H$ static charge contribution for the CH_3X series. In Table 5-3 we see that the CNDO/2 procedure predicts a value of 0.005 e for $(\Delta P)_1^H$ for CH_3F, and in Table 5-5, a value of 0.012 e for the same quantity for CH_3Cl. The fact that the calculated values of $(\Delta P)_1^H$ are small is encouraging, even though the actual magnitude is not constant for CH_3F and CH_3Cl. (Notice that the average value of the calculated $(\Delta P)_1^H$ for CH_3F and CH_3Cl is about +0.085 e.)

The $(\Delta P)_x^H$, and $(\Delta P)_z^H$, vectors and associated angles, θ_x and θ_z , for the CNDO-calculated tensors are compared with the experimental values in Table 5-6. The comparison is given graphically in Figures 5-1 and 5-2 respectively. The agreement is pretty good, except for the obvious discrepancy between the calculated and experimental $(\Delta P)_x^H$, vectors for

TABLE 5-6

THE CNDO $(\Delta P)^{H}_{x'}$ AND $(\Delta P)^{H}_{z'}$ VECTORS AND ASSOCIATED ANGLES θ FOR CH_3F AND CH_3Cl

	$(\Delta P)^{H}_{x'}$, (electrons)	θ[a] (degrees)	$(\Delta P)^{H}_{z'}$, (electrons)	θ (degrees)
CH_3F	0.032 [b] (0.014)	322.4 (61.5)	0.125 (0.145)	5.9 (8.2)
CH_3Cl	0.038 (0.043)	296.0 (303.3)	0.128 (0.083)	15.4 (42.9)

a. θ is defined as a clockwise rotation of the $(\theta P)^{H}_{T}$ vector from the C-H bond axis as viewed by looking down the positive y' axis centered on the H atom.
b. The experimental values are in parenthesis and were taken from Tables 4-4 and 4-3.

Figure 5-1: Comparison of the CNDO/2 calculated $(\Delta P)^{H}_{x}$, vectors with the experimental values for CH_3F and CH_3Cl.

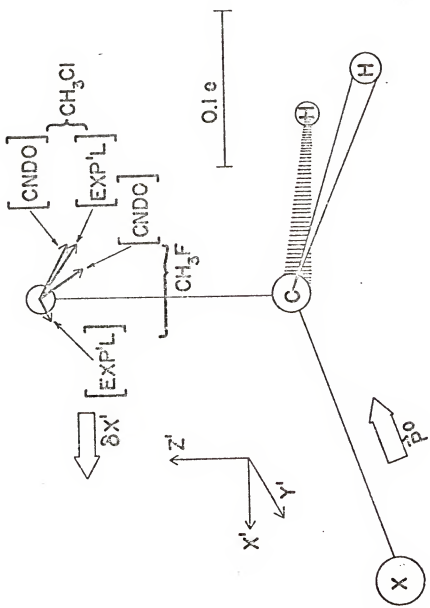
CNDO
EXP'L
CH3Cl
CNDO
CH3F
EXP'L
δX'
0.1 e
H
H
C
X
Z'
Y'
X'
ρ0

Figure 5-2: Comparison of the CNDO/2 calculated $(\Delta P)^{H}_{z}$, vectors with the experimental values for CH_3F and CH_3Cl.

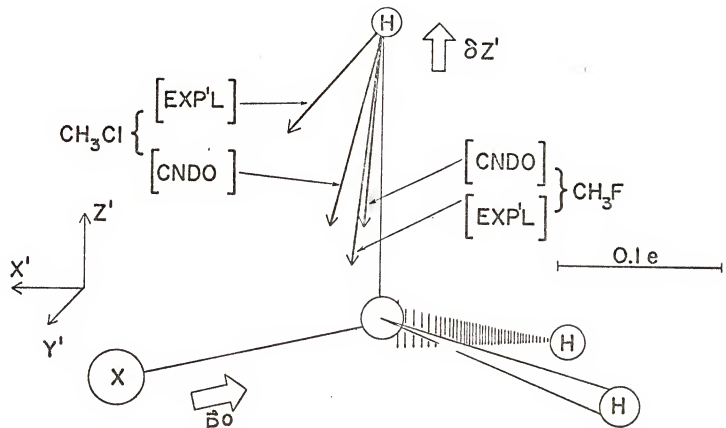
H
δZ'
[EXP'L]
CH3Cl
[CNDO]
[CNDO]
[EXP'L]
CH3F
Z'
X'
Y'
0.1 e
X
H
H
Po

CH_3F (see Figure 5-1). As we have mentioned, this particular vector is essentially undetermined experimentally, because of its large error. It is interesting to note, however, that the CNDO-calculated $(\Delta P)^H_x$, vector is in the fourth quadrant with the experimental $(\Delta P)^H_x$, vectors of CH_3Cl, CH_3Br and CH_3I, and not in the third quadrant, as indicated experimentally.

The qualitative agreement between the calculated and experimental $(\Delta P)^H_x$, vectors is very encouraging. We believe this result supports a conclusion that the "error" alluded to earlier in the CNDO calculation for CH_3Cl is confined largely to the chlorine tension, $\underline{P}^{Cl}_x$, and that the CNDO-calculated value for the hydrogen tensor $\underline{P}^H_x$ may be nearly correct.

Calculated Band Intensities

We shall now turn our attention to the actual band intensities predicted by CNDO for CH_3F and CH_3Cl. By using the complete CNDO calculated $\underline{P}_x$ matrix containing all $\underline{P}^\alpha_x$ tensors (Equation 2-25) and Equation 2-27 to 2-29, we obtain the $\underline{P}_Q$ tensor and from it we can calculate the band intensities using Equation 1-2 (Chapter 1). In our calculation, we did not actually compute the $\underline{P}^H_x$ tensors for the two hydrogen atoms that are out of the xz plane by the CNDO program. Instead, since the hydrogens are symmetrically equivalent, we simply rotated the H(3) tensor to coincide with the two remaining hydrogen atoms. This procedure is, of course, general so that for a molecule containing two or more identical atoms that are symmetrically equivalent, one need only compute the polar tensor for one of the atoms and then rotate

that tensor to obtain the tensor for the remaining symmetrically equivalent atoms. For fairly symmetric molecules, this feature may save a considerable amount of computer time in the quantum mechanical calculation. The tensor rotations were carried out by program TRANSC (Appendix III) and the computation of $\underline{P}_Q$ was done by program PVDTEN (Appendix III).

The results of the intensity calculations are given in Table 5-7, along with the experimentally observed intensities. For CH_3F, the agreement is, perhaps, better than we should expect, considering the approximate nature of the CNDO model. The ν_1, ν_2 and ν_4 bands are essentially in quantitative agreement with the experimental results, and ν_3 is the right order of magnitude. The ν_3 band is essentially a C-F stretching motion and as we have shown, the $\partial p_z/\partial z$ element has been underestimated and that element probably accounts for most of the intensity of this band. The ν_5 and ν_6 bands are well outside the observed error and have opposite relative values from the experimental results. In spite of the obvious discrepancies, the agreement is better than we had hoped for. With the exception of the ν_1 and ν_2 bands in CH_3Cl, CNDO greatly overestimated or underestimated the intensities in a non-systematic way. The ν_3 band, as in the case of CH_3F, is the halogen stretching mode and CNDO has grossly underestimated the intensity. This is a reflection of the error in the $\partial p_z/\partial z$ tensor element. We should point out that we did not take into account the experimental errors in $\underline{L}$ when computing the intensities given in Table 5-7. The inclusion

TABLE 5-7

THE CNDO/2 CALCULATED INFRARED BAND INTENSITIES FOR CH_3F AND CH_3Cl
(A_1 Units are km/mole)[a]

	CH_3F		CH_3Cl		CH_3Cl
	CNDO	Experimental	CNDO	Experimental	Calculated
ν_1	13.88	(24.73 ± 12.37)	14.95	(21.55 ± .71)	21.62
ν_2	2.23	(0.89 ± 1.91)	3.83	(6.80 ± .48)	11.81
ν_3	36.01	(94.96 ± 9.50)	0.54	(23.20 ± .46)	24.17
ν_4	58.36	(30.51 ± 10.59)	44.27	(4.84 ± .27)	44.27[b]
ν_5	0.057	(4.34 ± 2.10)	1.36	(6.14 ± .23)	1.36[b]
ν_6	12.20	(1.31 ± 0.90)	0.00101	(2.01 ± .04)	0.00101[b]
	TOTAL INTENSITIES FOR OVERLAPPED BANDS				
$\nu_1 + \nu_4$	72.24	(55.24 ± 22.96)	59.22	(26.39 ± .98)	65.89[c]
$\nu_2 + \nu_5$	2.28	(5.23 ± 4.01)	5.19	(12.94 ± .71)	13.17[c]
$\nu_3 + \nu_6$	48.21	(96.27 ± 10.40)	---	---	---

a. The experimental values were taken from Reference 18 and converted to A by $A = \Gamma\nu$. The last column headed CH_3Cl are the $A_{1,z}$ intensities obtained by replacing the CNDO calculated $(\partial p_z/\partial z)^{Cl}$ element by the experimental element, as explained in the text.

b. The CNDO calculated values.

c. These values were computed from the ν_1 and ν_2 intensities given in this column and the ν_4 and ν_5 CNDO values.

of the errors in $\underline{L}$ probably would not change our results by a significant amount. That is, we do not believe that resulting errors in the calculated intensities would be outside the observed errors of the experimental values.

Since we believe that the $(\partial p_z/\partial z)^{Cl}$ tensor element calculated by CNDO is wrong, we replaced that element by the experimental value of the $(\partial p_z/\partial z)^{Cl}$ tensor element from our preferred sign set to see how much improvement there was in the total intensities of the $A_{1,z}$ block (it will affect only the $A_{1,z}$ symmetry block). By adjusting the carbon tensor accordingly so that $\sum_{\alpha} P_x^{\alpha} = 0$, we computed the semi-empirical integrated intensities of the $A_{1,z}$ block of CH_3Cl reported in Table 5-7 in the last column. This simple change in the $\underline{P}_x^{Cl}$ and $\underline{P}_x^{C}$ tensors greatly improved the ν_1 and ν_3 intensities. There is no significant improvement for the symmetric C-H bending mode, ν_2 , however; in fact, the resulting calculated intensity of this mode has a larger deviation from the experimental value in the opposite sense.

The significance of this semi-empirical approach is not that we were able to improve the CH_3Cl intensities, but that such an approach, the combination of the experimental and theoretical tensor elements, may be very useful in the quantitative prediction of the infrared spectra of complex systems.

We believe that the preceding calculations of the integrated band intensities readily illustrated the ease and usefulness of the polar tensor technique for quantum mechanical calculations of intensities, even though the results from this preliminary study are not completely satisfying.

We carried through the analysis of the different contributions to the CNDO-calculated tensors as an illustration of its application and a possible indication of where CNDO procedure is overestimating or underestimating effects. Others have reparameterized the CNDO procedure (47) for better prediction of specific effects. Although this is an attractive alternative to our procedure (using the standard parameter values in our calculations), we feel that at present it is not worthwhile. It defeats the purpose of the CNDO procedure to reparameterize for every problem. The CNDO calculation provides an inexpensive general purpose quantum-mechanical calculation of molecular properties that generally leads to fairly reliable predictions. We believe that the CNDO calculation should be calibrated (not reparameterized indiscriminately) by comparison with more sophisticated quantum mechanical calculations.

CNDO Calculated Effective Charge

Comparison of the CNDO/2 calculated effective charge to the experimental effective charge for CH_3F and CH_3Cl is given in Table 5-8. The CNDO ξ_α values given in the table were calculated from the CNDO $\underline{P}_x^\alpha$ tensors given in Table 4-1 by use of Equation 2-31. The qualitative agreement between the CNDO/2 computed effective charge and the experimental values is fairly good for both CH_3F and CH_3Cl, in spite of the somewhat low value calculated (for ξ_{Cl} and ξ_C for CH_3Cl) due to the anomalous CNDO $\partial p_z/\partial z$ value for CH_3Cl. For the ξ_C and ξ_X values in both compounds, the CNDO values are somewhat

TABLE 5-8

COMPARISON OF THE CNDO CALCULATED EFFECTIVE CHARGES TO THE EXPERIMENTAL EFFECTIVE CHARGES FOR CH_3F AND CH_3Cl

(Units are electrons)

	CH_3F		CH_3Cl	
	CNDO[a]	Experimental[b]	CNDO[a]	Experimental[b]
ξ_H	0.130	(0.164 ± .007)	0.138	(0.119 ± .003)
ξ_X	0.670	(1.000 ± .004)	0.291	(0.557 ± .002)
ξ_C	0.884	(1.063 ± .417)	0.415	(0.588 ± .060)

a. Calculated from the CNDO polar tensor (Table 5-1) using Equation 2-31.
b. From Table 4-11.

underestimated, presumably because of an underestimation of the charge on the halogens as discussed earlier. It is quite possible that this underestimation may be a characteristic fault of the CNDO calculation, but notice that the trends in the calculated and experimental results for ξ_X are parallel. One should also keep in mind that the ξ_C values are determined by the ξ_X and ξ_H values and if "errors" are present in these values, ξ_C will reflect them.

In the case of ξ_H for CH_3F, the calculated value is slightly smaller than the experimental value for that compound, and for CH_3Cl the calculated ξ_H value is slightly larger than the experimental value. Notice, however, that in both cases, CH_3F and CH_3Cl, the calculated ξ_H values are almost constant and very close to the average experimental value of 0.130 e for the CH_3X series. Although CNDO predicts an exactly constant value of ξ_H for CH_3F and CH_3Cl, the experimental values do not appear to be quite the same for the two compounds, since the two values differ by more than 2.5 (the experimental error).

APPENDIX I

NORMAL COORDINATES OF CH_3X AND CD_3X

As we indicated in Chapter 3, we have recalculated the normal coordinates of the methyl halides in order to insure consistency in coordinate definitions. We used the normal coordinate programs WMAT and CHARLY from the Molecular Spectroscopy Laboratory of the University of Minnesota, made available to us by Dr. J. Overend. The programs were originally written for the CDC 6400 computer and were revised by Dr. G. Sanchez for use on the IBM 370/165 computer at the University of Florida. These programs have been described in detail elsewhere (19) and will not be discussed further here.

The CH_3X molecules belong to the C_{3v} symmetry point group and have three infrared active vibrations belonging to the totally symmetric A_1 representation and three belonging to the doubly degenerate E representation. (The values of ν_i's are from References 20 and 21.)

The molecular geometries of the methyl halides and the trideuterated isotopes used in this work are given in Table AI-1. The standard equilibrium Cartesian coordinates, calculated by program CART (see reference at bottom of Table 3-2) are given in Table AI-2 and are based on the Cartesian

axis defined in Figure AI-1. The internal displacement coordinates are defined in Figure AI-2, and the symmetry displacement coordinates are defined in Table AI-3 in terms of the un-normalized $\underline{U}$ matrix. The symmetrized $\underline{G}$ elements are given in Table AI-4 and AI-5 for CH_3X and CD_3X.

We carried through the normal coordinate calculations using both Overend's (18) and Duncan's (21) force constants and we found that there was no significant difference in the resulting polar tensors. Since Duncan's force field is better determined (see Chapter 1), we have reported only the results obtained from his force field. Duncan's symmetrized force constants are given in Table AI-6, and the resulting normal coordinate transformation matrices are given in Tables AI-7 and AI-8 for both the CH_3X and CD_3X series. The $\underline{L}^{-1}$ matrices are given in Tables AI-9 and AI-10. The calculated harmonic frequencies are given in Tables AI-11 and AI-12. A description of the infrared band assignments is given in Table AI-13.

Figure AI-1

Cartesian Coordinate Axes and Atom Sequence for CH_3X Used in the Normal Coordinate Analysis

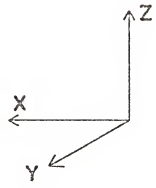

Cartesian Axis

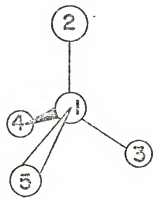

Atom Sequence

Atoms 1, 2, and 3 are in the xz plane.

Atom #	Atom	Atomic Mass (AMU)[a]
1	C	12.000000
2	X (X=F,Cl,Br,I)	18,99840, 34,96885, 78.9183, 126.9004
3	H(D)	1.007825 (2.014102)
4	H(D)	1.007825 (2.014102)
5	H(D)	1.007825 (2.014102)

a. Handbook of Chemistry and Physics, 50th Edition, Chemical Rubber Company, Cleveland, 1969.

Figure AI-2

Definition of Internal Displacement Coordinates for Methyl Halides[a]

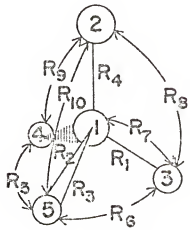

$R_1 = \delta r_{13}$[b]

$R_2 = \delta r_{14}$

$R_3 = \delta r_{15}$

$R_4 = \delta r_{12}$

$R_5 = \delta\alpha\ (4, 1, 5)$[c]

$R_6 = \delta\alpha\ (5, 1, 3)$

$R_7 = \delta\alpha\ (3, 1, 4)$

(continued to next page)

(Figure AI-2, continued)

$$R_8 = \delta\beta\ (3, 1, 2)^{d}$$

$$R_9 = \delta\beta\ (4, 1, 2)$$

$$R_{10} = \delta\beta\ (5, 1, 2)$$

---

a. Taken from Reference 34.
b. $\delta r_{i,j}$ means bond stretching coordinate between atoms i and j.
c. α (i, j, k) means angle bending coordinate for angle formed by atoms i, j, k. α is an HCH angle.
d. β is an XCH angle.

TABLE AI-1

EQUILIBRIUM MOLECULAR GEOMETRIES FOR CH_3X USED IN THE NORMAL COORDINATE CALCULATION[a]

	r_{CH}(Å)	r_{CX}(Å)	α_{HCH}
CH_3F	1.095	1.382	110°30'
CH_3Cl	1.084	1.778	110°50'
CH_3Br	1.084	1.935	111°20'
CH_3I	1.083	2.136	111°30'

a. Data taken from Reference 21.

TABLE AI-2

STANDARD EQUILIBRIUM CARTESIAN COORDINATES
FOR THE METHYL HALIDES, CH_3X
(Units are in Angstroms)

CH_3F

Atom	x	y	z
1	0.0	0.0	0.0
2	0.0	0.0	1.382
3	-1.038888	0.0	-0.346030
4	0.519444	-0.899703	-0.346030
5	0.519444	0.899703	-0.346030

CH_3Cl

1	0.0	0.0	0.0
2	0.0	0.0	1.778
3	-1.030523	0.0	-0.336272
4	0.515261	-0.892459	-0.336272
5	0.515261	0.892459	-0.336272

CH_3Br

1	0.0	0.0	0.0
2	0.0	0.0	1.935
3	-1.033613	0.0	-0.326650
4	0.516806	-0.895135	-0.326650
5	0.516806	0.895135	-0.326650

Continued to next page

(TABLE AI-2 continued)

CH_3I

Atom	x	y	z
1	0.0	0.0	0.0
2	0.0	0.0	2.136
3	-1.034707	0.0	-0.319799
4	0.517353	-0.896082	-0.319799
5	0.517353	0.896082	-0.319799

TABLE AI-3

SYMMETRY DISPLACEMENT COORDINATES FOR CH_3X EXPRESSED IN TERMS OF THE UN-NORMALIZED $\underline{U}$ MATRIX[a]

	R_1	R_2	R_3	R_4	R_5	R_6	R_7	R_8	R_9	R_{10}
S_1	1	1	1	0	0	0	0	0	0	0
S_{2a}[b]	0	0	0	0	1	1	1	-1	-1	-1
S_{2b}	0	0	0	0	1	1	1	1	1	1
S_3	0	0	0	1	0	0	0	0	0	0
$S_{4,x}$	2	-1	-1	0	0	0	0	0	0	0
$S_{5,x}$	0	1	-1	0	0	0	0	0	0	0
$S_{6,x}$	0	0	0	0	2	-1	-1	0	0	0

Continued to next page

(TABLE AI-3 continued)

	R_1	R_2	R_3	R_4	R_5	R_6	R_7	R_8	R_9	R_{10}
$S_{4,y}$	0	0	0	0	0	1	-1	0	0	0
$S_{5,y}$	0	0	0	0	0	0	0	2	1	1
$S_{6,y}$	0	0	0	0	0	0	0	0	1	-1

---

a. See Reference (16)

b. $S_2 = PS_{2a} - QS_{2b}$

$Q = (1 + K)/(2 + 2K^2)^{\frac{1}{2}}$

$P = (1 - K)/(2 + 2K^2)^{\frac{1}{2}}$

$K = \{ - 3 \sin(\beta) \cos(\beta) \} / \sin(\alpha)$

Redundant coordinate is $(QS_{2z} + PS_{2b})$

TABLE AI-4

UPPER TRIANGLE OF THE SYMMETRIZED G MATRIX FOR CH_3X

(all units are amu^{-1})[a]

Symmetry Block		CH_3F	CH_3Cl	CH_3Br	CH_3I
A_1	g_{11}	1.0172005	1.0162935	1.0149364	1.0140343
	g_{12}	-0.0949003	-0.0936552	-0.0902867	-0.0880854
	g_{13}	-0.0456120	-0.0447755	-0.0434943	-0.0426214
	g_{22}	1.9513454	1.9656754	1.9266357	1.9035587
	g_{23}	0.1733833	0.1743044	0.1729860	0.1722240
	g_{33}	0.1359693	0.1119302	0.0960046	0.0912135
E_x, E_y	g_{44}	1.1047525	1.1052065	1.1058836	1.1063356
	g_{45}	0.1481217	0.1511650	0.1535017	0.1552210
	g_{46}	-0.1200393	-0.1008428	-0.0947300	-0.0884736
	g_{55}	2.2960701	2.3571835	2.3790112	2.3982687
	g_{56}	0.2393007	0.2647356	0.2627645	0.2648623
	g_{66}	0.9969396	0.9480025	0.9284539	0.9171713

a. The valence bending-stretching interaction elements have been weighted by 1A and the valence bending-bending elements have been weighted by $(1A)^2$.

TABLE AI-5

UPPER TRIANGLE OF THE SYMMETRIZED G MATRIX FOR CD_3X
(all units are amu^{-1})[a]

Symmetry Block		CD_3F	CD_3Cl	CD_3Br	CD_3I
A_1	g_{11}	0.5214643	0.5205573	0.5192000	0.5182982
	g_{12}	-0.0949002	-0.0936524	-0.0902716	-0.0880544
	g_{13}	-0.0456120	-0.0447755	-0.0434943	-0.0426214
	g_{22}	1.1566544	1.1656857	1.1430759	1.1295519
	g_{23}	0.1733833	0.1742998	0.1729565	0.1721638
	g_{33}	0.1359693	0.1119302	0.0960046	0.0912135
E_x, E_y	g_{44}	0.6090165	0.6094702	0.6101485	0.6105996
	g_{45}	0.1481215	0.1511648	0.1535016	0.1552206
	g_{46}	-0.1200391	-0.1008427	-0.0947299	-0.0884736
	g_{55}	1.2463379	1.2805548	1.2940044	1.3055553
	g_{56}	0.0407912	0.0650535	0.0675585	0.0724000
	g_{66}	0.5834892	0.5261183	0.5065695	0.4945073

a. The valence bending-stretching interaction elements have been weighted by lA and the valence bending-bending elements have been weighted by $(lA)^2$.

TABLE AI-6

UPPER TRIANGLE OF THE SYMMETRIZED
$\underline{F}$ MATRIX FOR CH_3X
(all units are mdynes/Å)[a]

Symmetry Block		CH_3F	CH_3Cl	CH_3Br	CH_3I
A_1	f_{11}	5.248	5.493	5.536	5.533
	f_{12}	-0.222	0.028	0.076	0.126
	f_{13}	0.385	0.173	0.121	0.072
	f_{22}	0.757	0.636	0.600	0.559
	f_{23}	-0.690	-0.526	-0.469	-0.411
	f_{33}	5.692	3.500	2.940	2.394
E	f_{44}	5.276	5.364	5.436	5.450
	f_{45}	-0.132	-0.132	-0.146	-0.142
	f_{46}	0.176	0.061	0.081	0.128
	f_{55}	0.578	0.542	0.534	0.524
	f_{56}	-0.066	-0.019	-0.019	-0.011
	f_{66}	0.906	0.718	0.641	0.557

a. Taken from Reference 21.

TABLE AI-7

CALCULATED SYMMETRIZED L MATRIX FOR CH_3X
(all units are amu$^{-\frac{1}{2}}$)

Symmetry Block		CH_3F	CH_3Cl	CH_3Br	CH_3I
A_1	ℓ_{11}	1.004814	1.008100	1.007339	1.006582
	ℓ_{12}	0.086789	0.001071	-0.013873	-0.028588
	ℓ_{13}	-0.004100	-0.003938	-0.003150	-0.002689
	ℓ_{21}	-0.211729	-0.093734	-0.070199	-0.048175
	ℓ_{22}	1.367030	1.388852	1.379216	1.372646
	ℓ_{23}	0.194278	0.167260	0.139536	0.130703
	ℓ_{31}	-0.049811	-0.043251	-0.040972	-0.038827
	ℓ_{32}	0.068103	0.083930	0.093749	0.097128
	ℓ_{33}	0.358956	0.320959	0.292467	0.283323
E_x, E_y	ℓ_{44}	1.050864	1.051079	1.051319	1.051511
	ℓ_{45}	0.012734	0.020922	0.023556	0.019036
	ℓ_{46}	-0.016576	-0.001320	-0.006915	-0.017190
	ℓ_{54}	0.119930	0.113393	0.110444	0.117192
	ℓ_{55}	1.499687	1.514077	1.528255	1.535962
	ℓ_{56}	-0.180620	-0.227802	-0.176767	-0.159220
	ℓ_{64}	-0.102633	-0.101162	-0.090480	-0.074124
	ℓ_{65}	0.282452	0.319943	0.284446	0.272934
	ℓ_{66}	0.952171	0.914005	0.916166	0.914974

TABLE AI-8

CALCULATED SYMMETRIZED L MATRIX FOR CD_3X
(all units are amu$^{-\frac{1}{2}}$)

Symmetry Block		CD_3F	CD_3Cl	CD_3Br	CD_3I
A_1	ℓ_{11}	0.717525	0.721401	0.720552	0.719798
	ℓ_{12}	0.077600	0.011547	-0.001174	-0.013565
	ℓ_{13}	-0.024478	0.002148	0.002200	0.002223
	ℓ_{21}	-0.250852	-0.146994	-0.123636	-0.102532
	ℓ_{22}	0.994273	1.069451	1.061608	1.057103
	ℓ_{23}	-0.324261	0.018732	0.027807	0.039545
	ℓ_{31}	-0.080539	-0.065321	-0.060928	-0.057224
	ℓ_{32}	0.241159	0.148880	0.148887	0.147693
	ℓ_{33}	0.267067	0.292400	0.264811	0.257149
E_x, E_y	ℓ_{44}	0.780369	0.780630	0.781108	0.781384
	ℓ_{45}	-0.005721	0.000589	0.002940	0.000588
	ℓ_{46}	0.002858	0.009331	0.003177	-0.006225
	ℓ_{54}	0.197614	0.193876	0.192573	0.197260
	ℓ_{55}	1.096870	1.111297	1.119186	1.123386
	ℓ_{56}	0.064468	-0.089384	-0.065887	-0.068152
	ℓ_{64}	-0.156403	-0.137638	-0.124543	-0.107874
	ℓ_{65}	0.021440	0.138734	0.122412	0.124860
	ℓ_{66}	0.747373	0.698517	0.689981	0.683579

TABLE AI-9

CALCULATED SYMMETRIZED $\underline{L}$ INVERSE MATRIX FOR CH_3X
(all units are $amu^{-\frac{1}{2}}$)

Symmetry Block	L^{-1}	CH_3F	CH_3Cl	CH_3Br	CH_3I
A_1	ℓ_{11}	0.983857	0.992372	0.993631	0.994450
	ℓ_{12}	-0.064769	-0.001550	0.009578	0.020720
	ℓ_{13}	0.046292	0.012984	0.006132	-0.000121
	ℓ_{21}	0.136663	0.052519	0.037714	0.022665
	ℓ_{22}	0.742783	0.743353	0.749720	0.753579
	ℓ_{23}	-0.400459	-0.386735	-0.357284	-0.347427
	ℓ_{31}	0.110594	0.120001	0.127109	0.128501
	ℓ_{32}	-0.149914	-0.194592	-0.238972	-0.255497
	ℓ_{33}	2.868244	3.218544	3.534535	3.648592
E_x, E_y	ℓ_{44}	0.954261	0.952611	-0.953182	0.953720
	ℓ_{45}	-0.010844	-0.012781	-0.015541	-0.014560
	ℓ_{46}	0.014555	-0.001810	0.004197	0.015384
	ℓ_{54}	-0.061719	-0.052706	-0.055985	-0.062818
	ℓ_{55}	0.644506	0.628135	0.632574	0.632490
	ℓ_{56}	0.121184	0.156477	0.121628	0.108883
	ℓ_{64}	0.121167	0.123881	0.111529	0.095997
	ℓ_{65}	-0.192356	-0.221290	-0.197932	-0.189855
	ℓ_{66}	1.015856	1.039117	1.054165	1.061696

TABLE AI-10

CALCULATED SYMMETRIZED $\underline{L}$ INVERSE MATRIX FOR CD_3X
(all units are $amu^{-\frac{1}{2}}$)

Symmetry Block	L^{-1}	CD_3F	CD_3Cl	CD_3Br	CD_3I
A_1	ℓ_{11}	1.356573	1.382575	1.387374	1.390926
	ℓ_{12}	-0.105088	-0.013636	0.003198	0.019957
	ℓ_{13}	-0.003254	-0.009283	-0.011860	-0.015092
	ℓ_{21}	0.367464	0.186280	0.155505	0.126037
	ℓ_{22}	0.748494	0.941629	0.956402	0.968564
	ℓ_{23}	0.942466	-0.061694	-0.101719	-0.150036
	ℓ_{31}	0.077287	0.214015	0.231785	0.237144
	ℓ_{32}	-0.707577	-0.482500	-0.536983	-0.551849
	ℓ_{33}	2.892391	3.449344	3.830689	3.971611
E_x, E_y	ℓ_{44}	1.278629	1.277682	1.279922	1.281858
	ℓ_{45}	0.006776	0.001431	-0.002689	-0.001947
	ℓ_{46}	-0.005475	-0.016886	-0.006151	0.011479
	ℓ_{54}	-0.246505	-0.199466	-0.204490	-0.210488
	ℓ_{55}	0.911924	0.885487	0.884696	0.880739
	ℓ_{56}	-0.077719	0.115974	0.085422	0.085892
	ℓ_{64}	0.274651	0.291368	0.267305	0.240734
	ℓ_{65}	-0.024742	-0.175585	-0.157445	-0.161177
	ℓ_{66}	1.339117	1.405252	1.433064	1.449007

TABLE AI-11

CALCULATED HARMONIC WAVENUMBERS (cm^{-1}) FOR CH_3X

Symmetry Block		CH_3F	CH_3Cl	CH_3Br	CH_3I
	ω_1	3024.92	3075.53	3084.39	3081.52
A_1	ω_2	1488.11	1384.62	1331.35	1277.14
	ω_3	1062.74	738.88	617.66	539.08
	ω_4	3131.53	3164.36	3184.37	3187.13
E	ω_5	1493.47	1481.47	1472.11	1464.81
	ω_6	1207.14	1038.97	974.97	902.48

TABLE AI-12

CALCULATED HARMONIC WAVENUMBERS (cm^{-1}) for CD_3X

Symmetry Block		CD_3F	CD_3Cl	CD_3Br	CD_3I
	ω_1	2178.26	2201.91	2205.04	2200.39
A_1	ω_2	1136.25	1042.13	1003.43	962.63
	ω_3	1009.14	706.53	582.65	506.31
	ω_4	2323.17	2349.54	2362.86	2363.55
E	ω_5	1086.01	1072.36	1068.61	1064.06
	ω_6	924.09	780.29	725.19	667.97

TABLE AI-13

DESCRIPTION OF THE INFRARED BAND ASSIGNMENTS
OF THE METHYL HALIDES

ω	"Description of Motion"
ω_1	Symmetric CH stretch
ω_2	Symmetric XCH bend (umbrella motion)
ω_3	Symmetric CX stretch
ω_4	Asymmetric CH stretch
ω_5	Asymmetric HCH bend
ω_6	Asymmetric XCH bend

APPENDIX II

COMPUTER PROGRAMS

Program PVDTEN

Program PVDTEN calculated the $\underline{P}_S$, $\underline{V}$, and $\underline{P}_X$ tensors for a molecular system containing up to sixteen atoms. The program is designed to accept the symmetrized $\underline{L}^{-1}$ matrix and symmetrized $\underline{B}$ matrix used in a normal coordinate analysis to calculate $\underline{P}_S$ and $\underline{V}$. At the user's option, rotational corrections are computed and $\underline{P}_X$ is calculated. In addition, the program provides options for calculating $\underline{L}^{-1}$ from $\underline{L}$ and symmetrizing $\underline{B}$. An option for calculating $\underline{G}$ is available as an internal check on $\underline{L}$ ($\underline{L}\,\underline{L}' = \underline{G}$) and $\underline{B}$ ($\underline{B}\,\underline{M}^{-1}\underline{B}' = \underline{G}$). An option for calculating $\underline{A}$ and $\underline{G}^{-1}$ is also available. The program will punch the $\underline{V}$ and $\underline{P}_X^{\alpha}$ tensors on cards in the correct format for use in program TRANSC if desired.

Program PVDTEN consists of a main program and four subroutines (ROTCOR, LINV, SDYM, AMAT). The main program calculates $\underline{P}_S$ and $\underline{V}$ directly from $\underline{L}^{-1}$ and $\underline{P}_Q$ and the symmetrized $\underline{B}$. The subroutine ROTCOR calculates the rotational corrections and transfers them to the main program to be used with $\underline{V}$ for the $\underline{P}_X$ calculation. Subroutine LINV is called if $\underline{L}^{-1}$ is to be calculated from $\underline{L}$, $\underline{F}$, and $\underline{\Lambda}$; BSYM is called if $\underline{B}$ is to be symmetrized. Subroutine AMAT calculated $\underline{A}$ and $\underline{G}^{-1}$ {$\underline{G}^{-1} = (\underline{L}\underline{L}')^{-1}$ and $\underline{A} = \underline{M}^{-1}\underline{B}'\underline{G}^{-1}$} and contains an option for calculating $\underline{P}_S$

and $\underline{P}_Q$ from a given $\underline{P}_X$ matrix. A description of the in-put data is given below:

ITEM (each item begins a new card):

1. NOPROB -- The number of the problem. If the number of the problem is 7777, the program terminates; otherwise, problems may be stacked for consecutive runs. FORMAT (I4).
2. RECORD(I) -- Alphanumeric data for identification of the problem. The first column must be blank. FORMAT (1X, 12A6).
3. NS, NA, NI, NRC -- NS is the number of independent symmetry coordinates exclusive of any redundant coordinates; NA is the number of atoms; NI is the number of internal coordinates; and NRC is the number of redundant coordinates. FORMAT (4I3).

The inclusion of NRC is an artificial device so that the punched $\underline{B}$ from program WMAT (19) can be utilized in PVDTEN if redundant coordinates are used in WMAT.

4. IFLI, IFSB,IFCHL, IFCHLI, IFCHB, IFROC, IFPV, IFPD, IFAM -- This is the option control card. IFLI is the option flag for calculating $\underline{L}^{-1}$ from $\underline{L}$, $\underline{F}$, and $\underline{A}$. If IFLI = 1, $\underline{L}^{-1}$ is calculated from $\underline{L}$ by subroutine LINV. If IFLI = 0, $\underline{L}^{-1}$ is read directly into the program. IFSB is the option flag for symmetrizing $\underline{B}$. If IFSB = 1, the $\underline{B}$ matrix is symmetrized by subroutine BSYM; if IFSB = 0, the symmetrized $\underline{B}$ is read directly into the program. IFCHL is the option flag for checking $\underline{L}$ by calculating $\underline{G}$. If IFCHL = 1, $\underline{G}$ is computed from $\underline{L}$; if IFCHL = 0,

$\underline{G}$ is not computed from $\underline{L}$. IFCHLI is the option flag for checking $\underline{L}^{-1}$ as calculated by LINV. If IFCHLI = 1, $\underline{L}\,\underline{L}^{-1}$ is computed as a check on $\underline{L}^{-1}$; if IFCHLI = 0, no check is made. The options IFCHL and IFCHLI are in effect only if LINV has been called (IFLI = 1). IFCHB is the option flag for checking the symmetrized $\underline{B}$ matrix. If IFCHB = 1, $\underline{G}$ is computed, and if IFCHB = 0, it is not. This option is in effect only if BSYM has been called (IFBS = 1). IFROC is the option flag for calculating the rotational corrections. If IFROC = 1, rotational corrections are calculated by subroutine ROTCOR, and $\underline{P}_X$ may then be computed. IFPV and IFPD are the option flags for punching the $\underline{V}$ and $\underline{P}_X^{\alpha}$ tensors on cards for use in program TRANSC. If these two flags are equal to "1", the tensors are punched; if the flags are equal to "0", the tensors are not punched. IFAM is the option flag for calculating $\underline{A}$ and $\underline{G}^{-1}$ by subroutine AMAT. In order to utilize this subroutine, however, IFSB must be equal to "1". This is due to the fact that $\underline{G}$ used in AMAT is calculated by BSYM. Hence, if IFSB = 1 and IFAM = 1, then $\underline{A}$ and $\underline{G}^{-1}$ are computed. If IFSB = 0 and/or IFAM = 0, $\underline{A}$ and $\underline{G}^{-1}$ are not computed. FORMAT (9I3).

5. XM(I) -- The atomic masses are entered in the order used in the normal coordinate analysis. FORMAT (6F12.6).

If $\underline{L}^{-1}$ is to be calculated from $\underline{L}$, IFLI = 1, the following sets of data are required:

6. F(I) -- The frequencies (cm^{-1}) as computed by the normal

coordinate analysis. FORMAT (6F12.6).

7. XL(I,J) -- The symmetrized L matrix is entered by reading the row number, column number, and the L element. The row number following the last L element is set to - 06 (end code). Only non-zero elements need to be entered. FORMAT {4(2I3,F12.6)}.

8. FC(I,J) -- The upper triangle of the symmetrized F matrix is entered using the same format as item 7. Only non-zero elements need to be entered. The end code is - 07.

If $\underline{L}^{-1}$ is read directly, IFLI = 0, then items 6, 7, and 8 are omitted and only the symmetrized $\underline{L}^{-1}$ is read using the same format as item 7, except the end code is "0".

If B is to be symmetrized, IFSB = 1, the following sets of data are required:

9. B(I,J) -- The non-symmetrized B matrix (as punched by WMAT) is read using the same format as item 7, except the end code is - 05. Only non-zero elements need to be entered.

10. U(I,J) -- The non-normalized U matrix used in the normal coordinate analysis is entered in the same format as item 7, except the end code is - 03. Only non-zero elements need to be entered.

If B is already symmetrized, IFSB = 0, items 9 and 10 are omitted, and B is read directly using the format of item 7, except the end code is "0".

11. A(I,J) -- The $\partial \vec{p}/\partial Q_i$ matrix is entered by giving the row and column number followed by the absolute value of

$\partial\vec{p}/\partial Q_i$. The end code is "0", and only non-zero elements need to be entered. FORMAT {4(2I3,F12.6)}.

If rotational corrections are required, the following sets of data are read:

12. CC(I,J) -- The center of mass Cartesian coordinates are read giving the coordinate number (x = 1, y = 2, z = 3), the atom number, and the value of the coordinate, respectively. The end code is "0". Only non-zero elements need to be entered. FORMAT {4(2I3,F12.6)}.
13. u_x^0, u_y^0, u_z^0 -- The x, y, and z components of the permanent dipole moment are entered in the order x, y, z. FORMAT (3F12.6).
14. XI, YI, ZI -- The principal moments of inertia are entered in the order I_{xx}, I_{yy}, and I_{zz} with the same format as 13.

If no rotational corrections are required, IFROC = 0, items 12, 13, and 14 are omitted.

15. SIGN(I,J) -- The signs (σ_i) of the $\partial\vec{p}/\partial Q_i$'s are entered with the same format as item 11.
16. IFADSC -- A flag to signify whether additional sign combinations for the $\partial\vec{p}/\partial Q_i$'s are to follow. If IFADSC = 1, an additional set of signs are read using the same format as item 15. Thus, any number of sets of signs may be entered after the initial set (item 15) if each different set is preceeded by a card with IFADSC = 1. If IFADSC = 0, the program continues to the calculation of $\underline{A}$ and $\underline{G}^{-1}$ if IFAM = 1 or proceeds to the next problem

if IPAM = 0.

17. IPCAL -- An option flag in subroutine AMAT to indicate that $\underline{P}_S$ and $\underline{P}_Q$ are to be calculated from a $\underline{P}_X$ matrix. If IPCAL = 1, a $\underline{P}_X$ matrix is to follow (item 18). If IPCAL = 0, the program proceeds to the next problem. FORMAT (I3).

18. CAL(I,J) -- The calculated $\underline{P}_X$ matrix for the subsequent calculation of $\underline{P}_S$ and $\underline{P}_Q$ is read in using the format of item 11.

Items 17 and 18 can be used only if AMAT has been called.

To terminate the program, a problem number card (item 1) is placed at the end of the data with NOPROB = 7777.

PVDTEN was initially written to use symmetry coordinates, but internal coordinates could be used if certain variables are assigned to compensate for the differences between the coordinates. In the case of internal coordinates, NS would be equal to NI and a unit matrix could be entered for the required $\underline{U}$ matrix if the options in subroutines BSYM and AMAT were required.

The program length is about 181 K bytes and could easily be expanded to accept molecules larger than sixteen atoms by increasing the dimensions of the arrays.

A computer print-out of program PVDTEN is given below.

```
// EXEC F4HDXM      FORT H COMPILE (DECK), EXECUTE, CLASS M
/*PASSWORD      1,SPECTOR
//FORT.SYSIN DD *
      DIMENSION A(50,50),P(3,50),D(3,50),SIGN(3,50),SA(3,50),RECORD(12)
      COMMON NI,NS,NA,NA3,NRC,IFCHL,IFCHLI,IFCHB,NR(4),NC(4),DA(4),XM(50
     X),XLI(50,50),SB(50,50),V(3,50),ROTC(50,9),R(450),RM(50),G(50,50),X
     XL(50,50)
      REAL*8 RECORD
      WRITE(6,2227)
 2227 FORMAT('1')
    1 READ(5,2) NOPROB
    2 FORMAT(I4)
      IF(NOPROB-7777) 3,100,3
    3 READ(5,6) (RECORD(I),I=1,12)
      WRITE(6,5) NOPROB
    5 FORMAT(1X,'THIS IS PROBLEM',I4)
      WRITE(6,6) (RECORD(I),I=1,12)
    6 FORMAT(1X,12A6)
      READ(5,12) NS,NA,NI,NRC
   12 FORMAT(4I3)
      READ(5,120) IFLI,IFSB,IFCHL,IFCHLI,IFCHB,IFROC,IFPV,IFPD,IFAM
  120 FORMAT(9I3)
      NA3=NA*3
C
C     READ THE ATOMIC MASS OF THE ATOMS
C
      READ(5,140) (XM(I),I=1,NA)
  140 FORMAT(6F12.6)
      IF(IFLI.EQ.1) GO TO 111
      DO 7 I=1,50
      DO 7 J=1,50
    7 XLI(I,J)=0.0
C
C     READ L INVERSE
```

```
C
    8 READ(5,9) (NR(I),NC(I),DA(I),I=1,4)
    9 FORMAT(4(2I3,F12.6))
      DO 10 I=1,4
      K=NR(I)
      IF(K.EQ.0) GO TO 11
      L=NC(I)
   10 XLI(K,L)=DA(I)
      GO TO 8
   11 CONTINUE
      WRITE(6,17)
   17 FORMAT(1X,//1X,'THE L INVERSE MATRIX')
      DO 18 I=1,NS
      WRITE(6,19) I
   19 FORMAT(1X,'ROW',I4)
      WRITE(6,20) (XLI(I,J),J=1,NS)
   20 FORMAT(10F12.6)
   18 CONTINUE
      GO TO 112
  111 CALL LINV
  112 CONTINUE
      IF(IFSB.EQ.1) GO TO 113
      DO 13 I=1,50
      DO 13 J=1,50
   13 SB(I,J)=0.0
C
C     READ THE SYMMETRIZED B MATRIX
C
   14 READ(5,9) (NR(I),NC(I),DA(I),I=1,4)
      DO 15 I=1,4
      K=NR(I)
      IF(K.EQ.0) GO TO 16
      L=NC(I)
   15 SB(K,L)=DA(I)
```

```
      GO TO 14
   16 CONTINUE
      WRITE(6,21)
   21 FORMAT('1',1X,'THE SYMMETRIZED  B MATRIX')
      DO 22 I=1,NS
      WRITE(6,19) I
      WRITE(6,20) (SB(I,J),J=1,NA3)
   22 CONTINUE
      GO TO 114
  113 CALL BSYM
  114 CONTINUE
      DO 23 I=1,3
      DO 23 J=1,50
      A(I,J)=0.0
   23 CONTINUE
C
C      READ THE P(Q) MATRIX
C
C
   24 READ(5,9) (NR(I),NC(I),DA(I),I=1,4)
      DO 25 I=1,4
      K=NR(I)
      IF(K.EQ.0) GO TO 26
      L=NC(I)
   25 A(K,L)=DA(I)
      GO TO 24
   26 CONTINUE
      IF(IFRCC.EQ.1) GO TO 40
      GO TO 126
   40 CALL ROTCOR
  126 CONTINUE
      DO 27 I=1,3
      DO 27 J=1,50
      SIGN(I,J)=0.0
```

```
   27 SA(I,J)=0.0
C
C     READ THE FIRST SIGNS FOR THE DU/DQ'S
C
   28 READ(5,9) (NR(I),NC(I),DA(I),I=1,4)
      DO 29 I=1,4
      K=NR(I)
      IF(K.EQ.0) GO TO 30
      L=NC(I)
   29 SIGN(K,L)=DA(I)
      GO TO 28
   30 CONTINUE
      WRITE(6,144)
  144 FORMAT('1',1X,'THE SIGN COMBINATIONS')
      DO 132 I=1,3
      WRITE(6,19) I
      WRITE(6,20) (SIGN(I,J),J=1,NS)
  132 CONTINUE
      DO 31 I=1,3
      DO 31 J=1,NS
   31 SA(I,J)=SIGN(I,J)*A(I,J)
      WRITE(6,44)
   44 FORMAT(1X//1X,'THE P(Q)MATRIX')
      DO 32 I=1,3
      WRITE(6,19) I
      WRITE(6,20) (SA(I,J),J=1,NS)
   32 CONTINUE
C
C      CALCULATE THE P(S) MATRIX
C
      DO 33 I=1,3
      DO 33 K=1,NS
      P(I,K)=0.0
      DO 33 J=1,NS
```

```
      P(I,K)=P(I,K)+SA(I,J)*XLI(J,K)
   33 CONTINUE
      WRITE(6,34)
   34 FORMAT(1X//1X,'THE P(S) MATRIX')
      DO 35 I=1,3
      WRITE(6,19) I
      WRITE(6,20) (P(I,J),J=1,NS)
   35 CONTINUE
C
C     CALCULATE THE V MATRIX
C
      DO 36 I=1,3
      DO 36 K=1,NA3
      V(I,K)=0.0
      DO 36 J=1,NS
      V(I,K)=V(I,K)+P(I,J)*SB(J,K)
   36 CONTINUE
      WRITE(6,88)
   88 FORMAT(1X,//1X,'THE V MATRIX')
      DO 37 I=1,3
      WRITE(6,19)I
      WRITE(6,20) (V(I,J),J=1,NA3)
   37 CONTINUE
C     PRINT THE V TENSORS FOR EACH ATOM
C
      DO 50 M=1,NA
      N=3*M-2
      L=3*M
      WRITE(6,51) M
   51 FORMAT(1X,///1X,'THE V TENSOR FOR ATOM',I4)
      DO 50 I=1,3
      WRITE(6,19) I
      WRITE(6,52) (V(I,J),J=N,L)
   52 FORMAT(3F12.6)
```

```
C
C       CALCULATE THE SUM OF THE P(X) ELEMENTS FOR EACH ATOM
C
      IF(IFPV.EQ.0) GO TO 50
      WRITE(7,52) (V(I,J),J=N,L)
   50 CONTINUE
      IF(IFROC.EQ.0) GO TO 155
      K=1
      DO 150 M=1,NA
      N=3*M-2
      L=3*M
      DO 150 I=1,3
      DO 150 J=N,L
      D(I,J)=V(I,J)+R(K)
      K=K+1
  150 CONTINUE
C
C       CALCULATE THE P(X) MATRIX
C
      WRITE(6,151)
  151 FORMAT('1',1X//1X,'THE P(X) MATRIX')
      DO 137 I=1,3
      WRITE(6,19) I
      WRITE(6,20) (D(I,J),J=1,NA3)
  137 CONTINUE
      IJ=NA3-3
      DO 1112 I=1,3
      DO 1112 K=1,3
      SUM=0.0
      NN=IJ+K
      DO 1110 J=K,NN,3
      SUM=SUM+D(I,J)
 1110 CONTINUE
      WRITE(6,1111) I,K,SUM
```

```
 1111 FORMAT(1X/1X,'THE SUM OF THE P(X) MATRIX ELEMENTS FOR ROW',I4,'AND
     XELEMENT',I4,'IS',2X,F12.6)
 1112 CONTINUE
C
C       PRINT THE P(X) TENSOR FOR EACH ATOM
C
      DO 155 M=1,NA
      N=3*M-2
      L=3*M
      WRITE(6,156) M
  156 FORMAT(1X//1X,'THE P(X) TENSOR FOR ATOM',I4)
      DO 155 I=1,3
      WRITE(6,19) I
      WRITE(6,52) (D(I,J),J=N,L)
      IF(IFPD.EQ.0) GO TO 155
      WRITE(7,52) (D(I,J),J=N,L)
  155 CONTINUE
C
C     READ FLAG FOR ADDITIONAL SIGN COMBINATIONS
C
      READ(5,38) IFASC
   38 FORMAT(I3)
      IF(IFASC.EQ.0) GO TO 39
      GO TO 126
   39 CONTINUE
      IF(IFAM.EQ.1) CALL AMAT
      GO TO 1
  100 STOP
      END
      SUBROUTINE ROTCOR
      DIMENSION CC(50,50),CP(3)
      COMMON NI,NS,NA,NA3,NRC,IFCHL,IFCHLI,IFCHB,NR(4),NC(4),DA(4),XM(50
     X),XLI(50,50),SB(50,50),V(3,50),ROTC(50,9),R(450),RM(50),G(50,50),X
     XL(50,50)
```

```
      DO 1 I=1,50
      DO 1 J=1,50
    1 CC(I,J)=0.0
C
C       READ NON-ZERO ELEMENTS OF THE CENTER OF MASS CARTESIAN COORD.'S
C
    2 READ(5,3) (NR(I),NC(I),DA(I),I=1,4)
    3 FORMAT(4(2I3,F12.6))
      DO 4 I=1,4
      K=NR(I)
      IF(K.EQ.0) GO TO 5
      L=NC(I)
      CC(K,L)=DA(I)
    4 CONTINUE
      GO TO 2
    5 CONTINUE
      WRITE(6,6)
    6 FORMAT(1X,//1X,'THE CENTER OF MASS CARTESIAN COORDINATES')
      DO 7 J=1,NA
      WRITE(6,8) J
    8 FORMAT(1X,'X,Y,Z FOR ATOM',I3)
      WRITE(6,9) (CC(I,J),I=1,3)
    9 FORMAT(1X,3F12.6)
    7 CONTINUE
C       READ THE X,Y,Z COMPONENTS OF THE PERMANATE DIPOLE MOMENT IN
C       X,Y,Z, ORDER
      READ(5,10) (DP(I),I=1,3)
   10 FORMAT(3F12.6)
      WRITE(6,11)
   11 FORMAT(1X,//1X,'THE X,Y,Z COMPONENTS OF THE PERMANATE DIPOLE MOMEN
     XT')
      DO 12 I=1,3
      WRITE(6,13) DP(I)
   13 FORMAT(5X,F12.6)
```

```
   12 CONTINUE
C
C      READ THE PRINCIPLE MOMENTS OF INERTIA
C
      READ(5,10) XI,YI,ZI
      WRITE(6,14)
   14 FORMAT(1X,//1X,'THE X,Y,Z MOMENTS OF INERTIA')
      WRITE(6,15) XI,YI,ZI
   15 FORMAT(5X,F12.6,/5X,F12.6,/5X,F12.6)
      DO 16 I=1,NA
      ROTC(I,1)=XM(I)*((DP(3)*CC(3,I)/YI)+(DP(2)*CC(2,I)/ZI))
      ROTC(I,2)=-XM(I)*(DP(2)*CC(1,I)/ZI)
      ROTC(I,3)=-XM(I)*(DP(3)*CC(1,I)/YI)
      ROTC(I,4)=-XM(I)*(DP(1)*CC(2,I)/ZI)
      ROTC(I,5)=XM(I)*((DP(3)*CC(3,I)/XI)+(DP(1)*CC(1,I)/ZI))
      ROTC(I,6)=-XM(I)*(DP(3)*CC(2,I)/XI)
      ROTC(I,7)=-XM(I)*(DP(1)*CC(3,I)/YI)
      ROTC(I,8)=-XM(I)*(DP(2)*CC(3,I)/XI)
      ROTC(I,9)=XM(I)*((DP(2)*CC(2,I)/XI)+(DP(1)*CC(1,I)/YI))
   16 CONTINUE
      WRITE(6,17)
   17 FORMAT(1X,//1X,'THE ROTATIONAL CORRECTIONS')
      DO 20 I=1,NA
      WRITE(6,18) I
   18 FORMAT(1X,/1X,'ATOM',I3)
      WRITE(6,19) (ROTC(I,J),J=1,9)
   19 FORMAT(1X,3F12.6)
   20 CONTINUE
      K=0
      DO 21 I=1,NA
      DO 21 J=1,9
      K=K+1
      R(K)=ROTC(I,J)
   21 CONTINUE
```

```
      RETURN
      END
      SUBROUTINE LINV
      DIMENSION F(50),FC(50,50),TEMP(50,50)
      COMMON NI,NS,NA,NA3,NRC,IFCHL,IFCHLI,IFCHB,NR(4),NC(4),DA(4),XM(50
     X),XLI(50,50),SB(50,50),V(3,50),ROTC(50,9),R(450),RM(50),G(50,50),X
     XL(50,50)
      LC=NS
C
C     READ THE FREQUENCIES IN CM(-1)
C
      READ(5,7) (F(I),I=1,LC)
    7 FORMAT(6F12.6)
      WRITE(6,8)
    8 FORMAT(1X,//1X,'THE FREQUENCIES IN CM(-1)')
      WRITE(6,9) (I,F(I),I=1,LC)
    9 FORMAT(6(I3,F12.6))
C
C     CALCULATE FREQUENCY PARAMETERS
C
      DO 10 I=1,LC
      F(I)=0.588851*((F(I)/1000.0)**2)
   10 CONTINUE
      WRITE(6,11)
   11 FORMAT(1X,'THE FREQUENCY PARAMERERS')
      WRITE(6,9) (I,F(I),I=1,LC)
      DO 12 I=1,50
      DO 12 J=1,50
   12 XL(I,J)=0.0
C     READ L MATRIX
   13 READ(5,14) (NR(I),NC(I),DA(I),I=1,4)
   14 FORMAT(4(2I3,F12.6))
      DO 16 I=1,4
      K=NR(I)
```

```
      IF(K+6) 17,17,15
   15 L=NC(I)
      XL(K,L)=CA(I)
   16 CONTINUE
      GO TO 13
   17 CONTINUE
C     READ THE UPPER TRIANGLE OF THE F MATRIX
      DO 18 I=1,50
      DO 18 J=1,50
   18 FC(I,J)=0.0
   19 READ(5,20) (NR(I),NC(I),CA(I),I=1,4)
   20 FORMAT(4(2I3,F12.6))
      DO 22 I=1,4
      K=NR(I)
      IF(K+7) 23,23,21
   21 L=NC(I)
      FC(K,L)=CA(I)
   22 CONTINUE
      GO TO 19
   23 CONTINUE
      DO 24 I=1,LD
      DO 24 J=1,I
      FC(I,J)=FC(J,I)
   24 CONTINUE
C     WRITE THE L MATRIX
      WRITE(6,25)
   25 FORMAT(1X,//1X,'THE L MATRIX')
      DO 28 I=1,LD
      WRITE(6,26) I
   26 FORMAT(1X,'ROW',I4)
      WRITE(6,27) (XL(I,J),J=1,LD)
   27 FORMAT(10F12.6)
   28 CONTINUE
C     WRITE THE F MATRIX
```

```
      WRITE(6,29)
   29 FORMAT(1X,//1X,'THE F MATRIX')
      DO 30 I=1,LD
      WRITE(6,26) I
      WRITE(6,27) (FC(I,J),J=1,LD)
   30 CONTINUE
      IF(IFCHL.EQ.0) GO TO 33
C     CHECK THE L MATRIX--- LL(T)=G ---
      DO 31 I=1,LD
      DO 31 K=1,LD
      TEMP(I,K)=0.0
      DO 31 J=1,LD
      TEMP(I,K)=TEMP(I,K)+XL(I,J)*XL(K,J)
   31 CONTINUE
      WRITE(6,32)
   32 FORMAT(1X,//1X,'L MATRIX CHECK---LL(T)=G')
      DO 33 I=1,LD
      WRITE(6,26) I
      WRITE(6,27) (TEMP(I,J),J=1,LD)
   33 CONTINUE
C     CALCULATE L INVERSE
      DO 34 I=1,LD
      DO 34 K=1,LD
      XLI(I,K)=0.0
      DO 34 J=1,LD
      XLI(I,K)=XLI(I,K)+ (XL(J,I)*FC(J,K))/F(I)
   34 CONTINUE
      WRITE (6,35)
   35 FORMAT('1')
      WRITE(6,36)
   36 FORMAT(1X,'THE L INVERSE MATRIX')
      DO 37 I=1,LD
      WRITE(6,26) I
      WRITE(6,27) (XLI(I,J),J=1,LD)
```

```
   37 CONTINUE
      IF(IFCHLI.EQ.0) GO TO 40
C     CHECK L INVERSION
      DO 38 I=1,LD
      DO 38 K=1,LD
      TEMP(I,K)=0.0
      DO 38 J=1,LD
      TEMP(I,K)=TEMP(I,K)+XL(I,J)*XLI(J,K)
   38 CONTINUE
      WRITE(6,39)
   39 FORMAT(1X,//1X,'INVERSION CHECK---LL(-1)=E')
      DO 40 I=1,LD
      WRITE(6,26) I
      WRITE(6,27) (TEMP(I,J),J=1,LD)
   40 CONTINUE
      RETURN
      END
      SUBROUTINE BSYM
C     PROGRAM BSYM-THIS PROGRAM SYMMETRIZES THE B MATRIX PUNCHED BY
C     PROGRAM WMAT
C
      DIMENSION U(50,50),B(50,50)
      COMMON NI,NS,NA,NA3,NRC,IFCHL,IFCHLI,IFCHB,NR(4),NC(4),DA(4),XM(50
     X),XLI(50,50),SB(50,50),V(3,50),ROTC(50,9),R(450),RM(50),G(50,50),X
     XL(50,50)
      NS=NS+NRC
      DO 90 I=1,50
      DO 90 J=1,50
   90 B(I,J)=0.0
C
C     READ NONSYMMETRIZED B MATRIX
C
    7 READ(5,8) (NR(I),NC(I),DA(I),I=1,4)
    8 FORMAT(4(2I3,F12.6))
```

```
      DO 9 I=1,4
      K=NR(I)
      IF(K+5) 11,11,10
   10 L=NC(I)
    9 B(K,L)=DA(I)
      GO TO 7
   11 CONTINUE
      WRITE(6,12)
   12 FORMAT(1X,//1X,'THE NONSYMMETRIZED B MATRIX')
      DO 14 I=1,NI
      WRITE(6,44) I
      WRITE(6,45) (B(I,J),J=1,NA3)
   14 CONTINUE
      DO 15 I=1,50
      DO 15 J=1,50
   15 U(I,J)=0.000
C
C     READ NON-NORNALIZED U MATRIX
C
   16 READ(5,8) (NR(I),NC(I),DA(I),I=1,4)
      DO 18 I=1,4
      K=NR(I)
      IF(K+3) 19,19,17
   17 L=NC(I)
   18 U(K,L)=DA(I)
      GO TO 16
   19 CONTINUE
      WRITE(6,20)
   20 FORMAT(1X,//1X,'THE UNNORMALIZED U MATRIX')
      DO 22 I=1,NS
      WRITE(6,44) I
      WRITE(6,45) (U(I,J),J=1,NI)
   22 CONTINUE
C
```

```
C     NORMALIZE THE U MATRIX
C
      DO 23 I=1,NS
      UU=0.0
      DO 24 J=1,NI
      UU=UU+U(I,J)**2
   24 CONTINUE
      DO 25 J=1,NI
   25 U(I,J)=U(I,J)/SQRT(UU)
   23 CONTINUE
      WRITE(6,26)
   26 FORMAT(1X,//1X,'THE NORMALIZED U MATRIX')
      DO 27 I=1,NS
      WRITE(6,44) I
   27 WRITE(6,45) (U(I,J),J=1,NI)
C
C     SYMMETRIZE THE B MATRIX
      DO 28 I=1,NS
      DO 28 K=1,NA3
      SB(I,K)=0.0
      DO 28 J=1,NI
      SB(I,K)=SB(I,K)+U(I,J)*B(J,K)
   28 CONTINUE
      WRITE(6,29)
   29 FORMAT(1X,//1X,'THE SYMMETRIZED B MATRIX')
      DO 30 I=1,NS
      WRITE(6,44) I
      WRITE(6,45) (SB(I,J),J=1,NA3)
   30 CONTINUE
   31 CONTINUE
C
C     CHECK ON THE SYMETERIZED B MATRIX ---B.M(-1)B(T)=G---
C
      IF(IFCHB.EQ.0) GO TO 46
```

```
C
C     CALCULATE THE G MATRIX
C
      DO 75 I=1,50
      RM(I)=1.0
   75 CONTINUE
C
C
      K=0.0
      DO 41 I=1,NA
      K=K+1
      RM(K)=1.0/XM(I)
      RM(K+1)=1.0/XM(I)
      RM(K+2)=1.0/XM(I)
      K=K+2
   41 CONTINUE
      DO 42 I=1,NS
      DO 42 K=1,NS
      G(I,K)=0.0
      DO 42 J=1,NA3
      G(I,K)=G(I,K)+SB(I,J)*(SB(K,J)*RM(J))
   42 CONTINUE
      WRITE(6,43)
   43 FORMAT('1',1X,'B MATRIX CHECK ---BM(-1)  B(T)=G ---')
      DO 46 I=1,NS
      WRITE(6,44) I
   44 FORMAT(1X,'ROW',I4)
      WRITE(6,45) (G(I,J),J=1,NS)
   45 FORMAT(10F12.6)
   46 CONTINUE
   13 FORMAT(4(2I3,F12.6))
      NS=NS-NRC
      RETURN
      END
```

```
      SUBRCUTINE AMAT
      DIMENSION AM(50,50),GI(50,50),E(50,50),CAL(3,50),PQ(3,50)
      COMMON NI,NS,NA,NA3,NRC,IFCHL,IFCHLI,IFCHB,NR(4),NC(4),DA(4),XM(50
     X),XLI(50,50),SB(50,50),V(3,50),ROTC(50,9),R(450),RM(50),G(50,50),X
     XL(50,50)
C
C
C     CALCULATE G INVERSE
C
      DO 1 I=1,50
      DO 1 J=1,50
    1 GI(I,J)=0.0
      DO 2 I=1,NS
      DO 2 J=1,NS
      GI(I,J)=0.0
      DO 2 K=1,NS
      GI(I,J)=GI(I,J)+ XLI(K,I)*XLI(K,J)
    2 CONTINUE
C
C      PRINT THE G(-1) MATRIX
C
      WRITE(6,3)
    3 FORMAT('1',1X,'THE G INVERSE MATRIX',/)
      DO 6 I=1,NS
      WRITE (6,4) I
    4 FORMAT(1X,'ROW',2X,I4)
      WRITE(6,5)(GI(I,J),J=1,NS)
    5 FORMAT(10F12.6)
    6 CONTINUE
C
C     CHECK G INVERSION
C
      DO 8 I=1,NS
      DO 8 J=1,NS
```

```
      E(I,J)=0.0
      DO 8 K=1,NS
      E(I,J)=E(I,J)+GI(I,K)*G(K,J)
    8 CONTINUE
      WRITE(6,9)
    9 FORMAT(1X,//1X,'G INVERSION CHECK')
      DO 10 I=1,NS
      WRITE(6,4) I
      WRITE(6,5) (E(I,J),J=1,NS)
   10 CONTINUE
C
C     CALCULATE B(T)*G(-1)
C
      DO 11 I=1,50
      DO 11 J=1,50
   11 E(I,J)=0.0
      DO 12 I=1,NA3
      DO 12 J=1,NS
      E(I,J)=0.0
      DO 12 K=1,NS
      E(I,J)=E(I,J)+SB(K,I)*GI(K,J)
   12 CONTINUE
      K=0
      DO 13 I=1,NA3
      K=K+1
      DO 13 J=1,NS
      AM(I,J)=RM(K)*E(I,J)
   13 CONTINUE
C
C     WRITE THE A MATRIX
C
      WRITE (6,14)
   14 FORMAT(1X,//1X,'THE A MATRIX')
      DO 15 I=1,NA3
```

```
      WRITE(6,4) I
      WRITE(6,5) (AM(I,J),J=1,NS)
   15 CONTINUE
C
C       CHECK INVERSION
C
      DO 16 I=1,NS
      DO 16 J=1,NS
      E(I,J)=0.0
      DO 16 K=1,NA3
      E(I,J)=E(I,J)+SB(I,K)*AM(K,J)
   16 CONTINUE
      WRITE(6,17)
   17 FORMAT(1X,//1X,'A MATRIX CHECK--B*A=E--')
      DO 18 I=1,NS
      WRITE(6,4) I
      WRITE(6,5) (E(I,J),J=1,NS)
   18 CONTINUE
      READ(5,19) IFCAL
   19 FORMAT(I3)
      IF(IFCAL.EQ.0) GO TO 33
C
C     READ CALCULATED POLAR TENSOR IN ROW ORDER-NONZERO ELEMENTS ONLY-
C
      DO 20 I=1,3
      DO 20 J=1,50
      CAL(I,J)=0.0
   20 CONTINUE
   21 READ(5,22) (NR(I),NC(I),CA(I),I=1,4)
   22 FORMAT(4(2I3,F12.6))
      DO 23 I=1,4
      K=NR(I)
      IF(K.EQ.0) GO TO 24
      L=NC(I)
```

```
      CAL(K,L)=CA(I)
   23 CONTINUE
      GO TO 21
   24 CONTINUE
C
C     WRITE OUT THE CALCULATED DP/DX TENSOR
C
      WRITE(6,25)
   25 FORMAT('1',1X,'THE CALCULATED DP/DX TENSOR'/)
      DO 26 I=1,3
      WRITE(6,4) I
      WRITE(6,5) (CAL(I,J),J=1,NA3)
   26 CONTINUE
C
C     COMPUTE THE DP/DS TENSOR
C
      DO 27 I=1,3
      DO 27 J=1,NS
      E(I,J)=0.0
      DO 27 K=1,NA3
      E(I,J)=E(I,J)+CAL(I,K)*AM(K,J)
   27 CONTINUE
C
C     WRITE THE DP/DS TENSOR
C
      WRITE (6,28)
   28 FORMAT(1X,//1X,'THE CALCULATED DP/DS TENSOR')
      DO 29 I=1,3
      WRITE(6,4) I
      WRITE(6,5) (E(I,J),J=1,NS)
   29 CONTINUE
C
C      CALCULATE THE DP/DQ TENSOR
C
```

```
      DO 31 I=1,3
      DO 31 J=1,NS
      PQ(I,J)=0.0
      DO 31 K=1,NS
      PQ(I,J)=PQ(I,J)+E(I,K)*XL(K,J)
   31 CONTINUE
C
C     PRINT THE DP/DQ TENSOR
C
      WRITE (6,32)
   32 FORMAT(1X,//1X,'THE CALCULATED DP/DQ TENSOR')
      DO 33 I=1,3
      WRITE(6,4) I
      WRITE(6,5) (PQ(I,J),J=1,NS)
   33 CONTINUE
      RETURN
      END
```

Program TRANSC

Program TRANSC rotates a Cartesian 3 x 3 tensor $\underline{T}$ about the origin of the Cartesian coordinate system. The transformation is given by

$$t'_{i,k} = \vec{e}'_i \cdot \underline{T} \cdot \vec{e}'_k = \sum_{j,l=1}^{3} a_{i,j}\, a_{l,k}\, t_{j,l} \quad , \qquad \text{(AII-1)}$$

where $t'_{i,k}$ is the magnitude of the i, k$\underline{\text{th}}$ element of the new tensor $\underline{T}'$. The unit vectors $\vec{e}'_i$ and $\vec{e}'_k$ are parallel to the new i and k coordinate axes, respectively. The coefficients $a_{i,j}$ and $a_{l,k}$ are just the cosines of the angles between the original coordinate axes and the new coordinate axes.

Program TRANSC consists of a main program which transforms the tensor $\underline{T}$ to the new tensor, $\underline{T}'$, and one subroutine, ERROR, which propagates the dispersions in $\underline{T}$ through to $\underline{T}'$. A description of the in-put data is given below:

ITEM (each item begins on a new card):

1. NOPROB -- The number of the problem. If NOPROB = 7777, the program terminates; otherwise, problems may be stacked for consecutive runs. FORMAT (I4).
2. RECORD (I) -- Alphanumeric data for identification of the problem. The first column must be blank. FORMAT (IX, 12A6).
3. X(I,J) -- The nine angles (in degrees) between the old and new axes are entered in the order x'x, x'y, x'z, y'x, y'y, y'z...z'z, with three angles per card. FORMAT (3F12.8).
4. T(I,J) -- The original tensor is entered in row order with

three elements per card. FORMAT (3F12.8).

5. IFERR -- If dispersions in the old tensor are known and the resulting dispersions in the new tensor are required, then set IFERR = 1. This activates subroutine ERROR for the calculations of the new dispersions. If IFERR = 0, no dispersions are computed. The IFERR card is included for each transformation. FORMAT (I4).
6. ERR(I,J) -- If IFERR = 1, the dispersions in the old tensor are read using the same format as item 4. If IFERR = 0, the dispersions are omitted.
7. IFADT -- If additional tensors are to be transformed using the original angles of item 3, then the IFADT flag is set equal to "1". Any number of tensors may be transformed using the original angles if each tensor is preceeded by a card with IFADT = 1. (Note, however, that the IFERR card, item 5, must also be present for each additional tensor.) If IFADT = 0, the program proceeds to a new problem. FORMAT (I4).

TRANSC is about 4.5 K bytes in length. A listing of the program is given below.

```
//TRANSC   JOB (2003,1078,020,05,0200),'  JAMES NEWTON       ',CLASS=S
// EXEC F4GCXS      FORT G COMPILE (NODECK), EXECUTE, CLASS S
//FORT.SYSIN DD *
C
C
      COMMON A(3,3),T(3,3)
      DIMENSION         TT(3,3),TTT(3,3),X(3,3),RECORD(12)
      REAL*8 RECORD
    1 READ(5,10) NOPROB
   10 FORMAT(I4)
      IF(NOPROB-7777) 11,100,11
   11 CONTINUE
      READ(5,12) (RECORD(K),K=1,12)
   12 FORMAT(1X,12A6)
      WRITE(6,13) NOPROB
   13 FORMAT(1X,'THIS IS PROBLEM',I5)
      WRITE(6,12) (RECORD(K),K=1,12)
C
C      READ ANGLES IN ORDER X'X,X'Y,....Y'X....Z'Z
C
      DO 16 I=1,3
      READ(5,14) (X(I,J),J=1,3)
   16 CONTINUE
      WRITE(6,20)
   20 FORMAT(1X,//1X,'THE ANGLES')
      DO 21 I=1,3
      WRITE(6,18) (I,J,X(I,J),J=1,3)
   21 CONTINUE
C
C      CONVERT DEGREES TO RADIANS
C
      DO 40 I=1,3
      DO 40 J=1,3
      X(I,J)=X(I,J)/57.29577951
```

```
   40 CONTINUE
C
C      CALCULATE COS OF THE ANGLES
C
       DO 22 I=1,3
       DO 22 J=1,3
       A(I,J)=COS(X(I,J))
   22 CONTINUE
C
C       READ THE ORIGINAL TENSO IN ROW ORDER
C
       DO 15 I=1,3
       READ(5,14) (T(I,J),J=1,3)
   14 FORMAT(3F12.8)
   15 CONTINUE
C
C      WRITE OUT THE IN PUT DATA
C
       WRITE(6,17)
   17 FORMAT(1X,//1X,'THE ORIGINAL TENSOR')
       DO 19 I=1,3
       WRITE(6,18) (I,J,T(I,J),J=1,3)
   18 FORMAT(1X,3(2I3,1X,F12.6))
   19 CONTINUE
C
C       CALCULATION OF THE TRANSFORMED TENSOR
C
       DO 23 I=1,3
       DO 23 J=1,3
       TT(I,J)=0.000000
       DO 23 K=1,3
       DO 23 L=1,3
       TT(I,J)=TT(I,J)+A(I,K)*A(J,L)*T(K,L)
   23 CONTINUE
```

```
C
C     WRITE THE NEW TENSOR
C
      WRITE(6,24)
   24 FORMAT(1X,//1X,'THE TRANSFORMED TENSOR')
      DO 25 I=1,3
      WRITE(6,18) (I,J,TT(I,J),J=1,3)
   25 CONTINUE
C
C      CALCULATION OF THE TRACE OF THE OLD AND NEW TENSORS
C
      T1=0.000000
      T2=0.000000
      DO 45 I=1,3
      T1=T1+T(I,I)
      T2=T2+TT(I,I)
   45 CONTINUE
      WRITE(6,46) T1
   46 FORMAT(1X,//1X,'THE TRACE OF THE ORIGINAL TENSOR',2X,F12.6)
      WRITE(6,47)T2
   47 FORMAT(1X,'THE TRACE OF THE TRANSFORMED TENSOR',2X,F12.6)
C
C     CALCULATE THE PRODUCT OF THE NEW TENSOR AND ITS TRANSPOSE
C
      DO 55 I=1,3
      DO 55 K=1,3
      TTT(I,K)=0.0
      DO 55 J=1,3
      TTT(I,K)=TTT(I,K)+TT(I,J)*TT(K,J)
   55 CONTINUE
      WRITE(6,58)
   58 FORMAT(1X,//1X,'PRODUCT OF THE NEW TENSOR WITH ITS TRANSPOSE')
      DO 59 I=1,3
      WRITE(6,18) (I,J,TTT(I,J),J=1,3)
```

```
   59 CONTINUE
C
C      CALCULATE THE SQ. ROOT OF THE SUM OF THE SQ.' OF THE DIAGONAL
C      ELEMENTS OF THE PRODUCT OF THE NEW TENSOR AND ITS TRANSPOSE
C
       SUM=0.0
       DO 56 I=1,3
       SUM=SUM+TTT(I,I)**2
   56 CONTINUE
       ECH=SQRT(SUM)
       WRITE(6,57) ECH
   57 FORMAT(1X,//1X,'SQRT OF THE SUM OF SQ.S OF DIAGONAL ELEMENTS OF TH
      XE PRODUCT OF NEW TENSOR AND ITS TRANSPOSE',2X,F12.6)
       READ(5,10) IFERR
       IF(IFERR.EQ.1) CALL ERROR
       WRITE(6,50)
   50 FORMAT('1')
       READ(5,10) IFADT
       IF(IFADT.EQ.1) GO TO 22
       GO TO 1
  100 STOP
       END
       SUBROUTINE ERROR
       COMMON A(3,3),T(3,3)
       DIMENSION ERR(3,3),DISP(3,3)
C
C      READ DISPERSIONS IN THE OLD TENSOR
C
       DO 2 I=1,3
       READ(5,1) (ERR(I,J),J=1,3)
     1 FORMAT(3F12.8)
     2 CONTINUE
C
C       WRITE OUT THE DISPERSIONS
```

```
C
      WRITE(6,3)
    3 FORMAT(1X,//1X,'THE DISPERSIONS IN THE OLD TENSOR')
      DO 5 I=1,3
      WRITE(6,4) (I,J,ERR(I,J),J=1,3)
    4 FORMAT(1X,3(2I3,1X,F12.6))
    5 CONTINUE
C
C     CALCULATE THE DISPERSIONS IN THE NEW TENSOR
C
      DO 6 I=1,3
      DO 6 J=1,3
      DISP(I,J)=0.0
      DO 6 K=1,3
      DO 6 L=1,3
      DISP(I,J)=DISP(I,J)+(A(I,K)*A(J,L))**2*(ERR(K,L)**2)
    6 CONTINUE
      DO 7 I=1,3
      DO 7 J=1,3
    7 ERR(I,J)=SQRT(DISP(I,J))
C
C     WRITE OUT DISPERSIONS IN THE NEW TENSOR
C
      WRITE(6,8)
    8 FORMAT(1X,//1X,'DISPERSIONS IN THE TRANSFORMED TENSOR')
      DO 9 I=1,3
      WRITE(6,4) (I,J,ERR(I,J),J=1,3)
    9 CONTINUE
      RETURN
      END
/*
```

APPENDIX III

CORIOLIS CONSTANTS FOR THE CH_3X SERIES

The Coriolis constants ζ^{z}_{i} and $\zeta^{y}_{i,j}$ for the methyl halide series were calculated by the procedure outlined by Meal and Polo {J.H. Meal and S.R. Polo, J. Chem. Phys., 24, 1119 (1956)}. As described there, the $\underline{\zeta}^{\tau}$ (τ = x, y, or z) matrix is given by

$$\underline{\zeta}^{\tau} = \underline{L}^{-1}\, \underline{C}^{\tau}\, (\underline{L}^{-1})' \quad , \qquad \text{(AIII-1)}$$

where $\underline{L}^{-1}$ is the symmetrized inverse normal coordinate transformation matrix given in Appendix I, and $\underline{C}$ is defined as

$$\underline{C} = \underline{D}\, \underline{M}^{\tau}\, \underline{D}' \quad . \qquad \text{(AIII-2)}$$

The matrix $\underline{M}^{\tau}$ is a 3N x 3N matrix composed of N 3 x 3 submatrices along the diagonal as shown below.

$$\underline{M}^{\tau} = \begin{pmatrix} M_1^x & & & & & 0 \\ & M_1^y & & & & \\ & & M_1^z & & & \\ & & & \ddots & & \\ & & & & M_N^x & \\ & & & & & M_N^y \\ 0 & & & & & & M_N^z \end{pmatrix} .$$

The submatrices M^{τ} have the form

$$\underline{M}^{x} = \begin{pmatrix} 0 & 0 & 0 \\ 0 & 0 & 1 \\ 0 & -1 & 0 \end{pmatrix} \qquad \underline{M}^{y} = \begin{pmatrix} 0 & 0 & -1 \\ 0 & 0 & 0 \\ 1 & 0 & 0 \end{pmatrix}$$

$$\underline{M}^{z} = \begin{pmatrix} 0 & 1 & 0 \\ -1 & 0 & 0 \\ 0 & 0 & 0 \end{pmatrix} .$$

The matrix $\underline{D}$ is the mass weighted symmetrized $\underline{B}$ ($\underline{D} = \underline{B}\,\underline{M}^{-\frac{1}{2}}$) matrix used in the normal coordinate analysis. (Do not confuse $\underline{M}^{-\frac{1}{2}}$ with $\underline{M}^{\tau}$.)

Our calculated ζ constants are given in Table AIII-1. The experimental values are given in parentheses where available. The ζ^{y}_{i} values are the coupling constants between the degenerate E modes and the $\zeta^{z}_{i,j}$ values are the coupling constants between the i<u>th</u> $A_{1,z}$ mode and the j<u>th</u> E mode.

One should be aware of the fact that the zeta constants are not free of sign ambiguities, for as shown in Equation AIII-1 and AIII-2, ζ is a function of both $\underline{L}^{-1}$ and $\underline{B}$. Thus, to pick a sign of the zeta constant, one must know the $\underline{L}^{-1}$ matrix (that is, the sense of Q) and the original internal coordinate definitions ($\underline{B}$), since the sign of zeta is not derived directly from experiment (27, 34).

We are primarily interested in this work in the trends in $\zeta^{z}_{2,5}$ and $\zeta^{z}_{2,6}$. We see from the table that $\zeta^{z}_{2,5}$ is expected to be almost constant through the CH_3X series, and

values of $\zeta^{z}_{2,6}$ are expected to change smoothly. The fact that there does not appear to be any anomalous behavior in these calculated values of ζ^{z} through the series CH_3X prompts us to predict that the sign relationship between $\partial\vec{p}/\partial Q_2$ and $\partial\vec{p}/\partial Q_4$, as well as that between $\partial\vec{p}/\partial Q_3$ and $\partial\vec{p}/\partial Q_6$, is the same for the entire methyl halide series as found for CH_3F and CD_3Cl by DiLauro and Mills (15).

TABLE AIII-1

CALCULATED CORIOLIS CONSTANTS FOR THE CH_3X SERIES[a]
(Experimental Values in Parentheses)

	CH_3F	CH_3Cl	CH_3Br	CH_3I
$\zeta_i^y = \zeta_i^x$				
i = 4	0.069 (0.089)[b]	0.066 (0.065)[d]	0.058 (0.059)[d]	0.060 (0.065)[d]
5	-0.275 (-0.28)[b]	-0.268 (-0.272)[d]	-0.244 (-0.244)[d]	-0.243 (-0.239)[d]
6	0.289 (0.284)[b]	0.244 (0.238)[d]	0.217 (0.216)[d]	0.207 (0.212)[d]
$\zeta_{i,j}^z$				
i,j = 1,4	0.101 (0.060)[c]	0.050	0.034	0.015
2,5	-0.600 (-0.602)[c]	-0.600	-0.611 (0.601)[e]	-0.612
3,6	0.340 (0.318)[c]	0.248	0.210	0.186

a. All ζ's are dimensionless.
b. Values reported by Duncan et al. (20).
c. Experimental values reported by DiLauro and Mills (15).
d. Values reported by Duncan (21).
e. Absolute experimental value reported by Y. Morino and C Hirose, J. Mol. Spect., 24, 204 (1967).

REFERENCES

1. N.B. Colthup, L.H. Daly, and S.E. Wiberly, Introduction to Infrared and Raman Spectroscopy (Academic Press, New York, 1964).

2. A.S. Wexler, Applied Spect. Rev., 1, 29 (1967).

3. J. Overend, in Infrared Spectroscopy and Molecular Structure (M. Davies, Editor) (Elsevier, Amsterdam, 1963), p. 345.

4. W.B. Person and D. Steele, in Molecular Spectroscopy (D.A. Long, Editor), Specialist Periodical Report of the Chemical Society, No. 29, Vol. 2, 1974, pp. 357-438.

5. J.F. Biarge, J. Herranz, and J. Morcillo, Anales Real Soc. Espan. Fis. Quim. (Madrid), A57, 81, 1961.

6. W.B. Person, G.R. Peyton, and G. Jiang, Paper H5, Symposium on Molecular Spectra and Structure, Columbus, Ohio, June, 1972.

7. J. Morcillo, L.J. Zamorano, and J.M.V. Heredia, Spectrochim. Acta, 22, 1969 (1966).

8. J. Morcillo, J.F. Biarge, J.M.V. Heredia, and A. Medina, J. Mol. Structure, 3, 77 (1969).

9. D.F. Hornig and D.C. McKean, J. Am. Chem. Soc., 59, 1133 (1955).

10. W.T. King, G.B. Mast, and P.P. Blanchette, J. Chem. Phys., 56, 4440 (1972).

11. B.L. Crawford, Jr., J. Chem. Phys., 20, 977 (1952).

12. W.B. Person and J.H. Newton, J. Chem. Phys., 61, 1040 (1974).

13. I.M. Mills, in Infrared Spectroscopy and Molecular Structure (M. Davies, Editor) (Elsevier, Amsterdam, 1963), p. 166.

14. G.A. Segal and M.L. Klein, J. Chem. Phys., 47, 4236 (1967).

15. C. DiLauro and I.M. Mills, J. Mol. Spectry., 21, 386 (1966).

16. J. Aldous and I.M. Mills, Spectrochim. Acta, 18, 1073 (1962).

17. J. Aldous and I.M. Mills, Spectrochim. Acta, 19, 1567 (1963).

18. J.W. Russell, C.D. Needham, and J. Overend, J. Chem. Phys., 45, 3383 (1966).

19. G.E. Sanchez, Normal Coordinate Analysis of the Vibrations of Polyatomic Molecules, Ph.D. dissertation, University of Florida, Gainesville, Florida, 1971, Chapter 2 and Appendix 3.

20. J.L. Duncan, A. Allen, and D.C. McKean, Mol. Phys., 18, 289 (1970).

21. J.L. Duncan, D.C. McKean, and G.K. Speirs, Mol. Phys., 24, 553 (1972).

22. A.D. Dickson, I.M. Mills, and B. Crawford, Jr., J. Chem. Phys., 27, 445 (1957).

23. E.B. Wilson,Jr., J.C. Decius, and P.C. Cross, Molecular Vibrations (McGraw-Hill, New York, 1955).

24. Derek Steele, Theory of Vibrational Spectroscopy (W.B. Saunders Co., Philadelphia, 1971), Chapters 1-7.

25. F. Albert Cotton, Chemical Applications of Group Theory (Interscience Publishers, New York, 1966), Chapter 9.

26. J.H. Schachtschneider, "Vibrational Analysis of Polyatomic Molecules." VI. Shell Development Company Technical Report No. 57-65, Emeryville, California (1964), pp. 12-28.

27. I.M. Mills, Spectrochim. Acta, 16, 35 (1960).

28. Reference 23, Chapter 11.

29. Reference 26, p. 54.

30. D.C. McKean, R. Bruns, W.B. Person, and G.A. Segal, J. Chem. Phys., 55, 2890 (1971).

31. John A. Pople and David L. Beveridge, Approximate Molecular Orbital Theory (McGraw-Hill, New York, 1970).

32. We used the program from the Quantum Chemistry Program Exchange, #141, CNINDO, by P.A. Dolosk, for our calculations.

33. R.H. Schwendeman, J. Chem. Phys., 44, 2115 (1966).

34. I.M. Mills, W.L. Smith, and J.L. Duncan, J. Mol. Spect., 16, 349 (1965).

35. S. Kondo and W.B. Person, J. Mol. Spectroscopy, 52, 287 (1974).

36. N.L. Boas, Mathematical Methods in Physical Sciences (John Wiley and Sons, Inc., New York, 1966), p. 454.

37. R.E. Bruns and W.B. Person, J. Chem. Phys., 61, 1779 (1974).

38. A.L. Allred and E.G. Rochow, J. Inorg. Nucl. Chem., 5, 264 (1958).

39. J.A.A. Ketelaar, Chemical Constitution (Elsevier Publishing Company, New York, 1958), p. 91.

40. J.B. Marion, Classical Electromagnetic Radiation (Academic Press, New York, 1965), pp. 33-37.

41. W.P. Person, in Spectroscopy and Structure of Molecular Complexes (J. Yarwood, Editor) (Plenum Press, London, 1973), p. 53.

42. I.W. Levin and T.P. Lewis, J. Chem. Phys., 52, 1608 (1970).

43. L.P. Lindsay and P.N. Schatz, Spectrochim. Acta, 20, 1421 (1964).

44. W.B. Person and B. Zilles, unpublished results, University of Florida.

45. J. Hinze, M.A. Whitehead, and H.H. Jaffe', JACS., 85, 148 (1963).

46. P. Bennett, B.S. Thesis, University of Florida (1974).

47. S. Kondo and S. Saëki, Spectrochim. Acta, 29A, 735 (1973).

BIOGRAPHICAL SKETCH

James Henry Newton was born February 24, 1941, in Macon County, North Carolina. He attended elementary and high school in Highlands, North Carolina, and entered the University of North Carolina at Chapel Hill in September of 1959. After receiving his B.S. degree in chemistry from U.N.C. in August, 1964, he taught eighth grade and high school science in Highlands School for one year. In July, 1965, he joined Dayco Corporation in Waynesville, North Carolina as a research chemist in the Printing Products Division. In September, 1967, he returned to school at Furman University in Greenville, South Carolina, and received his M.S. degree in chemistry from that institution in 1969. He entered the Graduate School at the University of Florida in September of 1969 and received his Ph.D. in physical chemistry in December, 1974.

Mr. Newton is married to the former Christina Catherine Harbison, and they have two children.

I certify that I have read this study and that in my opinion it conforms to acceptable standards of scholarly presentation and is fully adequate, in scope and quality, as a dissertation for the degree of Doctor of Philosophy.

Willis B. Person, Chairman
Professor of Chemistry

I certify that I have read this study and that in my opinion it conforms to acceptable standards of scholarly presentation and is fully adequate, in scope and quality, as a dissertation for the degree of Doctor of Philosophy.

Earle E. Muschlitz, Jr.
Professor of Chemistry

I certify that I have read this study and that in my opinion it conforms to acceptable standards of scholarly presentation and is fully adequate, in scope and quality, as a dissertation for the degree of Doctor of Philosophy.

Martin T. Vala
Associate Professor of Chemistry

I certify that I have read this study and that in my opinion it conforms to acceptable standards of scholarly presentation and is fully adequate, in scope and quality, as a dissertation for the degree of Doctor of Philosophy.

Robert C. Stoufer
Associate Professor of Chemistry

I certify that I have read this study and that in my opinion it conforms to acceptable standards of scholarly presentation and is fully adequate, in scope and quality, as a dissertation for the degree of Doctor of Philosophy.

D. B. Dove

Derek B. Dove
Professor of Material Science
Engineering

This dissertation was submitted to the Graduate Faculty of the Department of Chemistry in the College of Arts and Sciences and to the Graduate Council, and was accepted as partial fulfillment of the requirements for the degree of Doctor of Philosophy.

December, 1974

Dean, Graduate School